Supporting Information

Tunable Oleo-Furan Surfactants by Acylation of Renewable Furans

Dae Sung Park[1,5,†], Kristeen E. Joseph[1,5, †], Maura Koehle[2,5], Christoph Krumm[1,4], Limin Ren[1], Jonathan N. Damen[1], Meera H. Shete[1,5], Han Seung Lee[1], Xiaobing Zuo[6], Byeongdu Lee[6], Wei Fan[3,5], Dionisios G. Vlachos[2,5], Raul F. Lobo[2,5], Michael Tsapatsis[1,5],Paul J. Dauenhauer[1,5,]*

[1]University of Minnesota, Department of Chemical Engineering and Materials Science
[2]University of Delaware, Department of Chemical Engineering
[3]University of Massachusetts Amherst, Department of Chemical Engineering
[4]Sironix Renewables, http://www.sironixrenewables.com/
[5]Catalysis Center for Energy Innovation, U.S. Department of Energy – Energy Frontier Research Center
[6]Argonne National Laboratory, X-Ray Science Division, Lemont, IL.
*****Corresponding Author: hauer@umn.edu
[†]Authors contributed equally

Contents

1.0 Materials and Methods

1.1 Materials

Hexane (95 %), Furan (99 %), and Trifluoroacetic anhydride (99 %) were purchased from Sigma-Aldrich. The saturated fatty acids, lauric acid (C12, 99 %, Acros), myristic acid (C14, 99 %, Sigma-Aldrich), stearic acid (C18, 95 %, Sigma-Aldrich), and cocinic acid (mixture of fatty acids, C8~C18, BOC Sciences) were used in furan acylation for the first step in overall reaction pathway. The reference standards, 2-n-heptylfuran (98 %) and 2-n-dodecylfuran (95 %) were purchased from Alfa Aesar and MP Biomedical, respectively. Lauric anhydride (98 %, TCI Chemicals) was also used for furan acylation with solid acid catalysts. H-BEA catalyst (CP814E, Si/Al = 12.5) and copper chromite catalyst were obtained from Zeolyst and Sigma-Aldrich, respectively. The H-BEA was calcined at 550 ºC for 12 h at the rate of 1 ºC min^{-1} in a tube furnace under air flow. The reduction of copper chromite was carried out at 300 ºC for 3 h under 10 % H_2/Argon flow.

For the purpose of evaluation and comparison of the renewable OFS surfactant performance, four different anionic commercial surfactants were purchased; linear alkylbenzene sulfonate (sodium dodecylbenzene sulfonate, 79.7%, Sigma-Aldrich), sodium lauryl sulfate (sodium dodecyl sulfate, 99.1%, Sigma-Aldrich), sodium lauryl ether sulfate (70.4%, BOC Sciences) and methyl ester sulfonate (Alpha-Step MC-48, 38.76%, Stepan)

1.2 Zeolite synthesis methods

Several types of self-pillared zeolites, Al/Sn-SPP and Al/Sn-MWW were used as catalysts in furan acylation with anhydride after calcination at 500 ºC for 4 h.

Sn-MWW synthesis: Sn-MWW was synthesized by modifying an existing literature method.[1] First, B-MWW precursor was de-boronated by 6M HNO_3 (1 g zeolite/ 50 mL HNO_3) at 100 °C under reflux for 1 day, this procedure was performed twice. Then 2.5 g of the de-boronated sample was mixed with 30 g of distilled water and 3.549 g of piperidine (99 %, Aldrich). After stirring for 1 hour, 0.146 g of tin tetrachloride pentahydrate ($SnCl_4 \cdot 5H_2O$, 98 %, Aldrich) was added into the above mixture and stirred for 2 hours. Then the final gel with chemical composition $1SiO_2$: 0.01 SnO_2: 1.0 piperidine: 40 H_2O was transferred to an autoclave and hydrothermally treated in a rotation oven at 170 °C for 14 days. The products were separated and fully washed by filtration and then dried at 70 °C overnight. Calcination of this sample was performed in static air at 580 °C for 10 hours.

Sn-SPP synthesis: First, 0.129 g of tin tetrachloride pentahydrate ($SnCl_4 \cdot 5H_2O$, 98 %, Sigma-Aldrich) was dissolved into 7.35 g of tetra(n-butyl)phosphonium hydroxide (TBPOH, 40 wt%, TCI America) followed by the addition of 7.5 g of tetraethyl orthosilicate (TEOS, 98 %, Sigma-Aldrich). After hydrolysis, 3.2 g of deionized water was added to the mixture. The mixture was stirred overnight, and a clear sol was obtained. The composition of the final sol was: 1.0 SiO_2 : 0.03 TBPOH : 4.0 EtOH : $30H_2O$: $0.01SnO_2$. The sol was sealed in a Teflon-lined stainless steel autoclave and hydrothermally treated in a pre-heated static oven at 115 °C for 5 days. The solid products were centrifuged, washed with distilled water and then dried at 70 °C overnight and calcined at 550 °C for 6 h in air under static conditions. The calcined samples were washed again

with water, dried at 70 °C overnight and calcined at 550 °C for 6 h in air under static conditions and this process was repeated to ensure removal of P_2O_5.

Al-MWW synthesis: Al-MWW was synthesized according to a literature method.[2] First, 0.72 g of sodium aluminate (MP Biomedicals, USA) and 2.48 g of sodium hydroxide (98.5 %, Sigma-Aldrich) were dissolved in 311 g of distilled water. Then, 19.1 g of hexamethyleneimine (HMI) (Aldrich) was added to the mixture and stirred for 30 min. Subsequently 23.6 g of fumed silica (Cab-o-sil M5) was added to the mixture and stirred overnight. The homogeneous gel was sealed in Teflon-lined stainless steel autoclaves and heated at 135 °C for 11 days. The products were separated and fully washed by filtration followed by drying at 70 °C overnight, then calcined at 580 °C in static air for 10 hours.

Al-SPP synthesis: 0.098 g of Aluminum isopropoxide (Sigma-Aldrich) was mixed with 3.23g of distilled water and 7.35 g of tetra(n-butyl)phosphonium hydroxide solution (TBPOH, 40wt %, TCI America). The mixture was added to 7.5 g of tetraethyl orthosilicate (TEOS, Sigma-Aldrich) and stirred overnight. The sol was sealed in a Teflon-lined stainless steel autoclave and hydrothermally treated in a pre-heated static oven at 115 °C for 5 days. The solid products were centrifuged, washed with distilled water and then dried at 70 °C overnight and calcined at 550 °C for 6 h in air under static conditions.

Ion exchange to obtain the proton form Al-zeolites: Typically, ion exchange was performed by stirring Al-zeolites with 1M ammonium nitrate (NH_4NO_3, Sigma-Aldrich) solution (1g zeolite + 100ml NH_4NO_3 solution) at 80 °C for 5h. After the stirring, zeolites products were centrifuged, washed with distilled water and then dried at 70 °C overnight and calcined at 500 °C for 4 h in air under static conditions. The whole procedure was performed twice for complete ion exchange.

Mg-Zr-O synthesis: The mixed oxide, Mg-Zr-O, catalyst was synthesized by sol-gel method. 0.01 mol of magnesium nitrate (Sigma-Aldrich, 99 %) and 0.009 mol of zirconyl nitrate (Sigma-Aldrich, 99 %) were mixed in DI water at room temperature. NaOH was added to the mixtures until the pH was 10, and the slurry was aged at room temperature for 72 h. The slurry was filtered and washed with DI water, and then, dried at 110 ºC for 24 h. The catalyst was then calcined at 600 ºC for 3h before being used for aldol-condensation reaction.[3]

K-BEA and K-Y synthesis: K-BEA and K-Y zeolites were prepared by typical ion-exchange method. 2.5 g of zeolite (H-BEA or H-Y) was added to 0.6 M solution of KNO_3 (Sigma-Aldrich, 99 %). The mixture was aged at 70 ºC for 10 h with vigorous stirring in a round bottom flask connected with a condenser. After filtration and washing with DI water, the powder was dried at 100 ºC for 24 h and calcined at 500 ºC for 4 h.[4]

1.3 Procedure for preparation of fatty acid anhydrides from corresponding fatty acids

Fatty acids can be converted to their corresponding anhydride by various existing methods such as heating the acid with a dehydrating agent like acetic anhydride whereby the carboxylic acid gets dehydrated to the anhydride and the acetic anhydride gets hydrated to the acid form. One

way of achieving this is by passing excess amounts of acetic acid vapor through molten fatty acid. Fatty acid anhydride can also be produced by heating the acid with liquid acetic anhydride in the presence of an organic solvent like toluene, ethylbenzene or tetrachloroethylene which forms an azeotrope with acetic anhydride.[5] This method promises good yields of fatty acid anhydrides using lesser amounts of acetic anhydride as compared to the previous vapor method. In this method, a mixture of fatty acid, acetic anhydride and the azeotropic agent (solvent) is heated to 120 °C at atmospheric pressure. As the reaction occurs, the azeotropic mixture of acetic acid and solvent is distilled off and any vaporized acetic anhydride is condensed and returned to the reaction vessel. An increase in the temperature of the reaction mixture marks the completion of reaction. A third method for the synthesis of fatty acid anhydrides makes use of a metal salts such as salts of cobalt, manganese, palladium, copper, nickel, chromium, rhodium, thorium and iron.[6] The reaction is carried out between 140 – 220 °C in an inert atmosphere. Water produced during the dehydration of fatty acid is removed as an azeotrope with a hydrocarbon solvent such as linear alkanes, benzene, toluene etc. Examples of metal salts that can be used as catalysts include $Co(OAc)_2 \cdot 4H_2O$, $Pd(OAc)_2$, $Cr(OAc)_3$, $Mn(OAc)_2 \cdot 4H_2O$, $Th(NO_3)_4 \cdot 4H_2O$, Rh_2O_3, $Cu(OAc)_2$ and $Fe(OAc)_3$.

1.4 Procedure for preparation of OFS-n-1/O (n=12, 14, 18, and mixtures from C8 to C18)

Furan acylation with fatty acids for production of OFS-n-1/O was conducted in a high pressure Parr Reactor and glass beaker. In a typical reaction, the furan (0.014 mol), fatty acid (0.014 mol), trifluoroacetic anhydride (0.02 mol) and n-tridecane (internal standard, 0.002 mol) were dissolved in hexane (10 mL), and 0.2 g of the Al-BEA catalyst was introduced to the mixture. Furan acylation with fatty anhydride was also performed in a Parr reactor with 0.014 mol of furan and 0.0014 mol of fatty anhydride in 15 mL of hexane with Brønsted acid and Lewis acid zeolites such as Al-BEA, Al-MWW, Al-SPP, Sn-BEA, Sn-MWW and Sn-SPP. The sealed reactor was purged with N_2 twice to remove the residual air in the reactor. The reactor was then heated to the reaction temperature (room temperature or 50 – 180 °C) under vigorous stirring (1,000 rpm). The reactor was then pressurized to 200 psi (at desired temperature) with N_2 to keep the reactants in liquid phase. After the desired reaction time, the reactor was cooled to room temperature and the gases were vented. The products were identified by a GC-MS (Agilent 7890A connected with Triple-Axis MS detector, Agilent 5975C) and quantified by a GC (Agilent 7890A) equipped with a HP-5 column and a flame ionization detector. The selectivity of the furyl-2-alkyl ketone was calculated by dividing the produced moles of furyl-2-alkyl ketone with the reacted moles of the furan. The final surfactant OFS-n-1/O was prepared according to the method given in Section 1.10 of the supplementary materials.

1.5 Procedure for preparation of OFS-n (n=12, 14, 18, and mixtures from C8 to C18)

The hydrogenation of OFS-n-1/O to make OFS-n was carried out in a 100 mL Parr reactor. The prepared furyl-2-alkyl ketone (2 mL) and n-tridecane (internal standard, 0.5 mL) were dissolved in hexane (30 mL), and 0.5 g of copper chromite catalyst was introduced to the mixture. The reactor was pressurized with hydrogen in a range of 100 – 350 psi at the desired reaction temperature (180 – 220 °C). The selectivity of the 2-n-alkylfuran was calculated by dividing the produced moles of 2-n-alkylfuran with the reacted moles of the furyl-2-alkyl ketone. The final surfactant OFS-n was prepared according to the method given in Section 1.10 of the supplementary

materials.

1.6 Procedure for preparation of OFS-12-2/C2H5

For making the mono-ethyl branched surfactant monomer (M-DF, Scheme S3), aldol-condensation of furyl-2-dodecyl ketone (2-dodecanoylfuran, DOF) with acetaldehyde was conducted in a 100 mL Parr reactor. The prepared DOF (0.0054 – 0.01 moles) and acetaldehyde (0.0054 – 0.054 moles) were dissolved in hexane (20 mL), and 0.2 g of solid acid/base catalysts was introduced to the mixture. The reactor was pressurized to 200 psi with N_2 to prevent vaporization of acetaldehyde and heated to 180 – 220 ºC. After purification of the aldol-condensation products, the mixture of unreacted DOF and aldol-product (Al_DOF) was used as the reactant for hydrogenation. The reduction of ketone to the hydrocarbon via hydrogenation was carried out at 220 ºC and 100 psi of H_2 for 7 h using copper chromite as the catalyst to produce M-DF (Scheme S3). The final surfactant OFS-12/C2H5 was prepared according to the method given in Section 1.10 of the supplementary materials.

1.7 Separation of furyl-2-alkyl ketone (alkyl chain=C12, C14, C18, and C8-C18 mixture)

The acylation products were concentrated using a rotary evaporator (Hei-VAP/G5, Heidolph) with a liquid nitrogen condenser. Several batch reactions were conducted without the internal standard chemical (n-tridecane) to collect the product mixture. The rotary evaporator was operated at room temperature for 30 min under high vacuum to remove the light molecules (hexane, furan, trifluoroacetic anhydride and trifluoroacetic acid). The remaining mixture was further concentrated at 70 ºC for 2h under high vacuum.

1.8 Separation and purification of 2-n-alkylfuran (alkyl chain=C12, C14, C18, and C8-C18 mixture) and M-DF

The products after hydrogenation were purified by using rotary evaporator initially followed by flash chromatography. The rotary evaporator was operated at 50 ºC for 1 h to evaporate the solvent and light molecules. Further purification was done by flash chromatography using a 12 inch length and 1 inch diameter column (CG-1189-07) packed with silica gel (230-400 mesh, particle size 40-63 μm). Hexane was used as the mobile phase to separate 2-n-dodecylfuran (DF) and M-DF (Scheme S3) from the product mixture, and a 50% acetone in hexane solution was used as the eluent to remove undesired products (eg. saturation of furan ring to form tetrahydrofuran based molecules such as M-DTHF as shown in Scheme S3 and some other unknown compounds).

1.9 Separation and purification of the aldol-condensation product (Al_DOF)

After aldol-condensation, the products, unreacted DOF and aldol-product, were concentrated and purified using rotary evaporator and flash chromatography. The rotary evaporator aided in the removal of all solvent and light molecules while, flash chromatography was used with a 1 inch diameter glass column, and 1,2-dichloroethane as the eluent to separate the desired products (DOF and Al_DOF) from all unknown chemicals.

During the process of separation and purification, the ratio of unreacted DOF to the aldol product (Al_DOF) changed from 77:23 to 70:30 due to losses during flash chromatography. Post hydrogenation, this ratio (DF:M-DF) changed to 66:34 which further reduced to ~60:40 post purification.

1.10 Sulfonation

All prepared surfactant monomers (including reference standards such as 2-n-heptylfuran) was sulfonated and neutralized to make oleo-furan sulfonate surfactants (OFS-n, OFS-n-1/O, OFS-n-2/2H5), sodium 2-R-furan-5-sulfonate (R = different alkyl chains), by the following method. The synthesized monomers (13 mmol) were added to a slurry of sulfur trioxide-pyridine complex (13 mmol) in anhydrous acetonitrile (12 mL). The mixture was stirred at room temperature for 3 days. At the end of 72h, 40 mL of water (70 ^{o}C) was introduced to the slurry, and the slurry was stirred for 1 h. The aqueous phase was separated by a separatory funnel after 1 h, and the aqueous solution was neutralized by using sodium carbonate till the pH was 7.0. The water was then evaporated off and the crystalline phase was collected by filtration and washed with iso-propanol (60 ^{o}C, 50 mL, 5 times).[7,8]

1.11 Characterization (NMR, Particle size distribution of micelles via DLS)

1.11.1 NMR

The synthesized surfactant monomers and oleo-furan sulfonate surfactants (OFS-n, OFS-n-1/O, OFS-12-2/C2H5) were analyzed by NMR spectroscopy (Bruker AX400, 400 MHz). The ^{1}H and ^{13}C NMR of the surfactant monomers was performed by dissolving ~20 μL of the compound in $CDCl_3$ containing 5 mM of tetramethylsilane (TMS) as an internal standard. The oleo-furan surfactants were also identified by NMR using DMSO-d_6 as the solvent. The results from NMR analysis are given in Section 3.0 and 6.0 of the supplementary materials text.

1.11.2 Particle size distribution of micelles via Dynamic Light Scattering (DLS)

Dynamic Light Scattering (DLS) has been used in the past for studying surfactant aggregates.[9] Micelle size distribution studies of the OFS-12 surfactant was performed using the Microtrac NANO-flex analyzer which employs a 180° scattering angle DLS technique. Three different surfactant concentration samples were prepared (5.0, 10.0 and 20.0 x CMC corresponding to 0.35, 0.70 and 1.40 wt.%) by dissolving the required amount of surfactant in deionized water and filtering the solution after surfactant dissolution using a 0.2μ micropore filter to remove any dust particles. Prior to each sample run, a blank solution (DI water) was used to set the baseline to zero. Fig S1 shows the average particle size distribution plots for the surfactant solutions. The average values were computed based on five individual trials each lasting 120 sec.

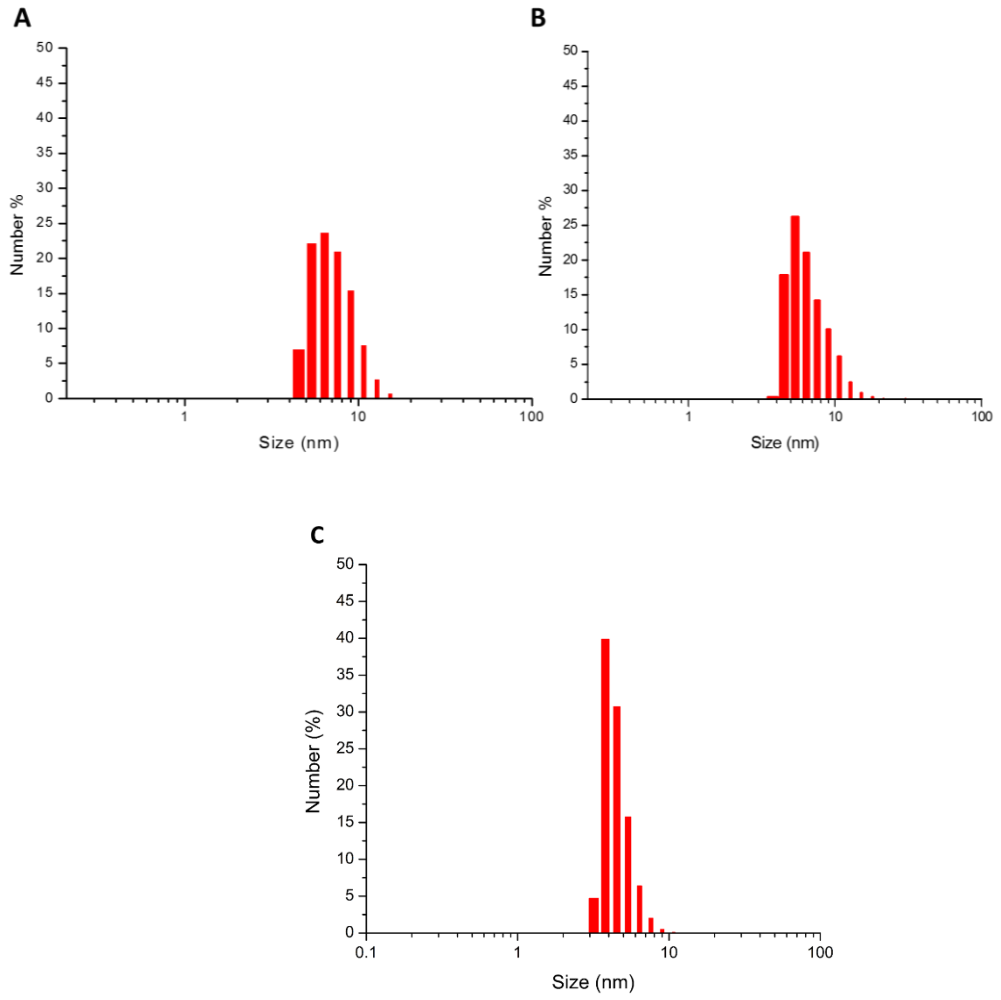

Fig. S1. Particle size (number) distribution for micelles in OFS-12 surfactant solution with concentration **A.** 5.0 x CMC (average size, 7 nm), **B.** 10.0 x CMC (average size, 6 nm) and, **C.** 20.0 x CMC (average size, 5 nm).

2.0 Reaction Results & Screening of Reaction Conditions

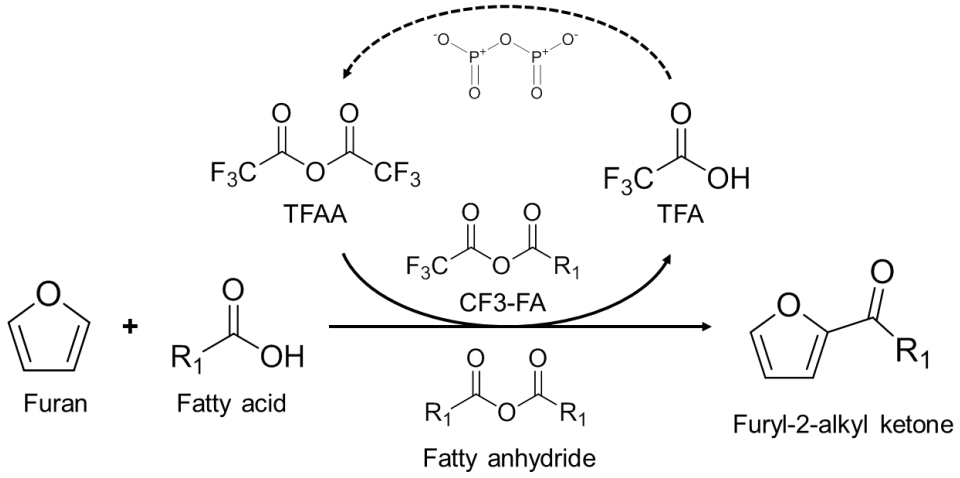

Scheme S1. Reaction pathway for furan acylation with fatty acid promoted by trifluoroacetic anhydride at room temperature (TFAA: Trifluoroacetic anhydride, TFA: Trifluoroacetic acid).

Table S1. Summarized results for the acylation of furan with lauric acid and trifluoroacetic anhydride (TFAA).

Conditions	Conversion (%)			Selectivity (%)
	Furan	Lauric acid	TFAA	2-dodecanoylfuran
25 ºC (No Cat.)	100	100	51.1	87.0
25 ºC	100	100	71.6	81.3
50 ºC	100	100	70.2	75.6
100 ºC	100	100	27.4	27.4
150 ºC	100	95.6	100	43.9
180 ºC	100	78.3	100	13.5
150 ºC (THF)	53.9	91.2	100	20.1

*Reaction Conditions: 200 psi (N_2), 0.014 mol of furan, 0.018 mol of lauric acid, and 0.028 mol of TFAA in hexane (10 mL), Al-BEA 0.2g, 6 h in Parr reactor.

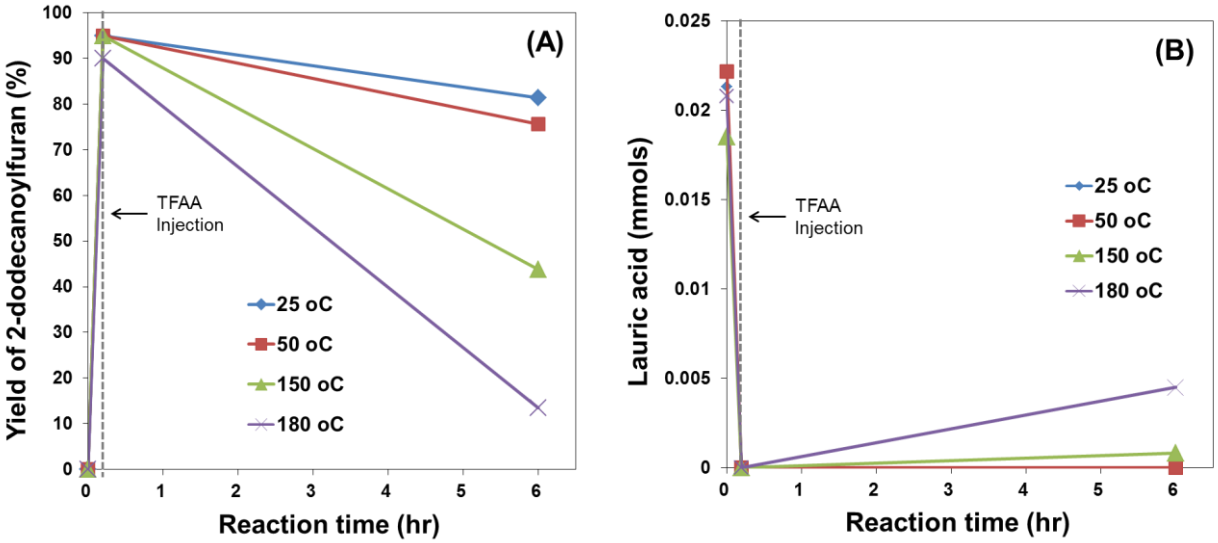

Fig. S2. The change in the yield of **A.** 2-dodecanoylfuran and, **B.** lauric acid concentration during a reaction. Reaction Conditions: 200 psi (N_2), 0.014 mol of furan, 0.018 mol of lauric acid, and 0.028 mol of TFAA in hexane (10 mL), Al-BEA 0.2 g, 6 h.

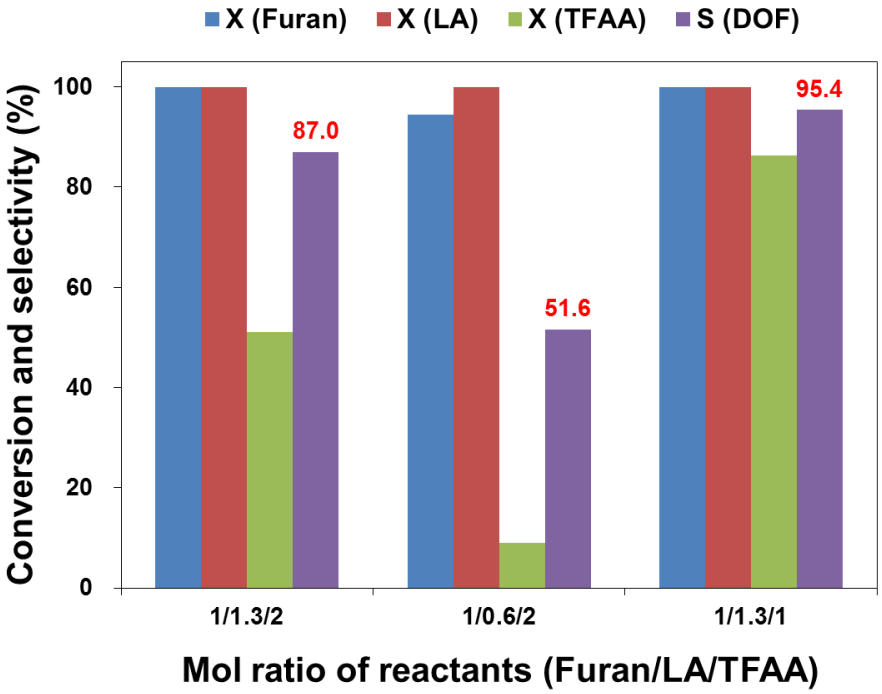

Fig. S3. Results for the acylation of furan and lauric acid with different mole ratios of reactants. LA: Lauric acid, TFAA: Trifluoroacetic anhydride, Mole ratio (1/1.3/1): 0.014 mol of furan / 0.018 mol of lauric acid / 0.014 mol of TFAA, Reaction conditions: Room temperature, 1 atm, no catalyst.

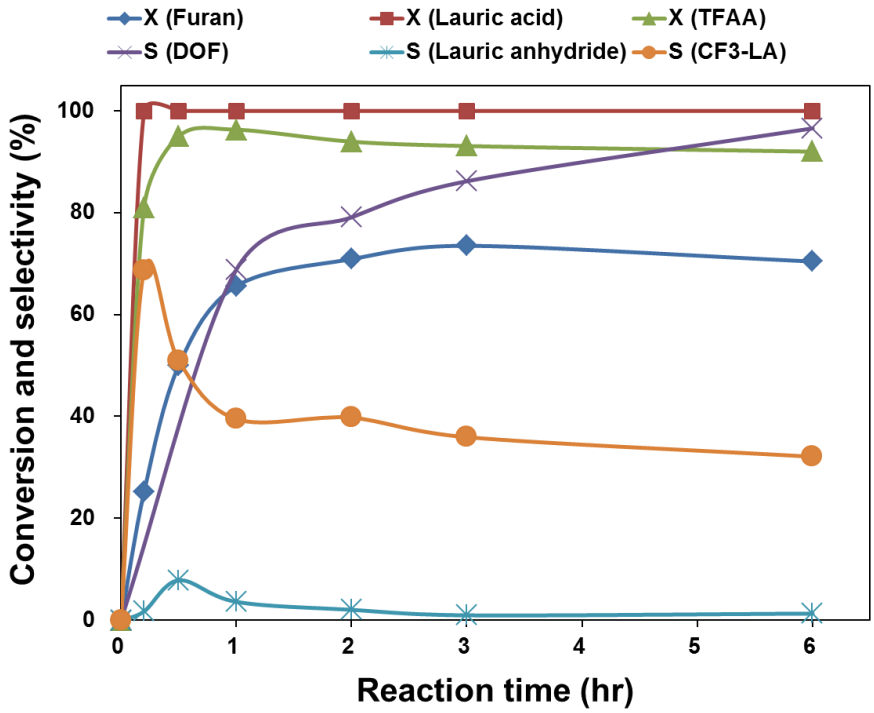

Fig. S4. Time-on-stream results for the acylation of furan and lauric acid with TFAA. DOF: 2-dodecanoylfuran, TFAA: Trifluoroacetic anhydride, Reaction conditions: 0.014 mol of furan, 0.018 mol of lauric acid, 0.02 mol of TFAA in 50 mL of hexane, 25 ºC, 1 atm.

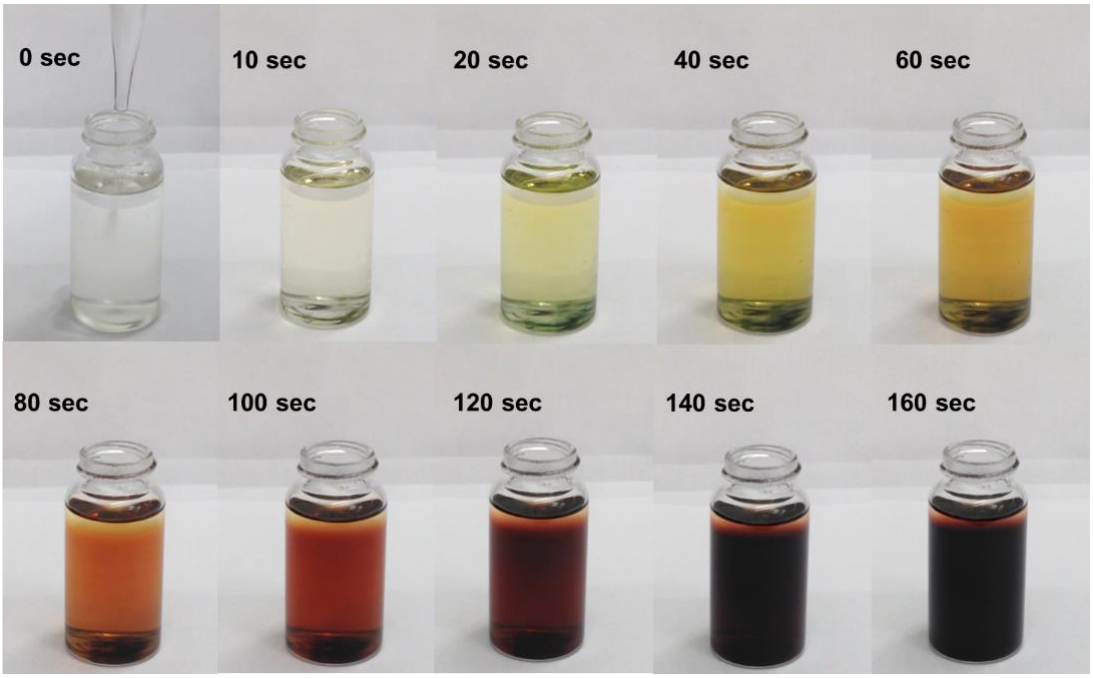

Fig. S5. Reaction progression of acylation of furan with lauric acid using TFAA with time. The reaction is complete and high yields are obtained within a few minutes. 0 s corresponds to the point of addition of TFAA.

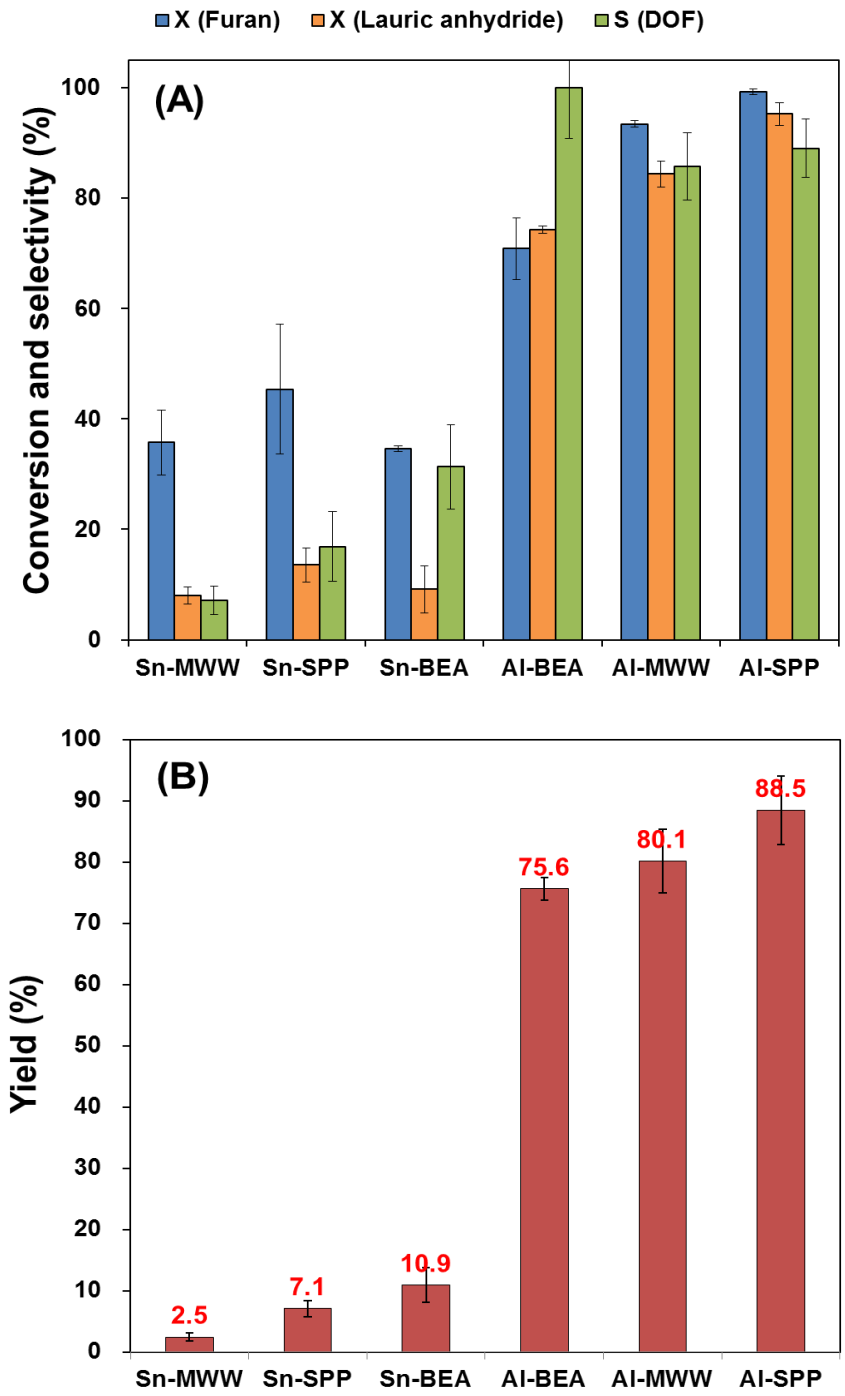

Fig. S6. Results for **A.** conversion and selectivity and **B.** yield in furan acylation with lauric anhydride over various solid acid catalysts (Reaction conditions: 180 °C, 200 psi of N_2, 5 h, 0.014 mol of furan, 0.014 mol of lauric anhydride in 15 mL hexane).

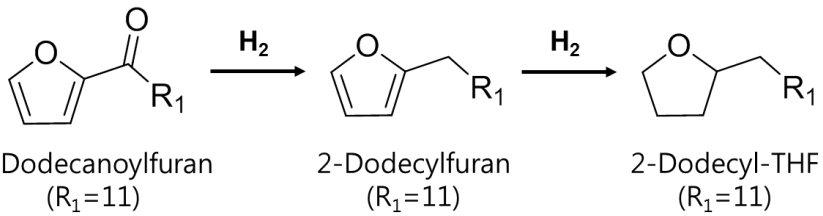

Scheme S2. Reaction pathway for liquid-phase hydrogenation of furyl-2-alkyl ketone over copper chromite ($2CuO\text{-}Cr_2O_3$).

Table S2. Summarized results for the hydrogenation of 2-dodecanoylfuran over copper chromite.

Conditions	Conversion (%)	Selectivity (%)		
	2-dodecanoylfuran	2-dodecylfuran	2-dodecyl-THF	Unknown
100 psi	100	91.6	7.3	1.1
150 psi	100	59.5	12.3	28.2
250 psi	100	54.8	18.3	26.9
350 psi	100	0.9	47.6	51.5
250 psi (Reduced 2CuO-Cr_2O_3)	99.6	18.3	74.9	6.9

*Reaction Conditions: 220 ºC, varying pressures of H_2 (at 220 ºC), 0.0077 mol of 2-dodecanoylfuran in hexane (30 mL), copper chromite 0.5g, 5 h.

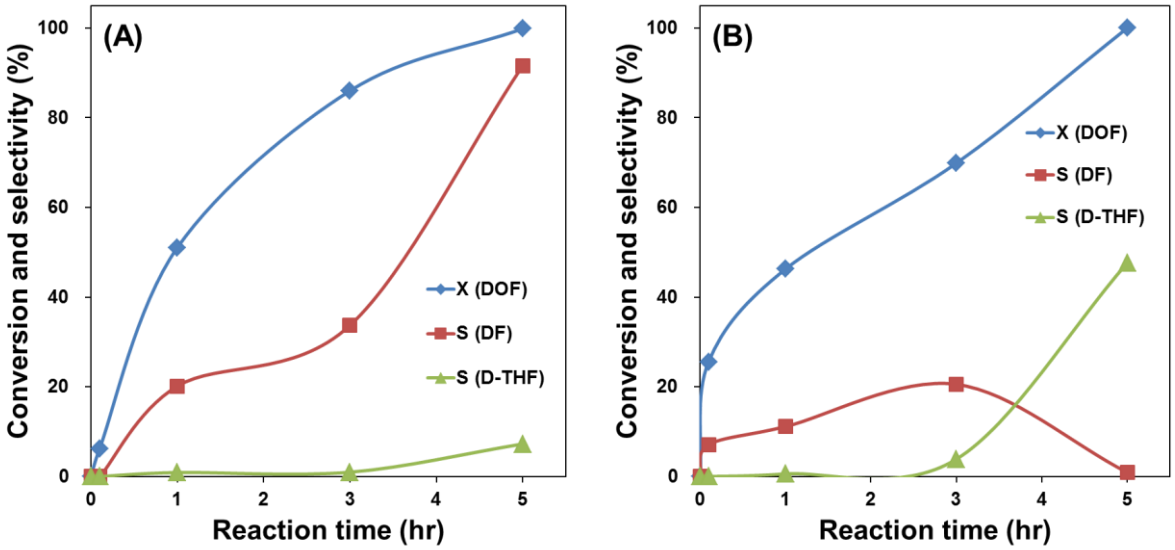

Fig. S7. Time-on-stream results (conversion of 2-dodecanoylfuran (DOF) and selectivities of 2-dodecylfuran (DF) and 2-dodecyl-tetrahydrofuran (D-THF)) for the hydrogenation of 2-dodecanoylfuran at **A.** 100 psi and **B.** 350 psi of H_2.

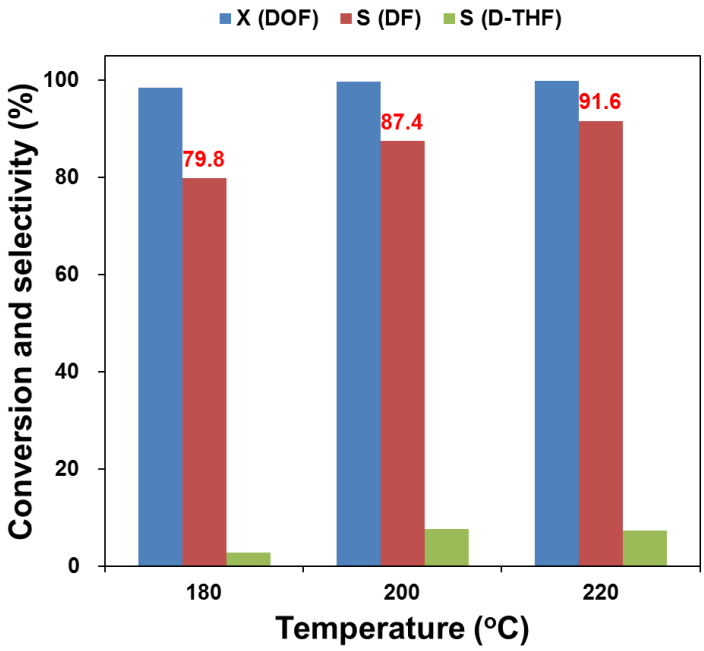

Fig. S8. Results for the hydrogenation of 2-dodecanoylfuran (DOF) at 180 – 220 °C in 100 psi of H_2. Reaction Conditions: 100 psi of H_2 (at reaction temperature), 0.0077 mol of 2-dodecanoylfuran in hexane (30 mL), copper chromite 0.5g, 5 h.

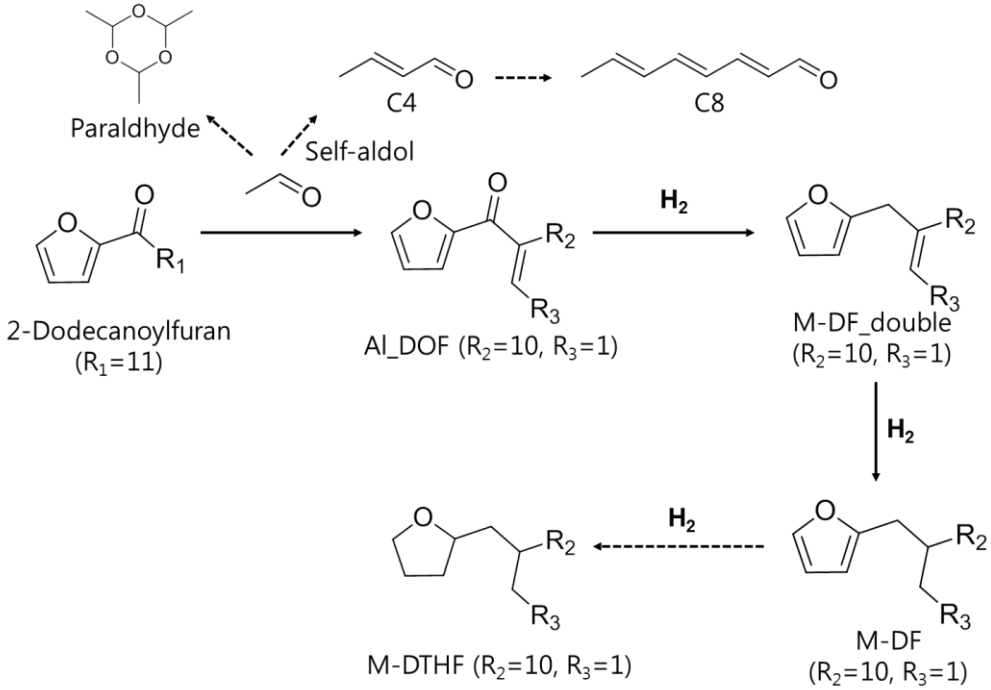

Scheme S3. Reaction pathways for aldol condensation of 2-dodecanoylfuran (DOF) with acetaldehyde and hydrogenation of the aldol-product (Al_DOF) to form mono-ethyl branched dodecylfuran (M-DF). One of the side products of the reaction is M-DTHF (mono-ethyl branched dodecyl-tetrahydrofuran) formed due to undesirable hydrogenation of the furan ring.

Table S3. Summarized results for the aldol condensation of 2-dodecanoylfuran (DOF) with acetaldehyde over various acid and base catalysts.

Conditions	Conversion (%)		Selectivity (%)				Yield (%)
	Acetaldehyde	DOF	C4	C8	Paraldehyde	Al_DOF	Al_DOF
Al-BEA (200 °C, 6h)	74.7	17.2	4.6	1.2	0.05	47.2	8.1
KBEA (200 °C, 6h)	62.3	12.0	9.5	1.3	0.03	75.5	9.1
HY (200 °C, 6h)	73.5	17.4	10.2	1.4	0.04	58.1	10.1
Mg-Zr-O (200 °C, 6h)	99.5	12.3	0.08	0.9	0.01	9.0	1.1
HY (220 °C, 6h)	78.8	17.6	8.5	1.4	0.02	42.5	7.5
HY (180 °C, 6h)	73.7	13.8	8.3	0.7	0.06	80.9	11.2
KY (180 °C, 6h)	72.1	16.2	10.5	0.8	0.03	63.0	10.2
HY (180 °C, 24h)	85.2	34.7	7.1	1.7	0.02	58.5	20.3
HY (180 °C, 48h)	93.9	47.2	7.7	18.7	0.04	35.6	16.6

*Reaction Conditions: 200 psi (N_2), 0.054 mol of acetaldehyde and 0.0054 mol of 2-dodecanoylfuran in hexane (20 mL), 0.2 g catalyst.

Table S4. Summarized results for the aldol condensation of 2-dodecanoylfuran (DOF) with acetaldehyde over various acid and base catalysts.

Catalysts	Conversion (%)		Selectivity (%)				Yield (%)
	Acetaldehyde	DOF	C4	C8	Paraldehyde	Al_DOF	Al_DOF
HY (1g, 24 h)	93.0	19.4	5.3	1.3	0.02	41.5	8.1
HY (0.2g, 24 h)	85.2	34.7	7.1	1.7	0.02	58.5	20.3
HY (0.1g, 24 h)	74.0	29.6	11.3	2.4	0.6	62.6	18.5
Si-SPP (0.1g, 24h)	82.0	27.4	8.1	3.5	0.06	63.3	17.3
Al-SPP (0.1g, 24h)	81.5	17.6	11.2	9.4	0.06	78.3	13.8
Al-MWW (0.1g, 24h)	90	20.6	3.8	3.2	0.05	70.9	14.6
NaOH (0.1g, 24h)	99	22.3	0.06	0.2	0.3	1.7	0.4
No Cat. (24 h)	72.3	33.0	7.8	1.1	0.2	70.8	23.4
No Cat. (48 h)	87.5	36.8	7.8	0.9	0.1	60.0	22.1
No Cat. (72 h)	93.1	58.3	4.1	0.6	0.04	24.5	14.3

*Reaction Conditions: 200 psi (N_2), 180 ºC, 0.054 mol of acetaldehyde and 0.0054 mol of 2-dodecanoylfuran in hexane (20 mL).

Table S5. Summarized results for the aldol condensation of 2-dodecanoylfuran (DOF) with acetaldehyde.

Mole ratio of reactants (AA:DOF)	Conversion (%)		Selectivity (%)				Yield (%)
	Acetaldehyde	DOF	C4	C8	Paraldehyde	Al_DOF	Al_DOF
15:1	60.4	32.6	16.2	2.0	0.5	67.1	21.9
10:1	72.3	33.0	7.8	1.1	0.2	70.8	23.4
5:1	72.8	17.0	7.9	0.5	0.2	70.9	12.1
1:1	70.0	4.0	1.4	0	0	57.2	2.3
1:2	82.7	11.1	0.9	0	0	61.2	6.8

*Reaction Conditions: 200 psi (N_2), 180 ºC, 24 h, (10:1) ratio: 0.054 mol of acetaldehyde and 0.0054 mol of 2-dodecanoylfuran in hexane (20 mL).

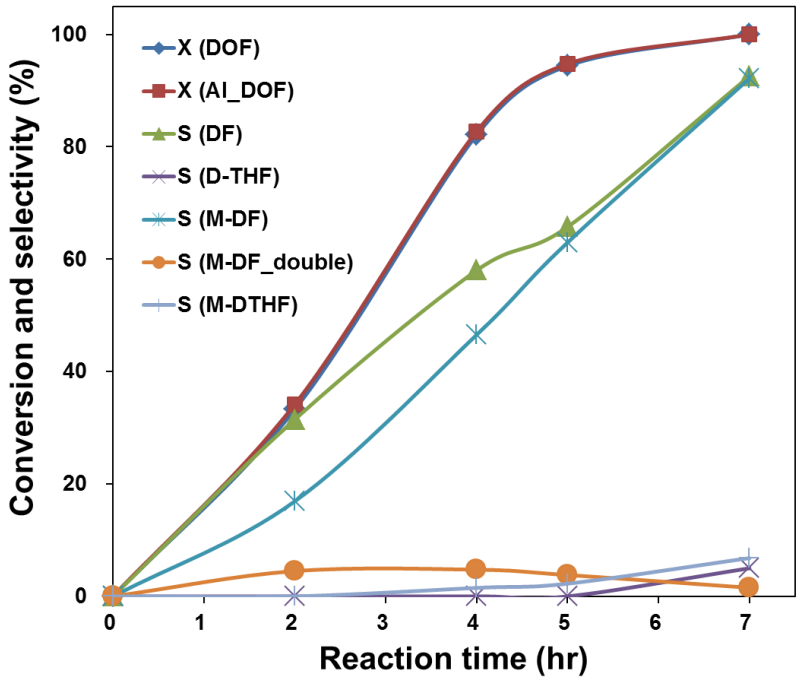

Fig. S9. Time-on-stream results for the hydrogenation of mixture of 2-dodecanoylfuran (DOF) and aldol-product (Al_DOF), (220 ºC, 100 psi of H_2, 0.5g of copper chromite, 7 h).

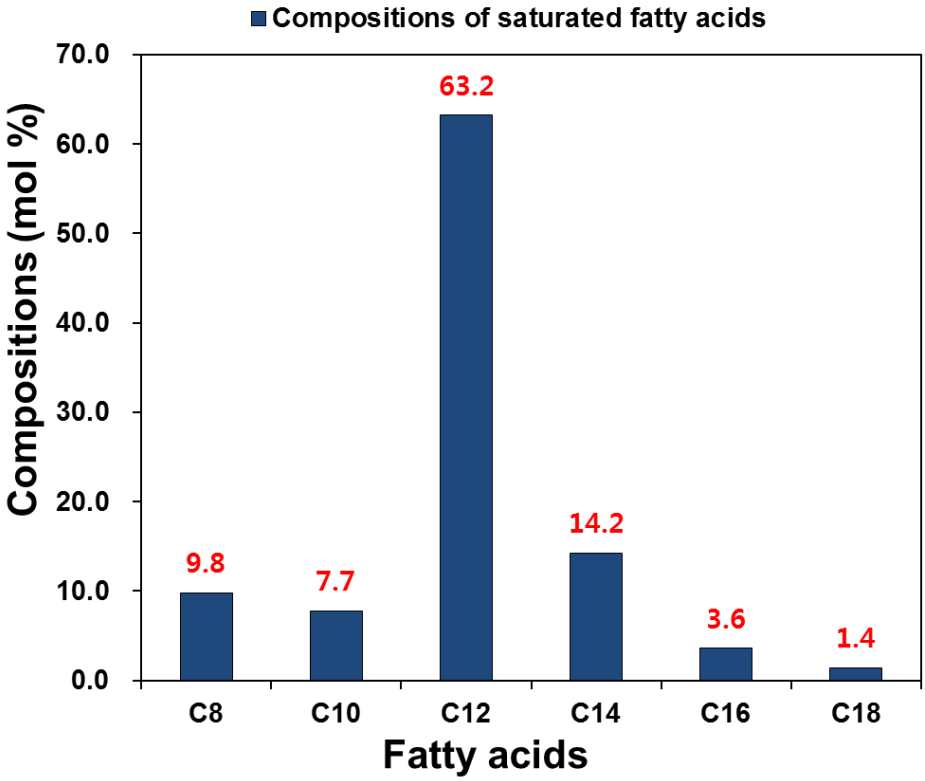

Fig. S10. Composition of the saturated fatty acids in standard cocinic acid quantified by GC-FID, unsaturated C18 fatty acid : < 3 mol %.

3.0 Identification of Chemicals

2-dodecanoylfuran (furyl-2-dodecyl-ketone)

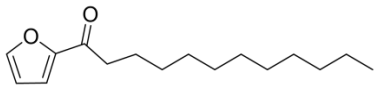

^{1}H-NMR (400 MHz, $CDCl_3$) δ 0.86-0.90 (t, 3H), 1.25 (brm, 16H), 1.67-1.75 (m, 2H), 2.80-2.84 (t, 2H), 6.53-6.54 (q, 1H), 7.20-7.21 (q, 1H), 7.58-7.59 (q, 1H) ppm.

^{13}C-NMR (100 MHz, $CDCl_3$) δ 14.11, 22.68, 24.50, 29.32, 29.37, 29.46, 29.60, 31.90, 38.52, 112.27, 117.49, 146.55, 152.69, 190.68 ppm.

GCMS (EI) m/z (relative intensity): 151 (3.4), 123 (20.1), 111 (10.9), 110 (99.9), 95 (31.6), 81 (2.6), 55 (5.5), 43 (4.4), 41 (6.2), 39 (3.6)

2-tetradecanoylfuran (furyl-2-tetradecyl-ketone)

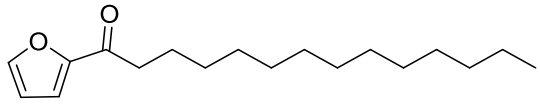

^{1}H-NMR (400 MHz, $CDCl_3$) δ 0.86-0.89 (t, 3H), 1.25 (brm, 20H), 1.67-1.75 (m, 2H), 2.78-2.82 (t, 3H), 6.51-6.52 (q, 1H), 7.16-7.17 (q, 1H), 7.56-7.57 (q, 1H)

^{13}C-NMR (100 MHz, $CDCl_3$) δ14.11, 22.69, 24.36, 29.34, 29.40, 29.48, 29.61, 29.65, 29.67, 31.92, 38.54, 112.08, 116.75, 146.13, 152.89, 189.87 ppm

GCMS (CI) m/z (relative intensity): 279.2 (100), 43.0 (26.8), 278.4 (19.5), 110.0 (19.5), 280.2 (18.4), 277.5 (13), 135.1 (6.2), 166.1 (4.4), 95.0 (4.4), 123.0 (3.8)

2-octadecanoylfuran (furyl-2-octadecyl-ketone)

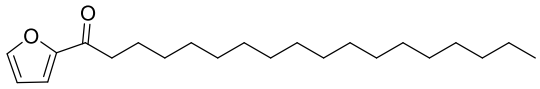

^{1}H-NMR (400 MHz, $CDCl_3$) δ 0.86-0.90 (t, 3H), 1.26 (brm, 28H), 1.68-1.75 (m, 2H), 2.80-2.84 (t, 2H), 6.53-6.54 (q, 1H), 7.20-7.21 (d, 1H), 7.59 (d, 1H) ppm.

^{13}C-NMR (100 MHz, $CDCl_3$) δ 14.11, 22.69, 24.49, 29.33, 29.37, 29.47, 29.61, 29.67, 29.70, 31.93, 38.51, 112.26, 117.48, 146.54, 152.69, 190.67 ppm.

GCMS (CI) m/z (relative intensity): 335.3 (100), 43 (46.8), 334.6 (29.4), 336.3 (23.5), 110.0 (19.4), 333.7 (19.4), 42 (5.4), 135.1 (5.2), 123.0 (4.2)

2-n-dodecylfuran

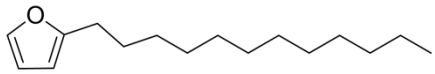

^{1}H-NMR (400 MHz, $CDCl_3$) δ 0.87-0.90 (t, 3H), 1.26 (brm, 18H), 1.60-1.67 (m, 2H), 2.59-2.63 (t, 2H), 5.96-5.97 (q, 1H), 6.27-6.28 (q, 1H), 7.29-7.30 (q, 1H) ppm.

^{13}C-NMR (100 MHz, $CDCl_3$) δ 14.12, 22.71, 27.99, 28.06, 29.21, 29.37, 29.38, 29.57, 29.65, 29.68, 31.94, 104.50, 110.02, 140.60, 156.66 ppm.

GCMS (EI) m/z (relative intensity): 236 (17.7), 123 (17.6), 96 (12.1), 95 (58.3), 94 (13.5), 82 (42.6), 81 (99.9), 53 (10.1), 43 (10.2), 41 (12.3)

2-n-tetradecylfuran

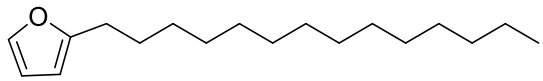

^{1}H-NMR (400 MHz, $CDCl_3$) δ 0.87-0.90 (t, 3H), 1.26 (brm, 22H), 1.60-1.67 (m, 2H), 2.59-2.63 (t, 2H), 5.96-5.97 (d, 1H), 6.27-6.28 (q, 1H), 7.29 (d, 1H) ppm.

^{13}C-NMR (100 MHz, $CDCl_3$) δ 14.13, 22.71, 28.00, 28.06, 29.21, 29.38, 29.57, 29.66, 29.68, 29.70, 29.71, 31.95, 104.50, 110.02, 140.61, 156.66 ppm.

GCMS (CI) m/z (relative intensity): 265.2 (82.7), 43.0 (100), 81 (99.6), 95.0 (48.4), 263.5 (46), 264.5 (41), 305.4 (34.5), 307.4 (33), 345.2 (23.2), 82.1 (22.5), 266.4 (16), 123.1 (14.3), 42.1 (12), 137.2 (11.8)

2-n-octadecylfuran

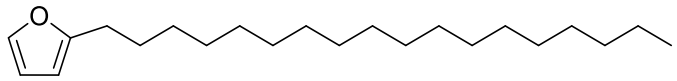

^{1}H-NMR (400 MHz, $CDCl_3$) δ 0.86-0.90 (t, 3H), 1.26 (brm, 30H), 1.59-1.66 (m, 2H), 2.59-2.63 (t, 2H), 5.96-5.97 (d, 1H), 6.26-6.27 (q, 1H), 7.28 (d, 1H) ppm.

^{13}C-NMR (100 MHz, $CDCl_3$) δ 14.13, 22.71, 27.99, 28.05, 29.21, 29.39, 29.50, 29.57, 29.66, 29.68, 29.72, 31.95, 104.49, 110.01, 140.61, 156.66 ppm.

GCMS (CI) m/z (relative intensity): 321.4 (22.6), 43.0 (100), 81.0 (61.7), 95.0 (55.6), 82.0 (29.2), 320.4 (21.8), 319.4 (17.9), 123.0 (11.7), 83.0 (11.3), 42.0 (11), 96.0 (10), 97.1 (10), 109.0 (9.2)

Mono ethyl branched 2-n-dodecylfuran (Mixture with 60 % of 2-n-dodecylfuran)

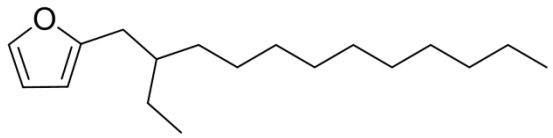

^{1}H-NMR (400 MHz, $CDCl_3$) δ 0.86-0.90 (t, 3H), 0.87-0.91 (t,3H), 1.26 (brm, 18H), 1.59-1.67 (q, 2H), 2.55-2.56 (d, 2H), 2.59-2.63 (t, 1H) 5.96-5.97 (t, 1H), 6.27-6.28 (q, 1H), 7.29-7.30 (q, 1H) ppm.

^{13}C-NMR (100 MHz, $CDCl_3$) δ 10.86, 14.13, 22.71, 25.92, 26.66, 28.00, 28.06, 29.21, 29.38, 29.58, 29.67, 29.69, 29.99, 31.94, 32.02, 33.06, 38.75, 105.73, 110.00, 140.64, 155.65 ppm

GCMS (EI) m/z (relative intensity): 264 (7.7), 235 (8.0), 123 (25.6), 82 (99.9), 81 (65.8), 71 (36.3), 57 (56.8), 43 (38.7), 41 (23.7), 28 (91.9).

OFS-7 (Sodium 5-heptylfuran-2-sulfonate)

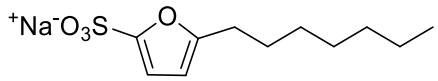

^{1}H-NMR (400 MHz, DMSO-d_6) δ 0.84-0.88 (t, 3H), 1.26-1.28 (brm, 8H), 1.52-1.59 (m, 2H), 2.54-2.57 (t, 2H), 5.98-5.99 (d, 1H), 6.26-6.27 (d, 1H) ppm.

^{13}C-NMR (100 MHz, DMSO-d_6) δ 13.95, 22.08, 27.41, 27.55, 28.41, 28.54, 31.21, 105.07, 108.32, 155.15, 155.43 ppm.

OFS-12 (Sodium 5-dodecylfuran-2-sulfonate)

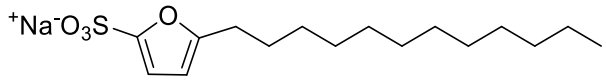

^{1}H-NMR (400 MHz, DMSO-d_6) δ 0.84-0.87 (t, 3H), 1.24 (brm, 22H), 1.53-1.59 (m, 2H), 2.53-2.57 (t, 2H), 5.96-5.97 (d, 1H), 6.23-6.24 (d, 1H) ppm.

^{13}C-NMR (100 MHz, DMSO-d_6) δ 13.95, 22.09, 27.39, 27.54, 28.58, 28.70, 28.74, 28.97, 29.00, 29.03, 31.28, 104.98, 108.09, 154.98, 155.69 ppm.

OFS-14 (Sodium 5-tetradecylfuran-2-sulfonate)

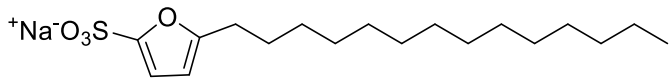

^{1}H-NMR (400 MHz, DMSO-d_6) δ 0.84-0.87 (t, 3H), 1.24 (brm, 22H), 1.52-1.59 (m, 2H), 2.53-2.57 (t, 2H), 5.96-5.97 (d, 1H), 6.24 (d, 1H) ppm.

^{13}C-NMR (100 MHz, DMSO-d_6) δ 13.96, 22.10, 27.40, 27.55, 28.59, 28.71, 28.76, 28.99, 29.01, 29.05, 31.30, 105.00, 108.15, 155.03, 155.63 ppm.

4.0 Evaluation of the Surfactants

Evaluation of surfactant performance was carried out by analyzing properties of surfactants in solution such as critical micelle concentration (CMC), Krafft point, 'foaminess', wettability (Draves index) and hard water stability (hardness tolerance).

4.1 Critical Micelle Concentration (CMC)

CMC is an important property of a surfactant and is the concentration above which the surfactant forms micelles and any additional surfactant added to the solution will also form micelles.[10] The value of CMC of the surfactant was measured by recording the decrease in surface tension with increasing surfactant concentration. 6-8 samples with increasing surfactant concentration were prepared by dissolving the required amount of surfactant in deionized water. The solution temperature was kept high enough to ensure that all of the surfactant is in solution i.e. the solution temperature was kept above the Krafft point of the surfactant. Surface tension measurements were made using the Krüss digital tensiometer K10ST via the Wilhelmy plate method. The temperature of the solution was monitored during the course of measurement. The surface tension of each concentration was measured three times and CMC was reported as the value of concentration corresponding to the point of intersection of two straight lines drawn to fit the plot of surface tension vs. ln(surfactant concentration).

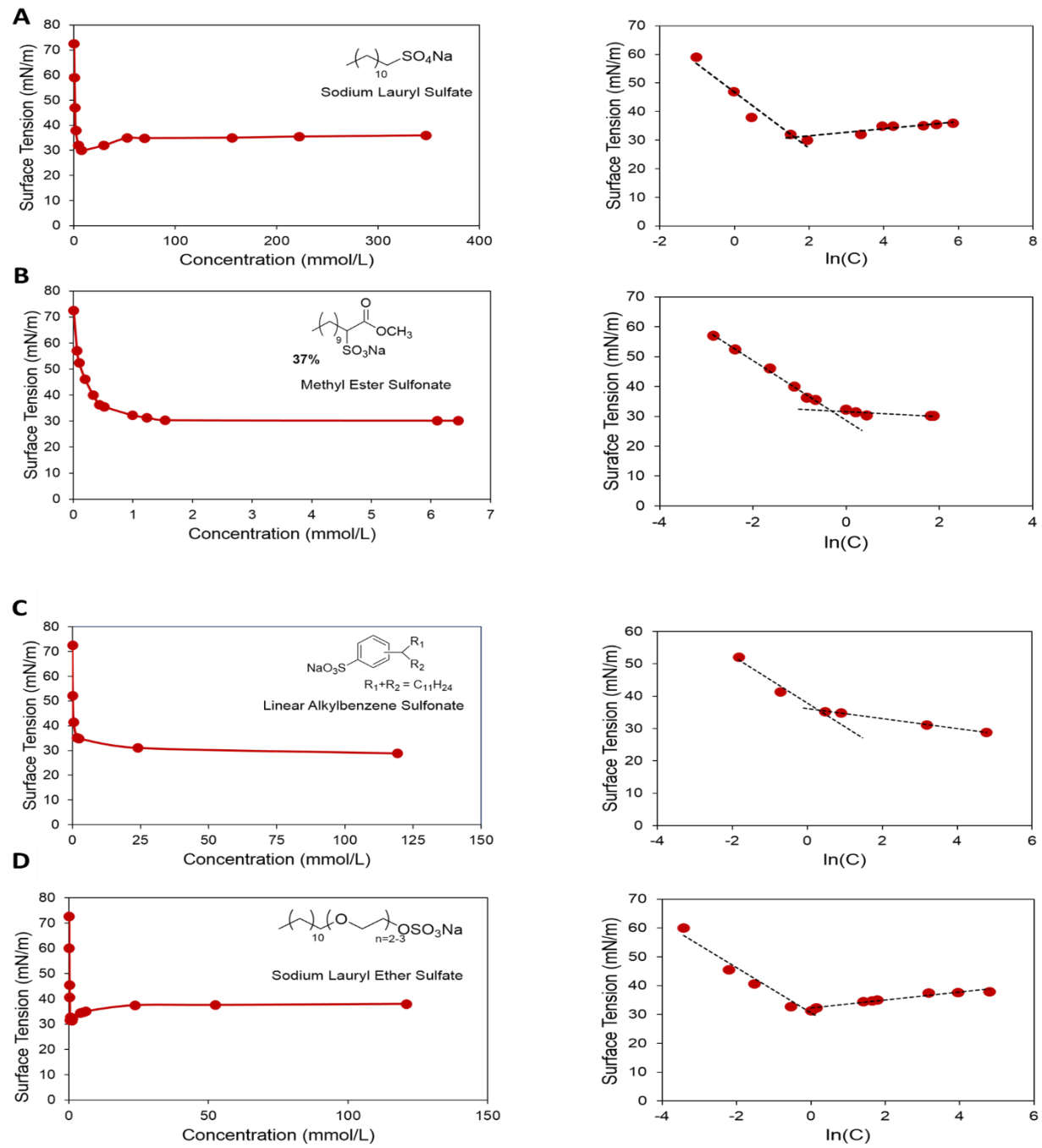

Fig. S11. Surface tension versus surfactant concentration of commercial surfactants: **A.** Sodium Lauryl Sulfate (SLS), **B.** Methyl Ester Sulfonate (MES), **C.** Linear Alkylbenzene Sulfonate (LAS) and, **D.** Sodium Lauryl Ether Sulfate (SLES). The point of intersection of the two dashed lines in the surface tension vs ln(C) plot yields the value of CMC.

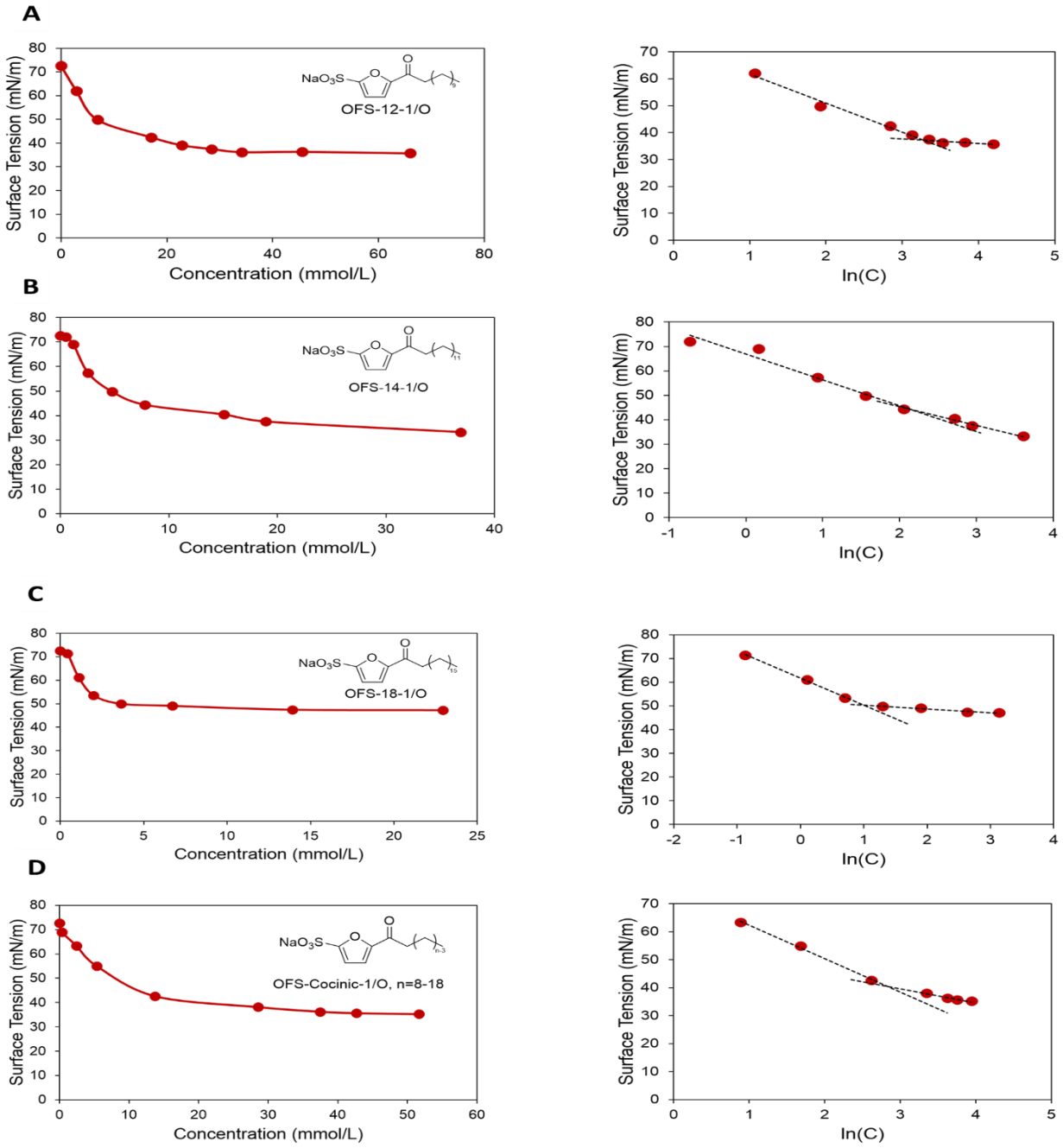

Fig. S12. Surface tension versus surfactant concentration of renewable OFS-n-1/O surfactants: **A.** OFS-12-1/O, **B.** OFS-14-1/O, **C.** OFS-18-1/O and, **D.** OFS-Cocinic-1/O, n = 8-18. The point of intersection of the two dashed lines in the surface tension vs ln(C) plot yields the value of CMC.

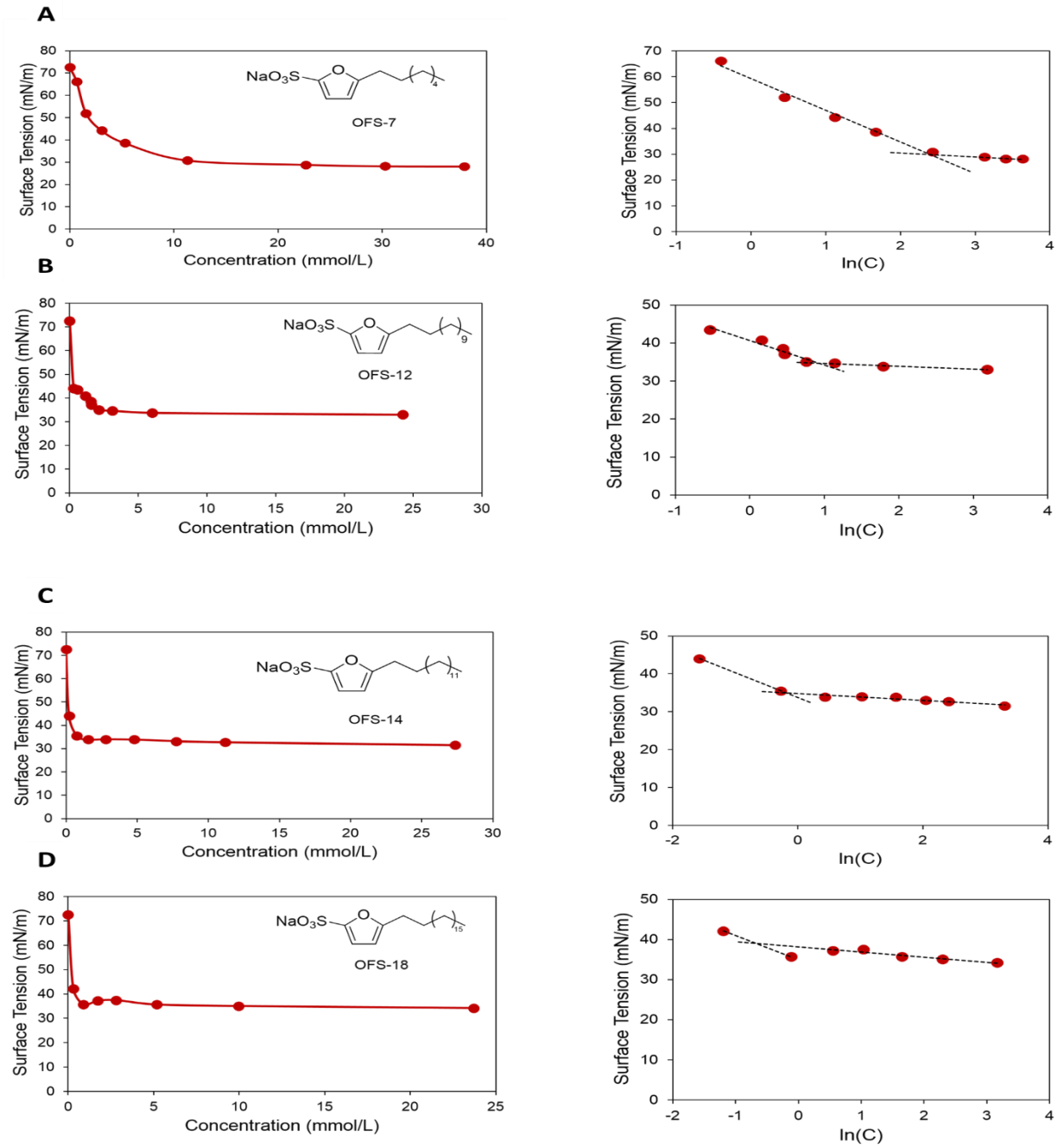

Fig. S13A-D. Surface tension versus surfactant concentration of renewable OFS-n surfactants: **A.** OFS-7, **B.** OFS-12, **C.** OFS-14, **D.** OFS-18, **E.** OFS-Cocinic, n = 8-18, **F.** 40:60 mol% OFS-12-2/C2H5:OFS-12 and, **G.** 85:15 mol% OFS-12-1/O:OFS-12. The point of intersection of the two dashed lines in the surface tension vs ln(C) plot yields the value of CMC.

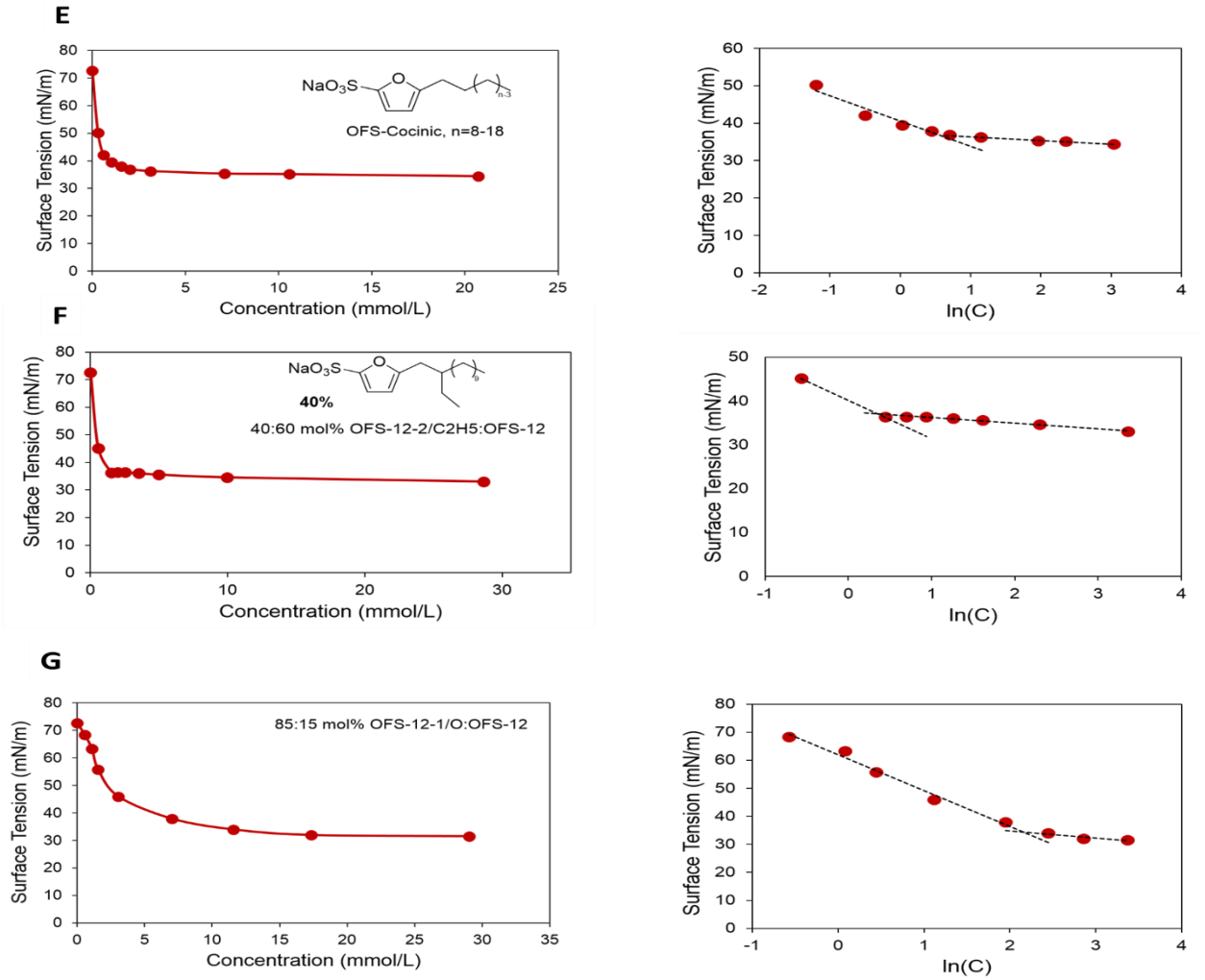

Fig. S13E-G. Surface tension versus surfactant concentration of renewable OFS-n surfactants: **A.** OFS-7, **B.** OFS-12, **C.** OFS-14, **D.** OFS-18, **E.** OFS-Cocinic, n = 8-18, **F.** 40:60 mol% OFS-12-2/C2H5:OFS-12 and, **G.** 85:15 mol% OFS-12-1/O:OFS-12. The point of intersection of the two dashed lines in the surface tension vs ln(C) plot yields the value of CMC.

Table S6. Summary of CMC values for all surfactants in ppm and mmol/L (mM).

	CMC[a]	
Surfactant	[ppm]	mmol/L
Commercial		
SLS, Sodium Lauryl Sulfate	2010	6.97
MES, Methyl Ester Sulfonate	130	0.41
LAS, Linear Alkylbenzene Sulfonate	460	1.33
SLES, Sodium Lauryl Ether Sulfate	380	1.01
OFS, Oleo-Furan Sulfonates		
OFS-12-1/O	11520	33.11
OFS-14-1/O	3127	8.26
OFS-18-1/O	1156	2.65
OFS-Cocinic-1/O	4890	14.01
OFS-7	2669	9.99
OFS-12	720	2.13
OFS-14	267	0.72
OFS-18	316	0.75
OFS-Cocinic	512	1.51
40:60 mol% OFS-12-2/C2H5:OFS-12	496	1.43
85:15 mol% OFS-12-1/O:OFS-12	2445	7.01

[a]Critical Micelle Concentration, measured above Krafft point

4.2 Krafft Point/Temperature

Krafft point or Krafft temperature is the minimum temperature at which surfactants form micelles. Below Krafft point, the surfactants precipitate out of solution and remain in the crystalline phase.[10] A 1.0 wt% solution of surfactant in deionized water was prepared for all surfactants except in the case of OFS-12-1/O where a 2.0 wt% solution was used instead, since its CMC is roughly about 1.1 wt%. 50 mL of the prepared solution was poured into a beaker surrounded by a freezing mixture of ice and salt (sodium chloride) mounted on a laboratory hot plate with magnetic stirring. The Krafft point (T_K) of the surfactants was measured by estimating the degree of counterion dissociation using a conductivity meter (COND 6+, Oakton/Eutech Instruments) immersed in the surfactant solution capable of measuring both, conductivity and temperature. The magnetic stirring speed was set to 650 rpm and the solution was first allowed to cool to 0 ºC. Upon attainment of this temperature, the solution was slowly heated and the conductivity was measured in every 0.5 ºC increments until it reached a steady value. The Krafft point was taken as the temperature where the conductivity vs. temperature plot exhibited a sharp change in slope. Visually, this corresponded to the surfactant solution transitioning from a turbid system due to the precipitated surfactant crystals below the Krafft point to a clear solution indicating the dissolution of surfactants and the formation of micelles in water.

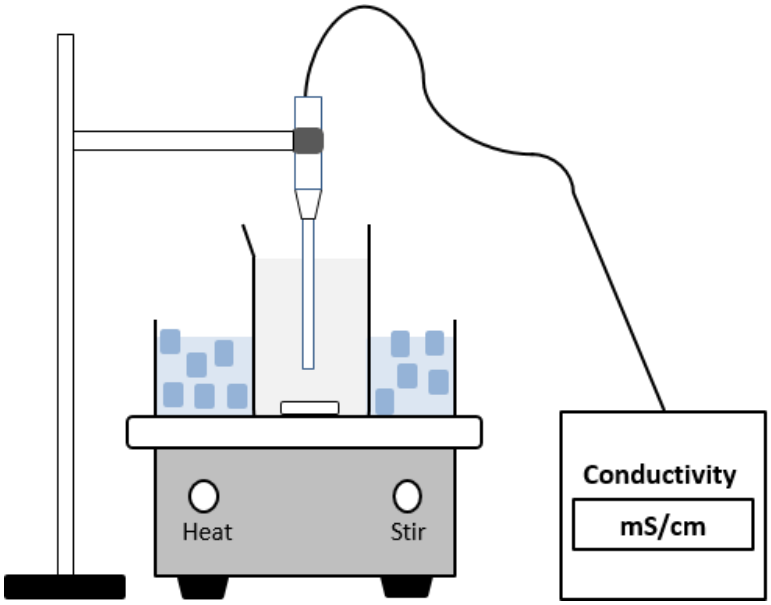

Fig. S14. Schematic of apparatus used for measurement of Krafft point

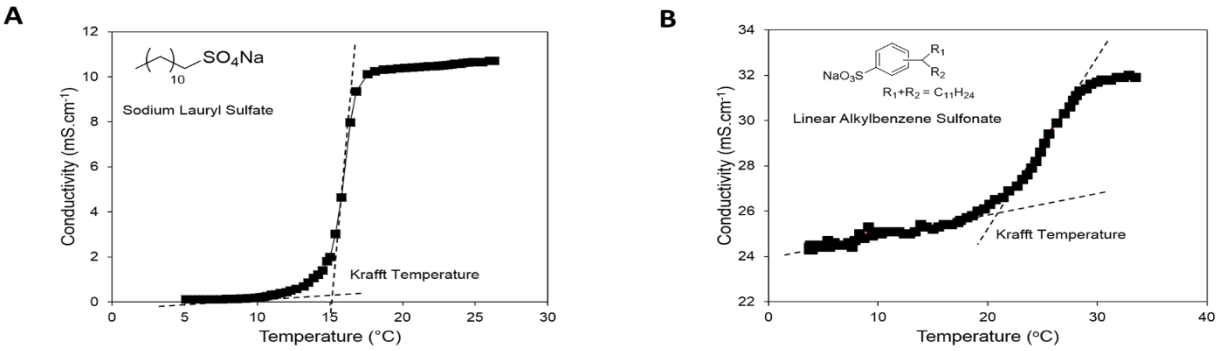

Fig. S15. Conductivity versus temperature of 1.0 wt% commercial surfactant solutions for determination of Krafft point: **A.** Sodium Lauryl Sulfate (SLS) and, **B.** Linear Alkylbenzene Sulfonate (LAS).

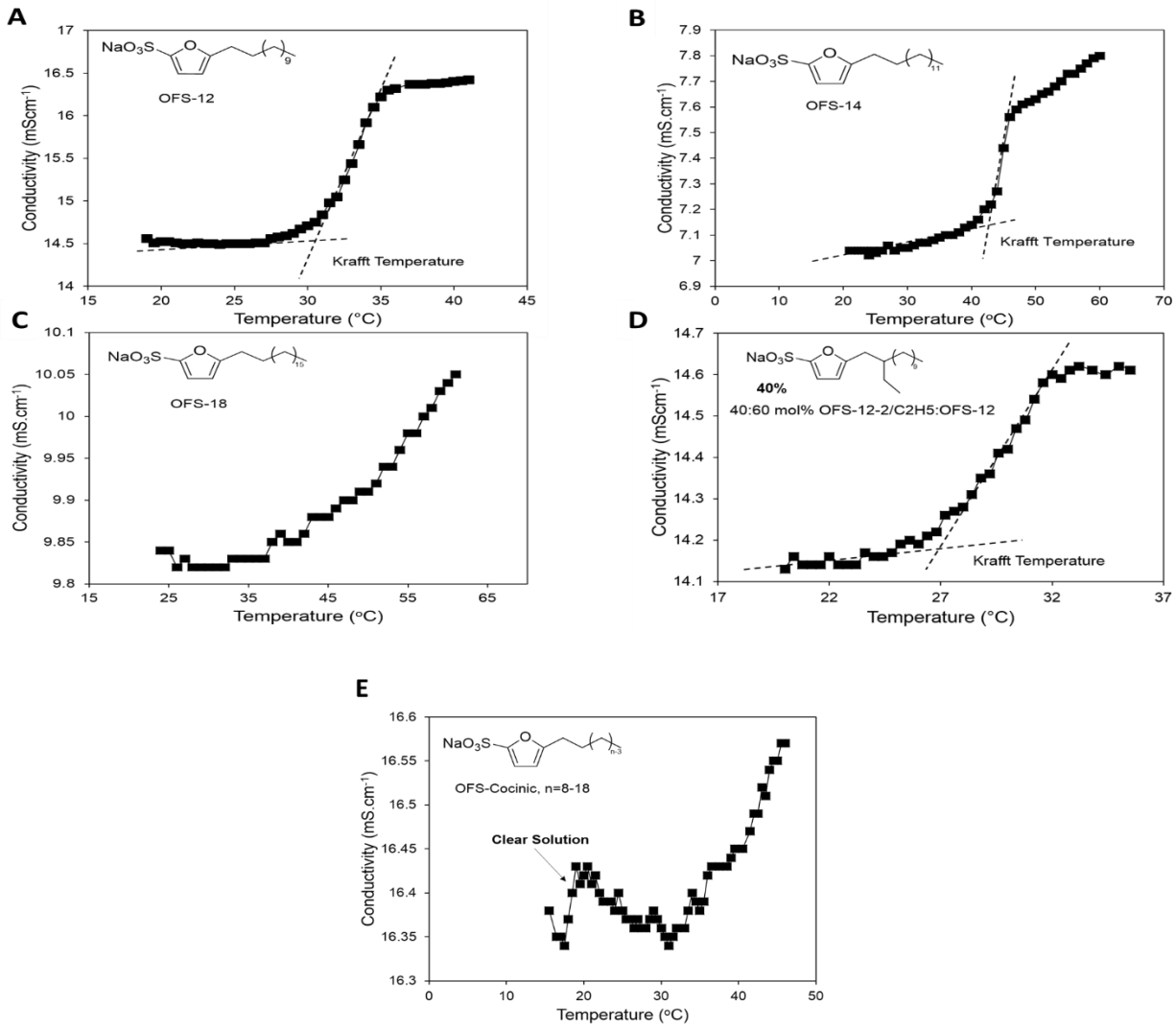

Fig. S16. Conductivity vs temperature of 1.0 wt% renewable OFS-n surfactant solutions for determination of Krafft point: **A.** OFS-12, **B.** OFS-14, **C.** OFS-18, **D.** 40:60 mol% OFS-12-2/C2H5:OFS-12 and, **E.** OFS-Cocinic, n = 8-18.

In the case of OFS-18, maximum temperature operation limits of the conductivity probe did not allow the estimation of Krafft point, and thus the value is reported as >50 ºC. For the OFS-Cocinic, n = 8-18 surfactant, the conductivity vs temperature plot was erratic, which is attributed to the presence of 6 different surfactants in the mixture. The solution changed from turbid to clear at approximately 18.5 ºC which was, therefore, reported as the Krafft point. Methyl Ester Sulfonate (MES), Sodium Lauryl Ether Sulfate (SLES), OFS-7 and all OFS-n-1/O surfactant solutions remained clear even at 0 ºC; the Krafft point was thus reported as <0 ºC.

Table S7. Summary of Krafft points for all surfactants.

Surfactant	Krafft Point[a] [°C]
Commercial	
SLS, Sodium Lauryl Sulfate	15.0 ± 1.2
MES, Methyl Ester Sulfonate	< 0
LAS, Linear Alkylbenzene Sulfonate	20.0 ± 2.5
SLES, Sodium Lauryl Ether Sulfate	< 0
OFS, Oleo-Furan Sulfonates	
OFS-12-1/O	< 0
OFS-14-1/O	< 0
OFS-18-1/O	< 0
OFS-Cocinic-1/O	< 0
OFS-7	< 0
OFS-12	30.0 ± 1.0
OFS-14	41.5± 0.9
OFS-18	> 50
OFS-Cocinic	18.5 ± 0.5
40:60 mol% OFS-12-2/C2H5:OFS-12	25.7 ± 0.5
85:15 mol% OFS-12-1/O:OFS-12	< 0

[a]Measured at 1.0 wt% surfactant in water except for OFS-12-1/O

4.3 Surfactant Foaming

The foaming properties of the surfactants were studied by bubbling air through a 0.5 wt% surfactant solution in 100 mL of deionized water. The surfactant solution was poured into a 500 mL glass graduated cylinder. Air was bubbled through a 1/8 inch diameter and 16 inch length SS 316 tubing, which was immersed in the solution. A clearance of 1 inch was maintained between the end of the tubing and the bottom of the cylinder. The air flow rate was maintained at 30 sccm using a Brooks 5850E mass flow controller. The cylinder was mounted on a laboratory hot plate with magnetic stirring. A magnetic stirrer rotating at 380 rpm was also used to ensure uniform distribution of bubbles. All measurements were done above the Krafft point of the surfactant solutions. For those surfactants with a Krafft point above room temperature (OFS-12, OFS-14), the graduated cylinder was surrounded by a heated sand bath mounted on the hot plate. The temperature of the sand bath was set such that the solution temperature is just above its Krafft point. Air was bubbled through the solution until the foam height reached a steady value and the height was recorded every thirty seconds by means of a camera. The initial rate of foam growth was measured by calculating the slope of the linear region of the height vs. time plot before it attained equilibrium. The height of the foam column is indicative of the foaming capacity of the surfactant; the foam height after 60 min of air bubbling was, thus, used as a parameter to report foaming capacity. All surfactant foam heights reached an equilibrium value within 60 min with sodium lauryl ether sulfate (SLES) being an exception. For the purpose of comparison, Sodium Lauryl Sulfate (SLS) was chosen as a 'reference' surfactant and the initial foam growth rates and 60 min foam heights of all other surfactants were normalized with respect to SLS i.e. foam growth rate metric is reported as ratio of slope of linear region of surfactant *i* to that of SLS (r_i/r_{SLS}) and the foam height metric is reported as the ratio of foam height of surfactant *i* after 60 min (3600 s) to that of SLS ($h_{i\text{-}60}/h_{i\text{-}SLS}$) as shown in Table S8.

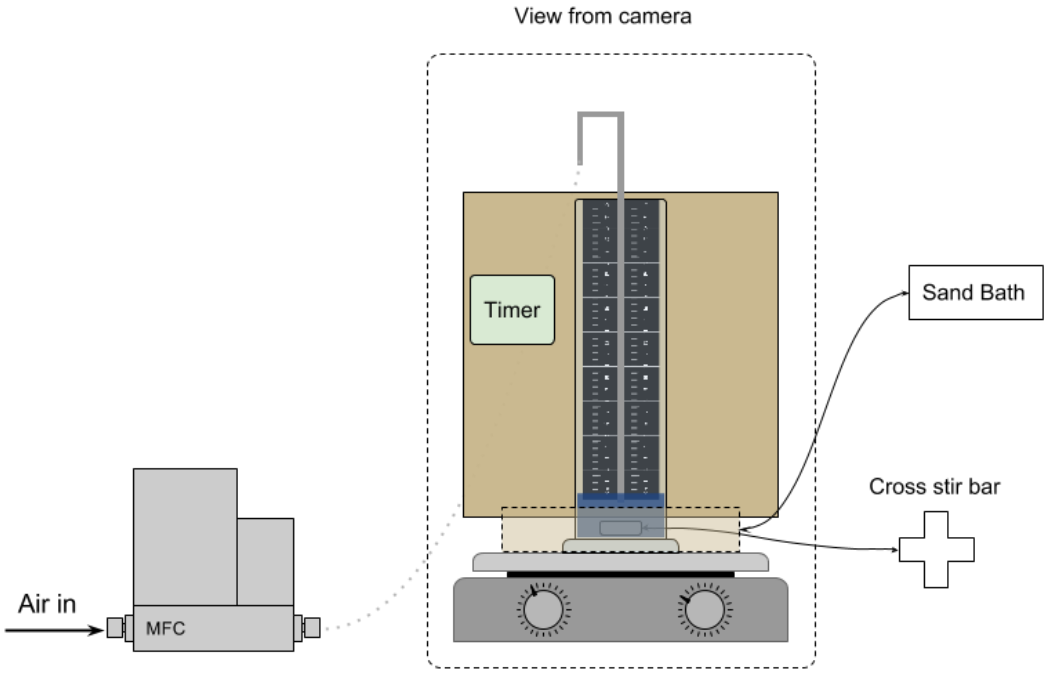

Fig. S17. Schematic of foaming apparatus and set-up.

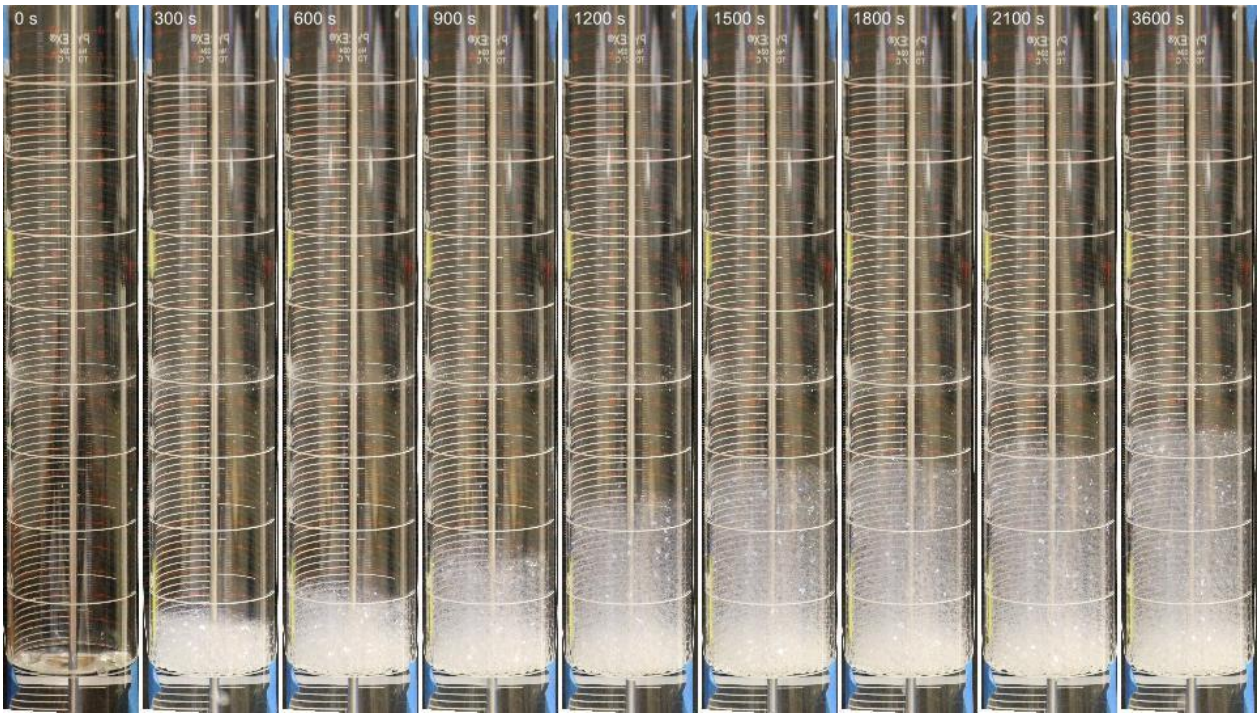

Fig. S18. Foam growth of 0.5 wt% solution of Sodium Lauryl Sulfate (SLS) for increasing times (left to right) up to 1 h (times in seconds are indicated on upper left insets)

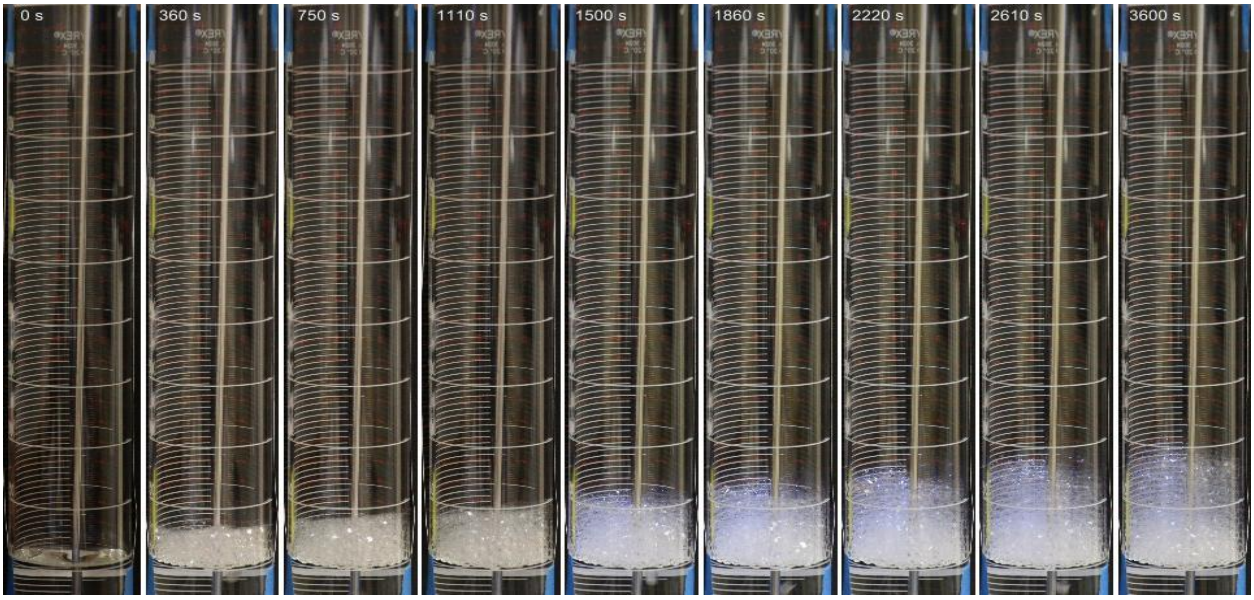

Fig. S19. Foam growth of 0.5 wt% solution of Methyl Ester Sulfonate (MES) for increasing times (left to right) up to 1 h (times in seconds are indicated on upper left insets)

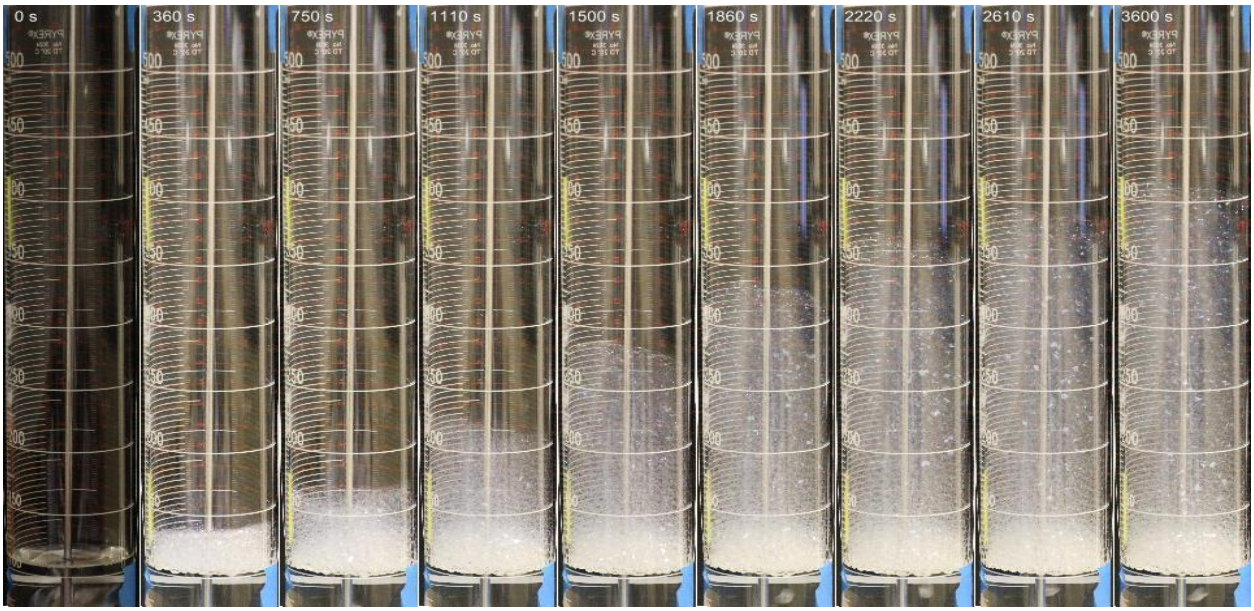

Fig. S20. Foam growth of 0.5 wt% solution of Linear Alkylbenzene Sulfonate (LAS) for increasing times (left to right) up to 1 h (times in seconds are indicated on upper left insets).

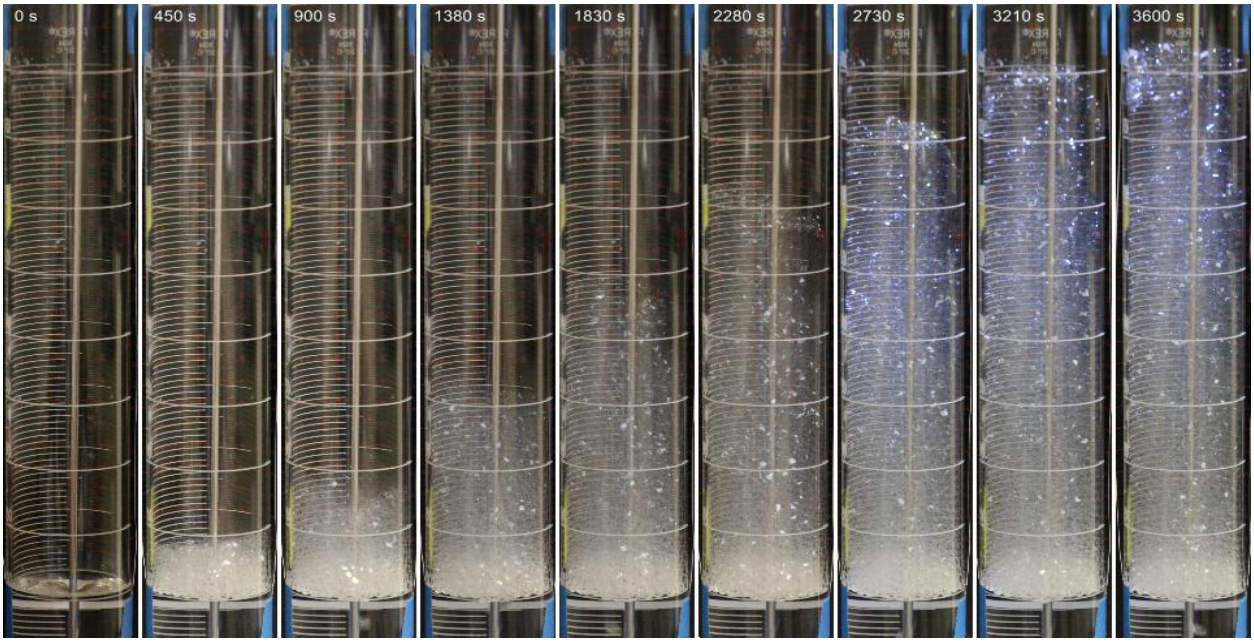

Fig. S21. Foam growth of 0.5 wt% solution of Sodium Lauryl Ether Sulfate (SLES) for increasing times (left to right) up to 1 h (times in seconds are indicated on upper left insets)

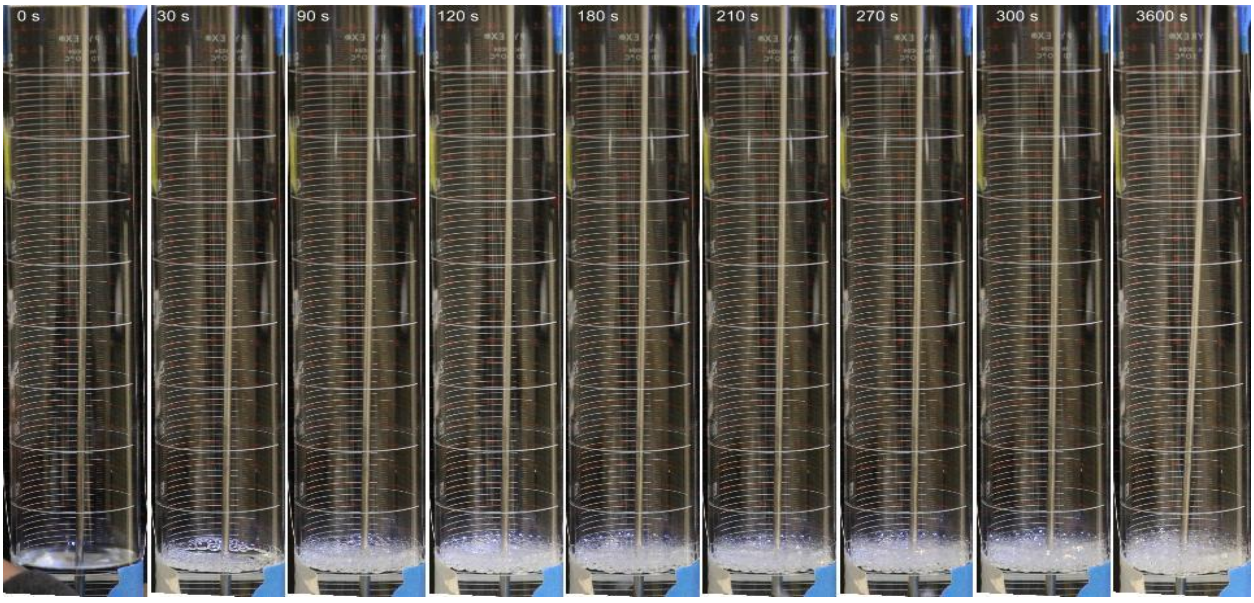

Fig. S22. Foam growth of 0.5 wt% solution of OFS-7 for increasing times (left to right) up to 1 h (times in seconds are indicated on upper left insets)

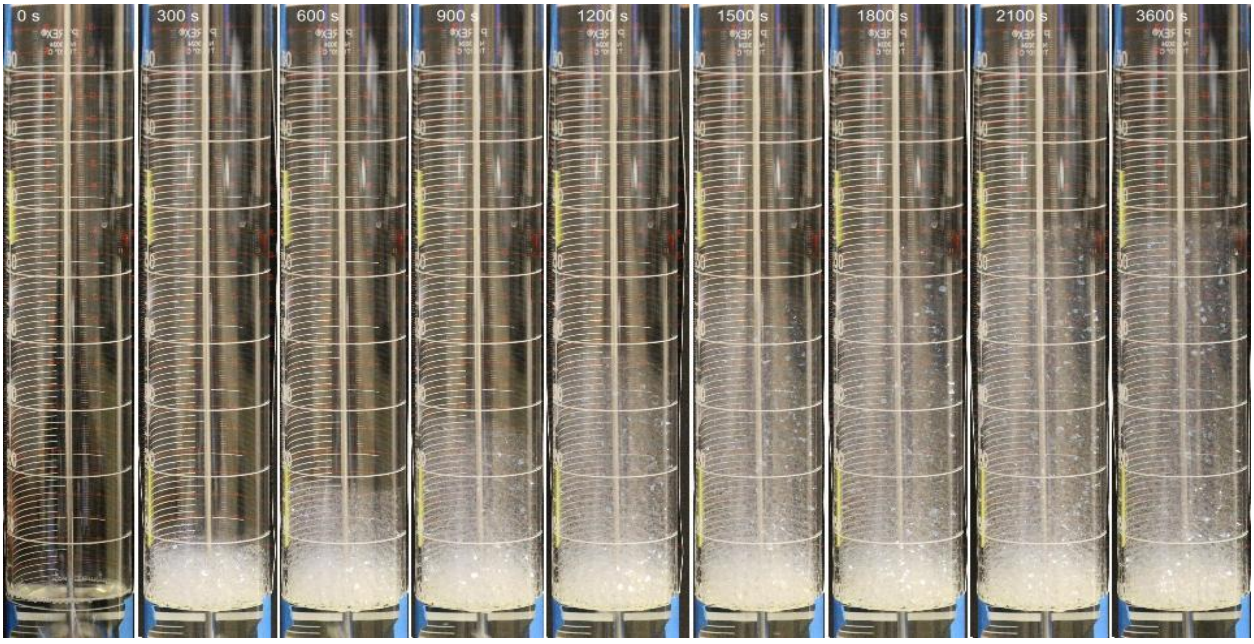

Fig. S23. Foam growth of 0.5 wt% solution of OFS-12 for increasing times (left to right) up to 1 h (times in seconds are indicated on upper left insets)

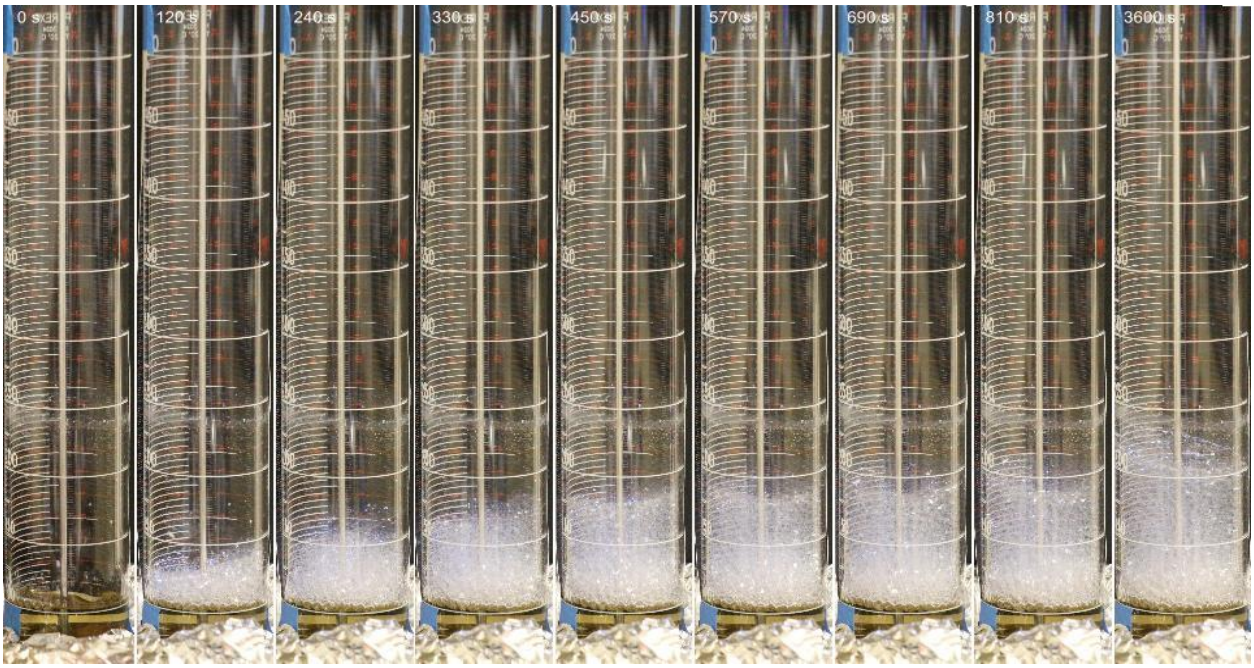

Fig. S24. Foam growth of 0.5 wt% solution of OFS-14 for increasing times (left to right) up to 1 h (times in seconds are indicated on upper left insets)

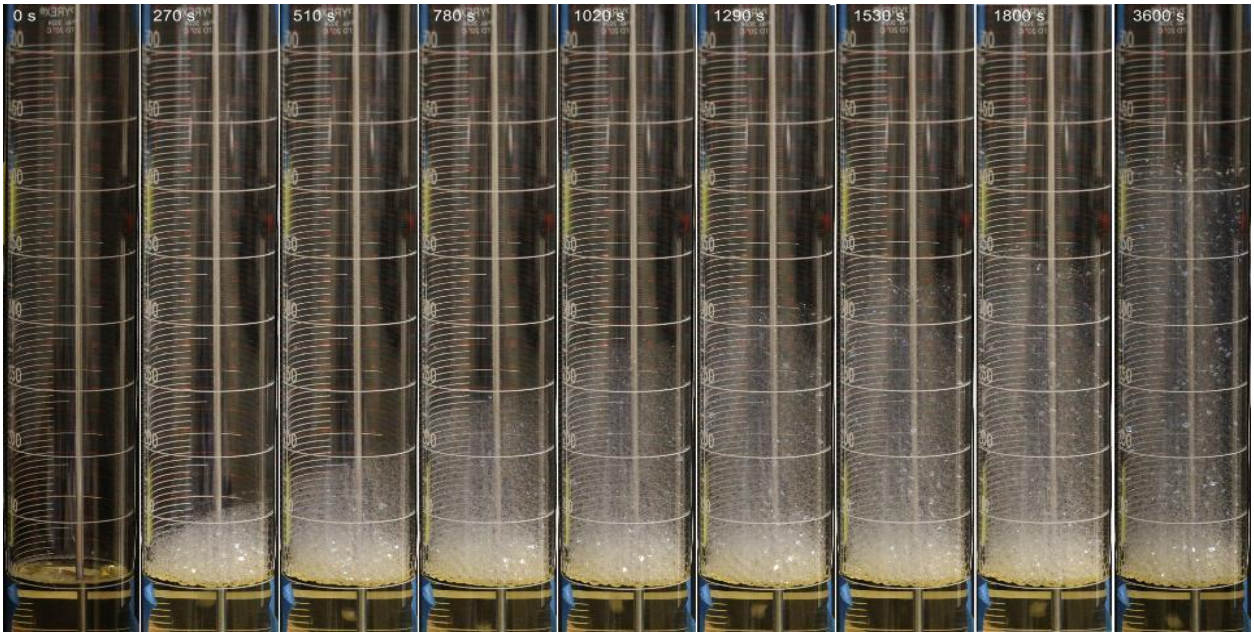

Fig. S25. Foam growth of 0.5 wt% solution of OFS-Cocinic-n=8-18 for increasing times (left to right) up to 1 h (times in seconds are indicated on upper left insets).

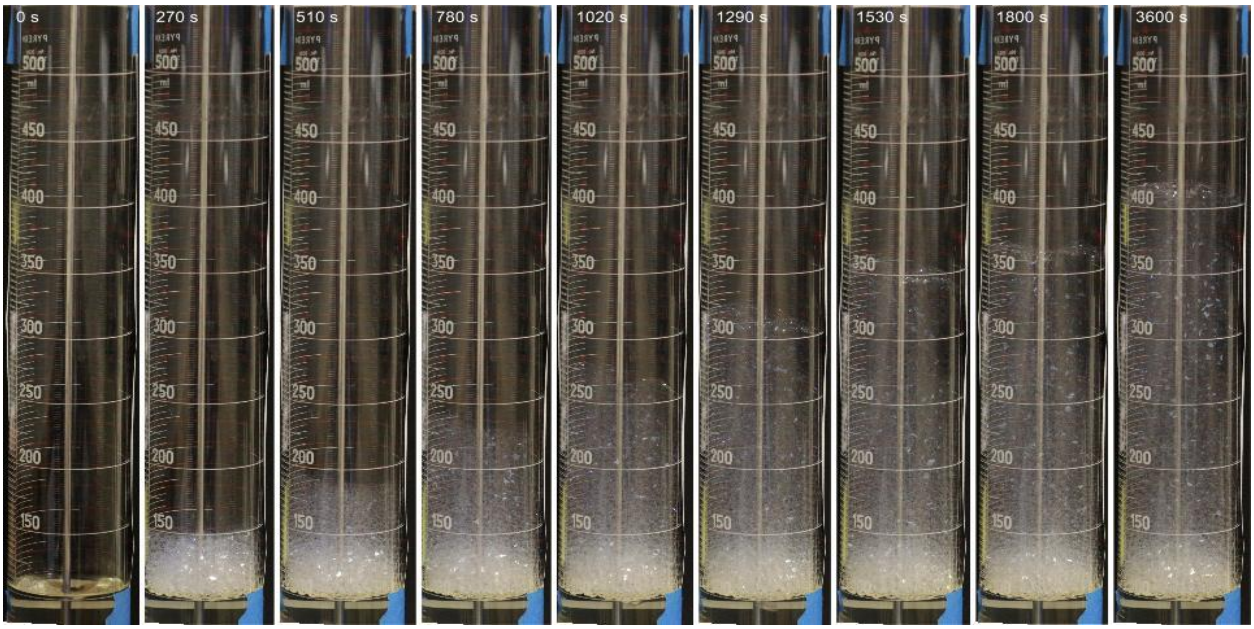

Fig. S26. Foam growth of 0.5 wt% solution of 40:60 mol% OFS-12-2/C2H5:OFS-12 for increasing times (left to right) up to 1 h (times in seconds are indicated on upper left insets).

Fig. S27. Foam growth of 0.5 wt% solution of OFS-18-1/O for increasing times (left to right) up to 1 h (times in seconds are indicated on upper left insets).

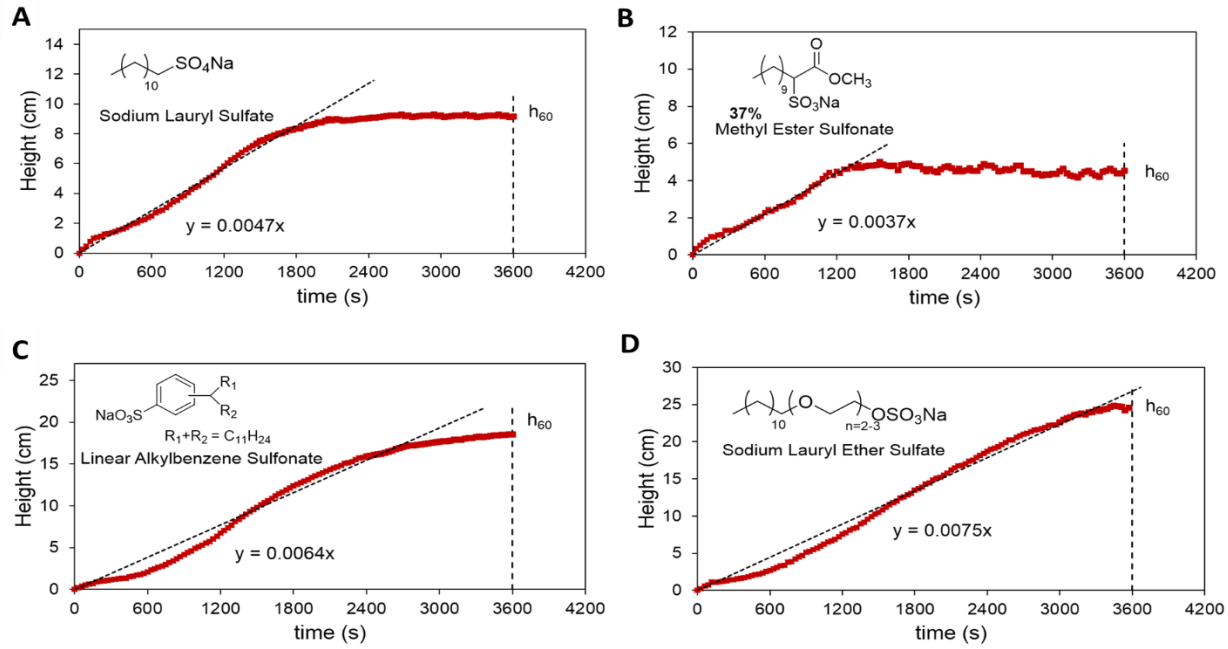

Fig. S28. Foam height vs. time of 0.5 wt% commercial surfactant solutions: **A.** Sodium Lauryl Sulfate (SLS), **B.** Methyl Ester Sulfonate (MES), **C.** Linear Alkylbenzene Sulfonate (LAS) and, **D.** Sodium Lauryl Ether Sulfate (SLES). The slope of the linear region (dashed line) represents the initial foam growth rate (r) while the height of the foam column (h_{60}), after 60 min (3600s), is used as a foaming capacity indicator.

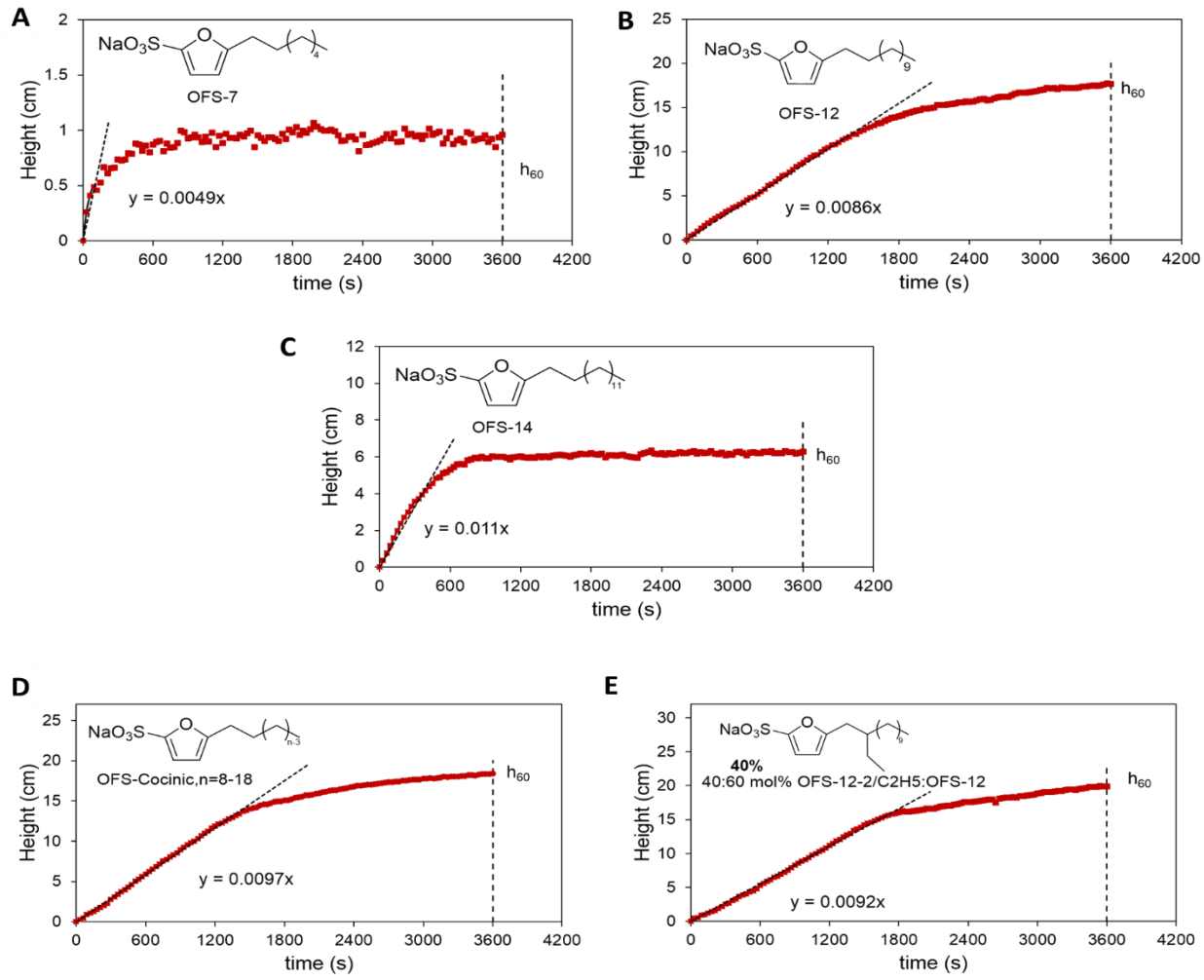

Fig. S29. Foam height versus time of 0.5 wt% renewable OFS-n surfactant solutions: **A.** OFS-7, **B.** OFS-12, **C.** OFS-14, **D.** OFS-Cocinic, n = 8-18 and, **E.** 40:60 mol% OFS-12-2/C2H5:OFS-12. The slope of the initial linear region represents the initial foam growth rate (r) while the height of the foam column (h_{60}), after 60 min (3600s), is used as a foaming capacity indicator.

Table S8. Summary of foaming parameters of all surfactants; normalized initial growth rates and foam heights after 60 min with respect to SLS.

Surfactant	Foam Growth Rate[a] r_i / r_{SLS} [-]	Foam Height$_{60}$[a,b] $h_{i\text{-}60} / h_{i\text{-}SLS}$ [-]
Commercial		
SLS, Sodium Lauryl Sulfate	1.00	1.00
MES, Methyl Ester Sulfonate	0.79	0.54
LAS, Linear Alkylbenzene sulfonate	1.36	2.20
SLES, Sodium Lauryl Ether Sulfate	1.60	2.94
OFS, Oleo-Furan Sulfonates		
OFS-12-1/O	0	0
OFS-14-1/O	0	0
OFS-18-1/O	0	0
OFS-Cocinic-1/O	0	0
OFS-7	1.04	0.12
OFS-12	1.83	2.11
OFS-14	2.34	0.75
OFS-18	-	-
OFS-Cocinic	2.06	2.19
40:60 mol% OFS-12-2/C2H5:OFS-12	1.96	2.37
85:15 mol% OFS-12-1/O:OFS-12	-	-

[a]Measured at 0.5 wt% in water. [b]After 60 min (3600 s).

4.4 Draves Wetting Index

The wettability or the wetting properties of the surfactant were measured according to the ASTM D2281 standard.[10,11] 500 mL of 0.25 wt% surfactant solution was poured slowly into a 500 mL graduated cylinder to ensure that no foam was created while pouring. Any foam that was created was removed using a bulb-pipet. The temperature of the surfactant solution was maintained around its Krafft point by employing a heated sand bath throughout the course of the experiment.

A cotton skein (Test Fabrics, Item# 1203007), weighing approximately 5g, was folded and fastened to an S-shaped 3 g copper hook tied to a 40 g lead anchor (lead slug) using a fine linen thread ¾ inch long (Test Fabrics, Item# WEIGHT & HOOK). The ends of the skein were cut at the opposite end and the skein was made compact by drawing the cut skein through fingers before testing the surfactant. It was then dropped into the graduated cylinder containing the solution and the time taken for the thread to relax and the skein to sink to bottom was recorded as the wetting time (T_D) for 0.25 wt% solution.

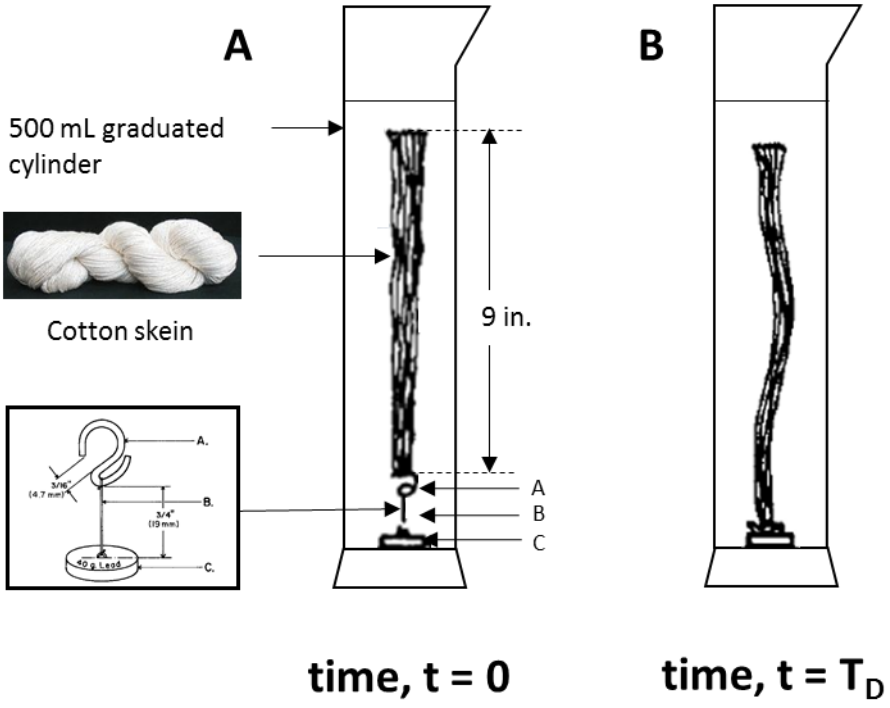

Fig. S30. Schematic of the apparatus used for the Draves test[11] **A.** The skein is just immersed into the solution at t = 0 s. **B.** The skein sinks after wetting time T_D

Table S9. Summary of Draves wetting time for all surfactants.

Surfactant	Draves Wetting[a] [s]
Commercial	
SLS, Sodium Lauryl Sulfate	6.3 ± 2.7
MES, Methyl Ester Sulfonate	15.1 ± 3.8
LAS, Linear Alkylbenzene Sulfonate	4.9 ± 3.2
SLES, Sodium Lauryl Ether Sulfate	15.4 ± 4.0
OFS, Oleo-Furan Sulfonates	
OFS-12-1/O	> 3600
OFS-14-1/O	> 3600
OFS-18-1/O	> 3600
OFS-Cocinic-1/O	> 3600
OFS-7	> 3600
OFS-12	48.9 ± 13.3
OFS-14	39.4 ± 7.0
OFS-18	-
OFS-Cocinic	58.0 ± 9.4
40:60 mol% OFS-12-2/C2H5:OFS-12	18.5 ± 1.9
85:15 mol% OFS-12-1/O:OFS-12	-

[a]Measured at 0.25 wt% surfactant in water

4.5 Hardness Tolerance

Precipitation of the anionic surfactant from hard water is an undesired process in detergency. The tendency of the anionic surfactants to precipitate is quantified by analyzing hardness tolerance. Hardness tolerance is the minimum concentration of counterion, such as, Ca^{2+} and Mg^{2+}, precipitating with surfactant, resulting in deactivation of the surfactant performance.[12-14] Calcium chloride was used as a divalent counterion, and surface tension of the surfactant solution was measured with increasing concentration of $CaCl_2$ from 1 mM to 450 mM. The value of calcium concentration above which the surface tension of the surfactant solution increased was recorded as the tolerance value of the surfactant towards calcium as indicated by the dashed red line in Fig. S32 – S35. At the tolerance value, the Ca^{2+} ions disrupt the micelle structure and this value of calcium concentration is referred to as micelle stability. All experiments were carried out at a concentration equal to twice CMC of each surfactant, and the point of transition from a clear solution to a turbid one was also monitored. Fig. S31 illustrates this effect for a linear alkylbenzene sulfonate (LAS) solution. Below the turbid point, the surfactant solution was clear as shown by insets A and B in Fig. S31 which changed to a cloudy solution at calcium concentrations equal to and greater than the turbid point (inset C and D). The point of micelle stability was marked by an increase in the surface tension of the surfactant solution with an increase in calcium concentration. In Fig. S31, inset B corresponds to the micelle stability concentration and inset C corresponds to the turbid concentration.

For the OFS-n surfactants, a momentary turbidity was observed in the surfactant solution upon addition of $CaCl_2$ due to localized concentration gradients which disappeared upon stirring unlike the OFS-n-1/O, LAS and SLS surfactants where the turbidity/precipitation continued to persist even upon vigorous stirring.

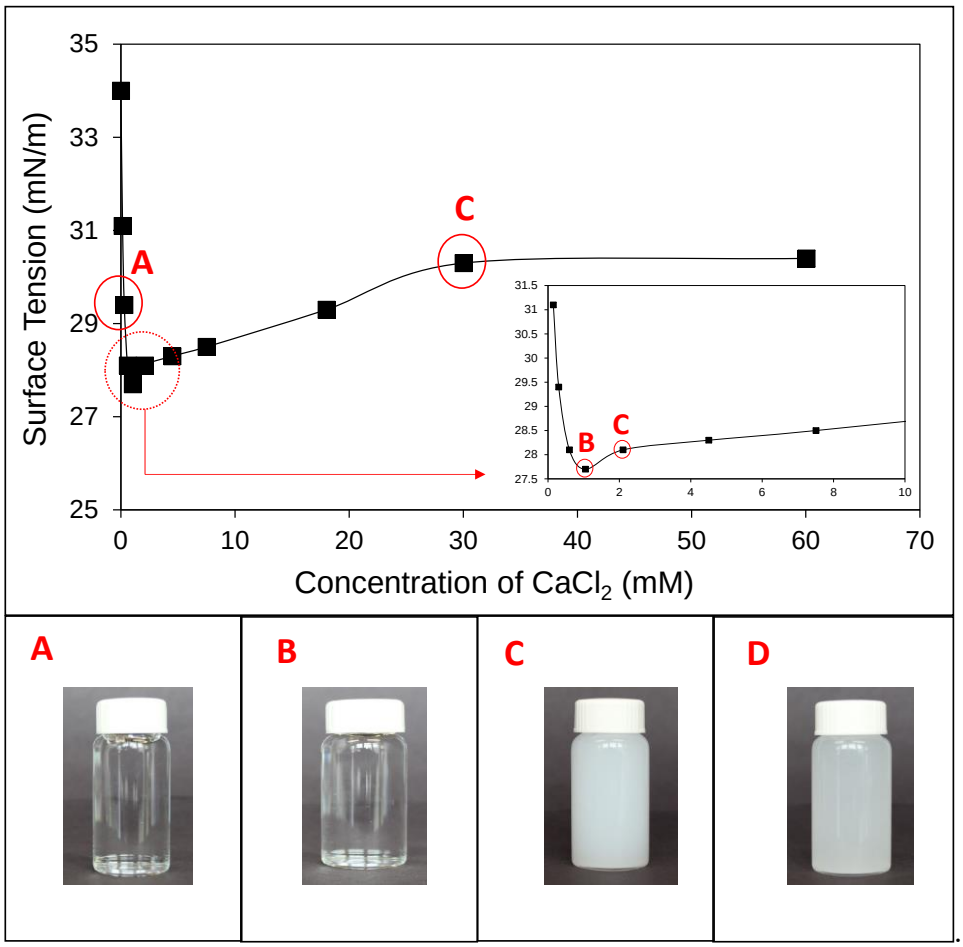

Fig. S31. Surface tension versus $CaCl_2$ concentration for LAS solution demonstrating the effect of increasing calcium concentration. (Concentration of the surfactant: twice CMC). Micelle stability is defined as the calcium concentration at the increasing point of surface tension, and turbid concentration marks the onset of turbidity in the surfactant solution The solution transitions from clear to turbid as shown in insets A-D: **A.** Clear solution at low calcium concentration (33 ppm, corresponding to soft water conditions). **B.** LAS solution at 100 ppm of Ca^{2+} corresponding to the tolerance value (micelle stability). **C.** Cloudy solution at the turbid concentration (230 ppm, corresponding to hard water conditions). **D.** Cloudy solution with the formation of calcium precipitates (3300 ppm, corresponding to extreme hard water conditions).

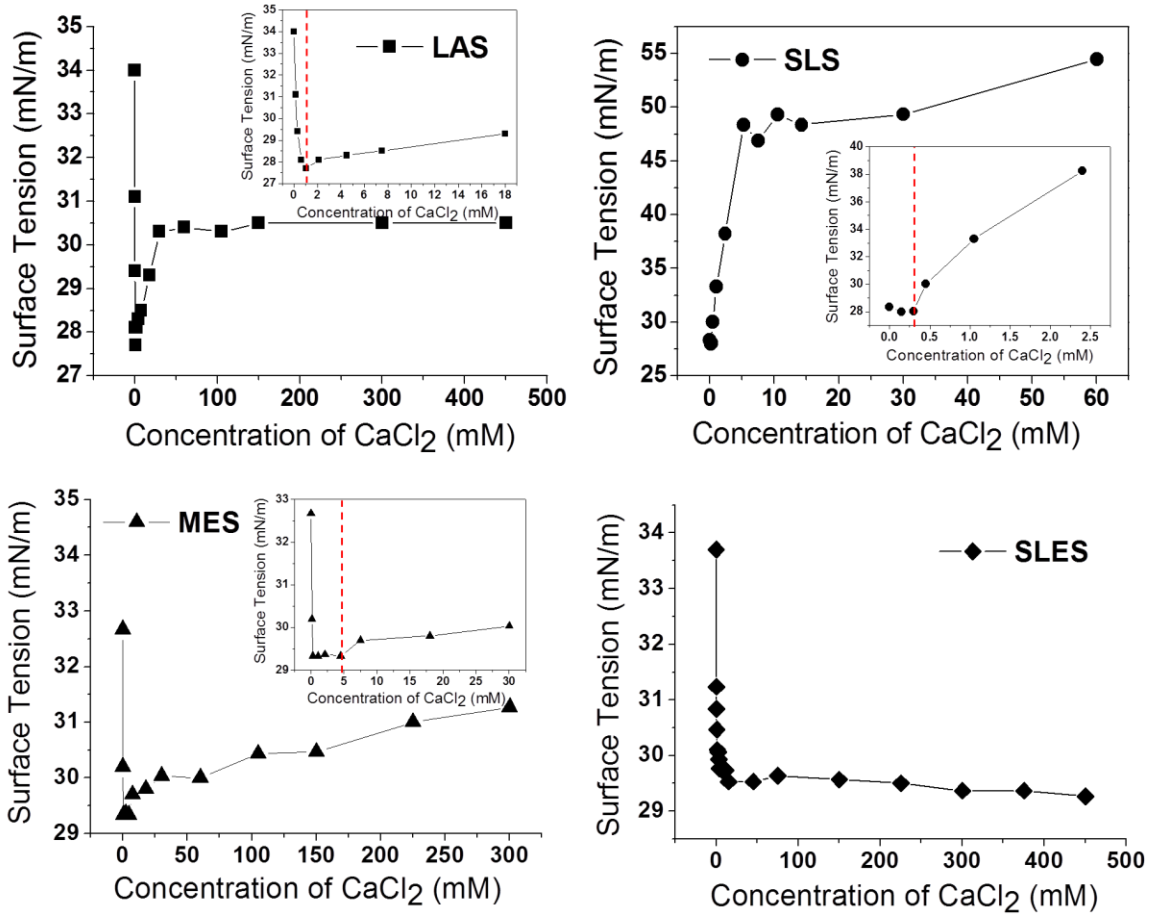

Fig. S32. Surface tension versus $CaCl_2$ concentration of the standard commercial surfactants, LAS, SLS, MES, and SLES (Concentration of the surfactant: Twice CMC, Hardness tolerance / micelle stability concentration: Calcium concentration at the increasing point of the surface tension indicated by the red dashed line).

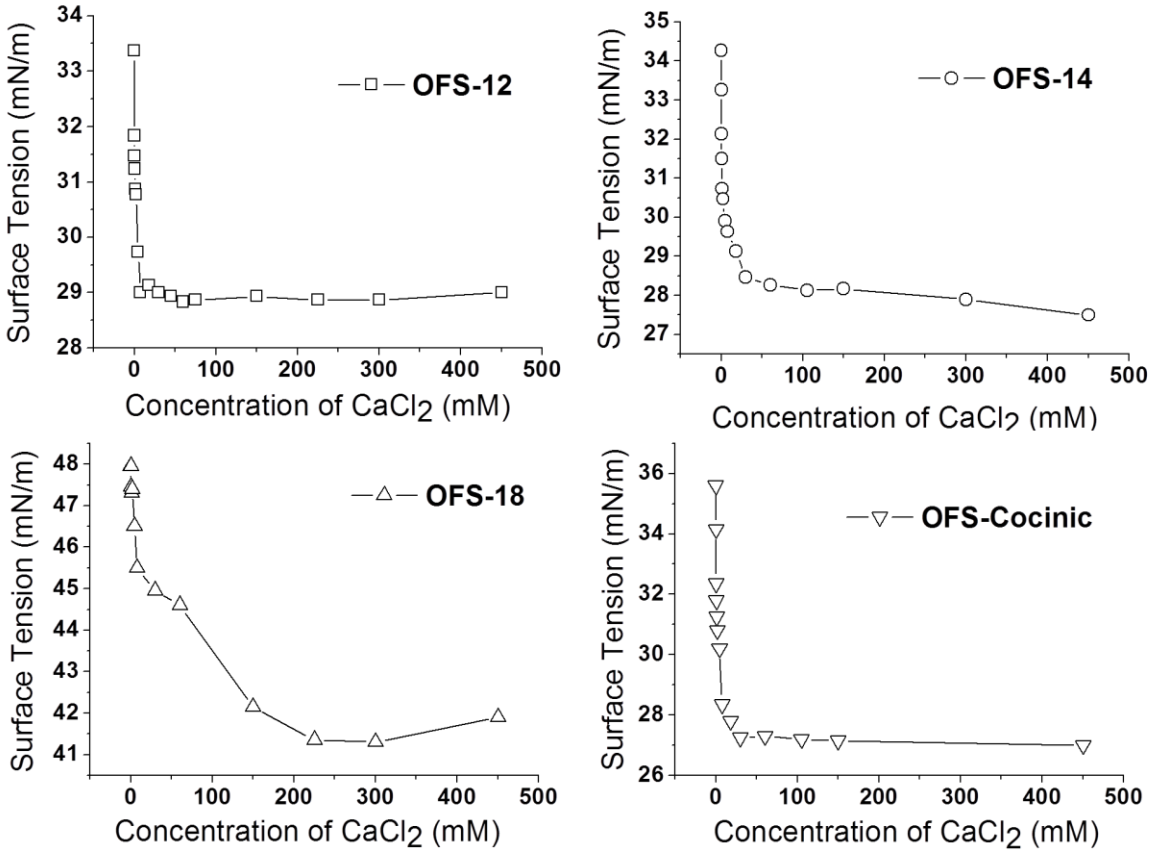

Fig. S33. Surface tension vs. $CaCl_2$ concentration of the linear OFS-n surfactants (Concentration of the surfactant: Twice CMC, Hardness tolerance / micelle stability concentration: Calcium concentration at the increasing point of the surface tension).

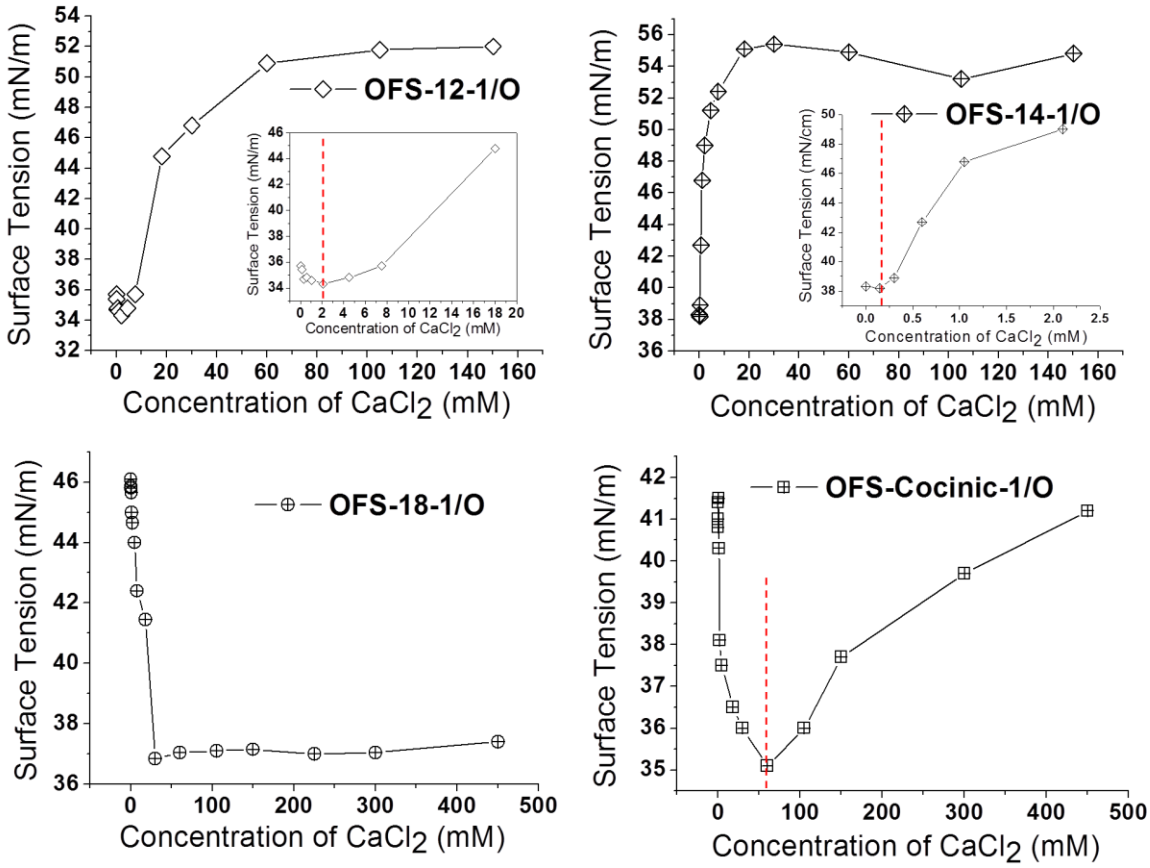

Fig. S34. Surface tension versus $CaCl_2$ concentration of the OFS-n-1/O surfactants (Concentration of the surfactant: Twice CMC, Hardness tolerance / micelle stability concentration: Calcium concentration at the increasing point of the surface tension indicated by the red dashed line).

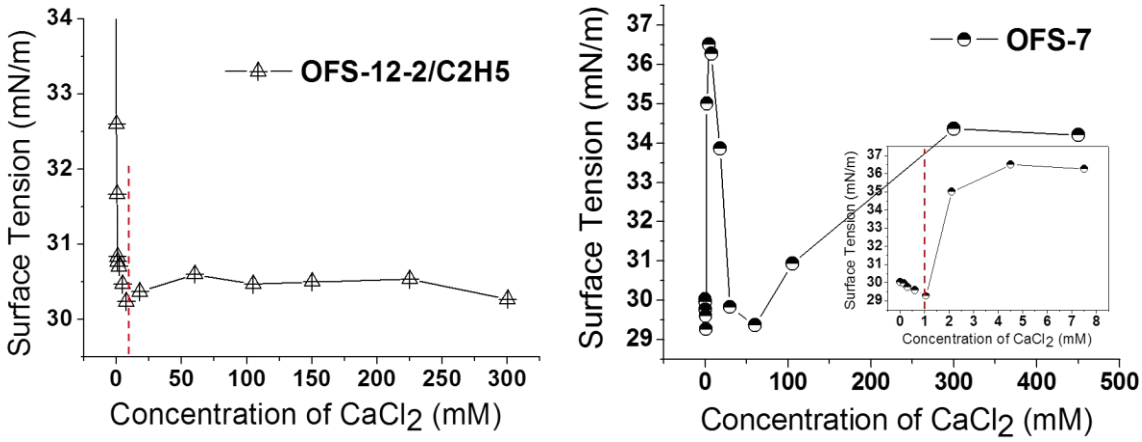

Fig. S35. Surface tension versus $CaCl_2$ concentration of OFS-12-2/C2H5 and OFS-7 (Concentration of the surfactant: Twice CMC, Hardness tolerance / micelle stability concentration: Calcium concentration at the increasing point of the surface tension indicated by the red dashed line).

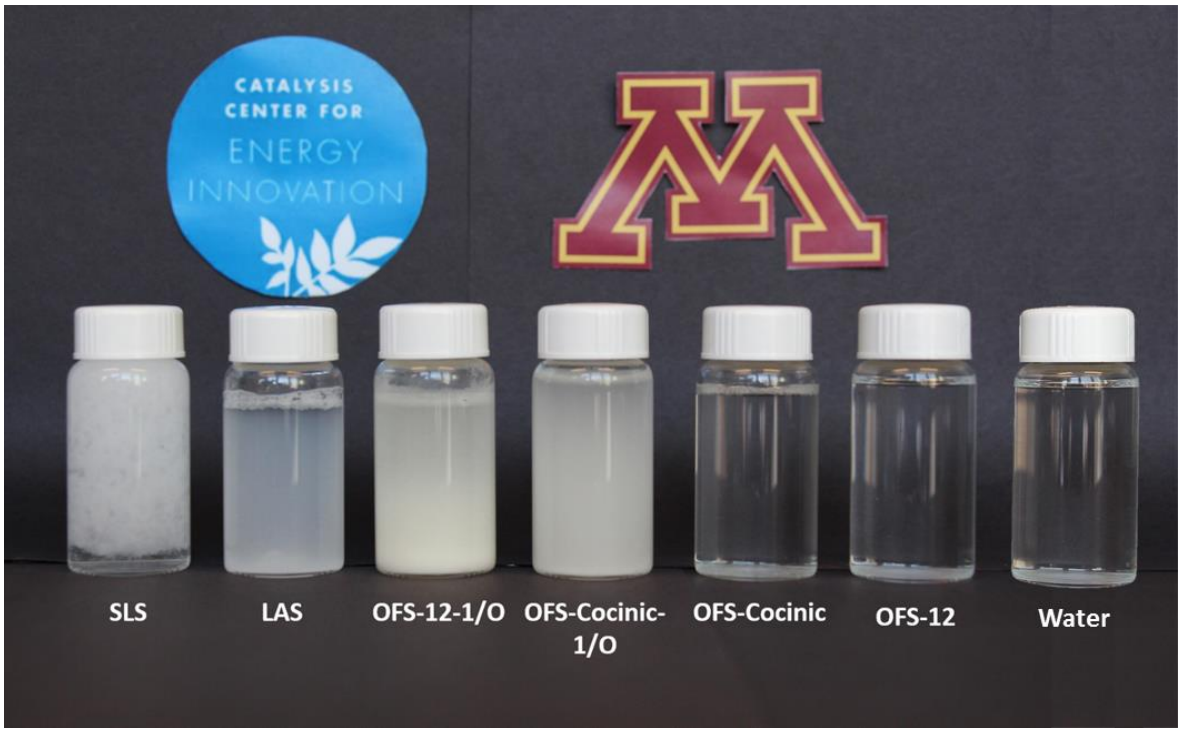

Fig. S36. Surfactant solutions after addition of $CaCl_2$ (Surfactant concentration: Twice CMC, Concentration of $CaCl_2$: 50,000 ppm). Image was taken after two weeks of making the solution.

Table S10. Summary of hard water stability tests for all surfactants.

Surfactant	Micelle stability conc. [ppm of $CaCl_2$][a]	Turbid conc. [ppm of $CaCl_2$][a]
Commercial		
SLS, Sodium Lauryl Sulfate	33	33
MES, Methyl Ester Sulfonate	500	>50,000
LAS, Linear Alkylbenzene Sulfonate	100	230
SLES, Sodium Lauryl Ether Sulfate	>50,000	>50,000
OFS, Oleo-Furan Sulfonates		
OFS-12-1/O	230	230
OFS-14-1/O	33	66
OFS-18-1/O	>50,000	2,000
OFS-Cocinic-1/O	6,600	500
OFS-7	110	230
OFS-12	>50,000	10,000
OFS-14	>50,000	2,000
OFS-18	33,000	2,000
OFS-Cocinic	>50,000	10,000
40:60 mol% OFS-12-2/C2H5:OFS-12	2,000	2,000
85:15 mol% OFS-12-1/O:OFS-12	-	-

[a]Measured at twice CMC of the surfactants

5.0 Gas Chromatography (GC) Profiles

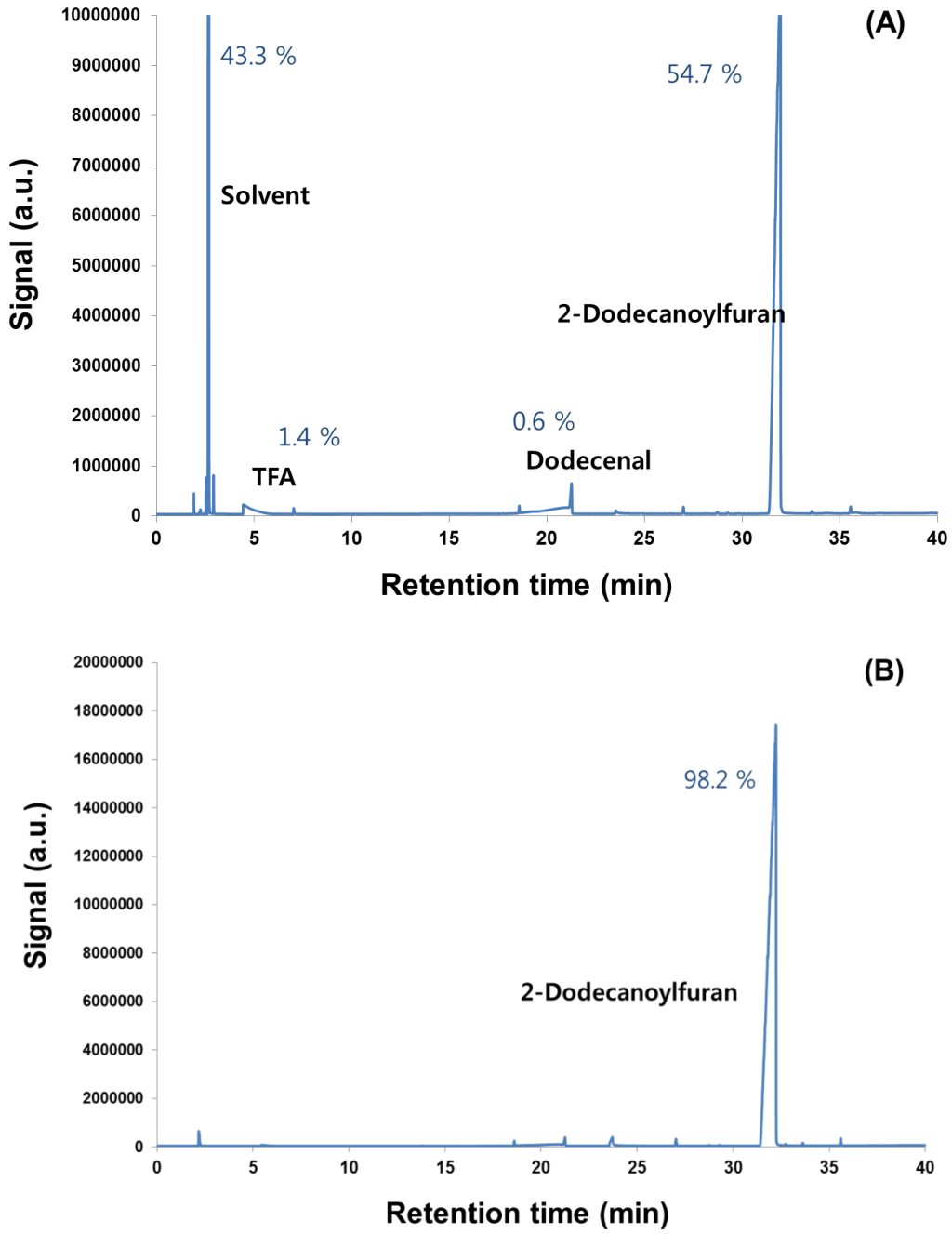

Fig. S37. Typical GC profiles of product mixtures **A.** After acylation and, **B.** Post purification of 2-dodecanoylfuran by rotary evaporator.

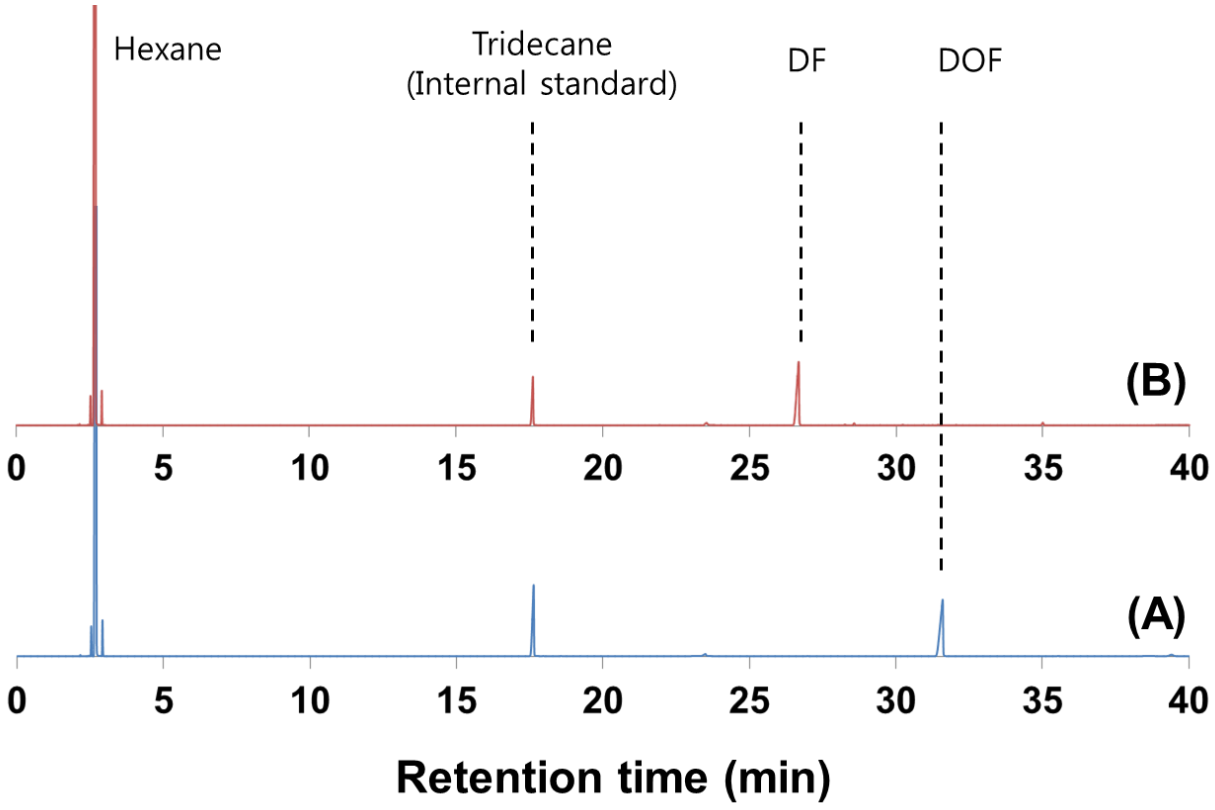

Fig. S38. Typical GC profiles of **A.** Reactant mixture and **B.** Products in hydrogenation of 2-dodecanoylfuran (DOF: 2-dodecanoylfuran, DF: 2-dodecylfuran).

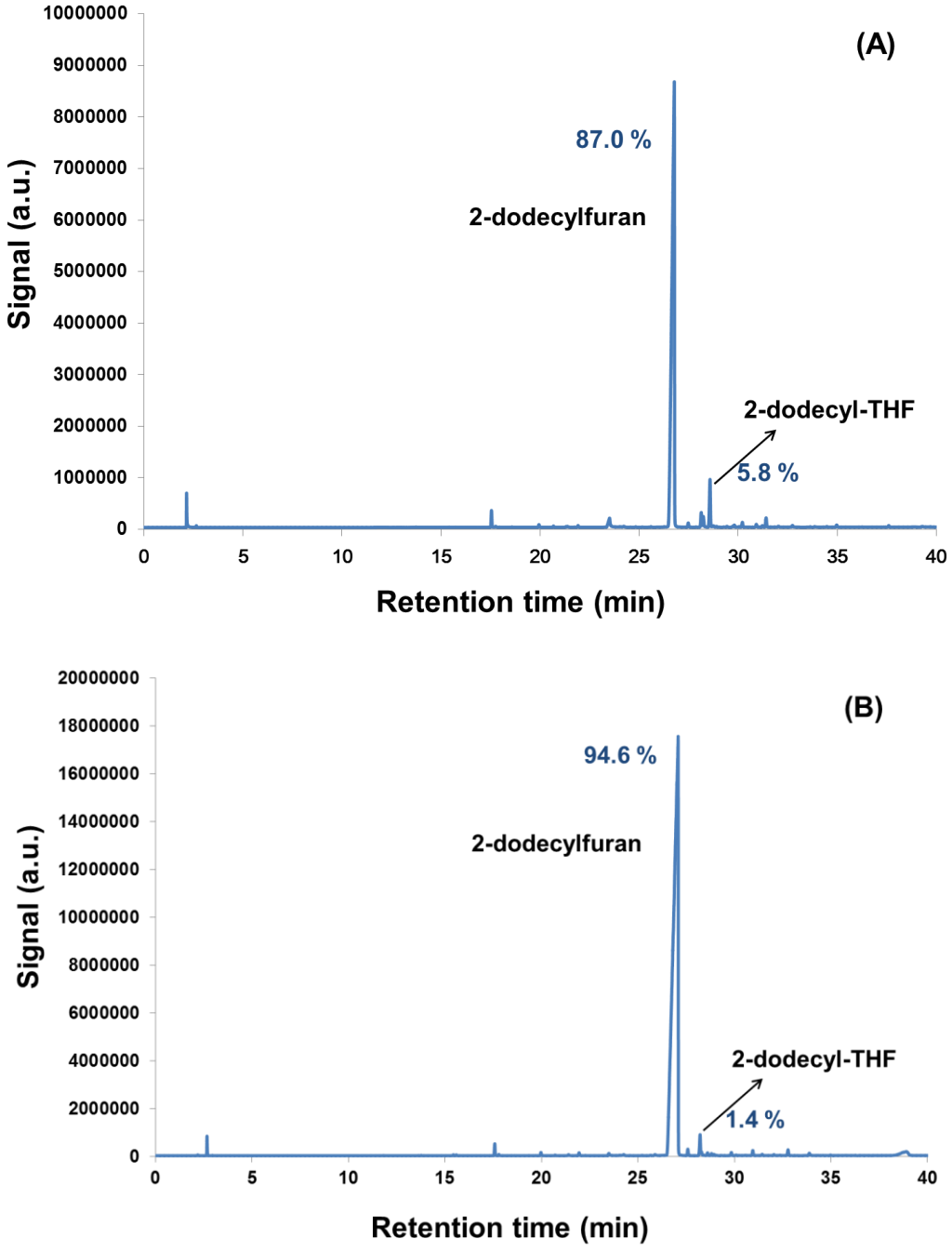

Fig. S39. Typical GC profiles of product mixtures after hydrogenation. **A.** Concentrated samples by rotary evaporator and, **B.** Purified and separated by flash chromatography.

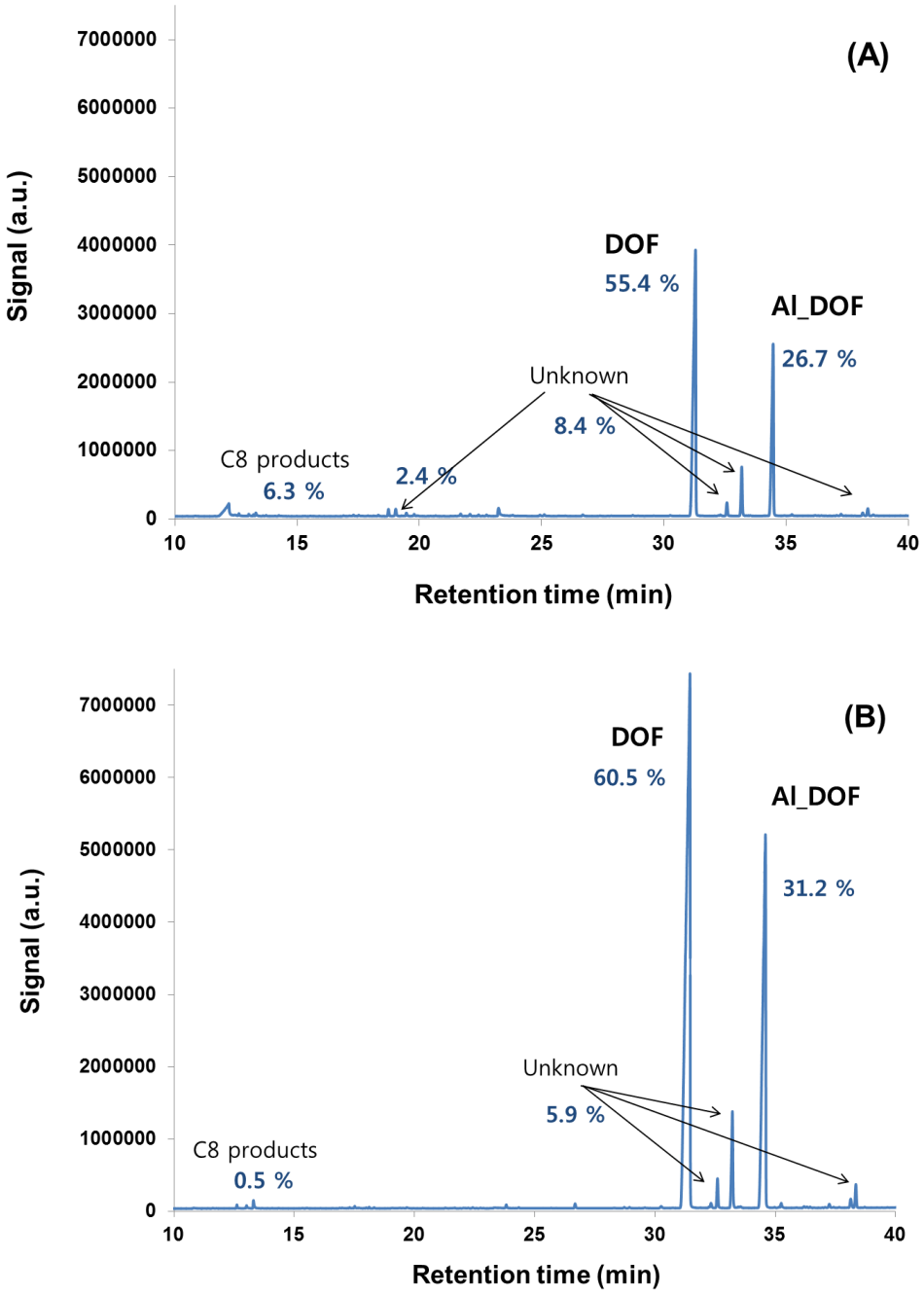

Fig. S40. Typical GC profiles of product mixtures after aldol condensation. **A.** Concentrated samples by rotary evaporator and, **B.** Purified and separated by flash chromatography.

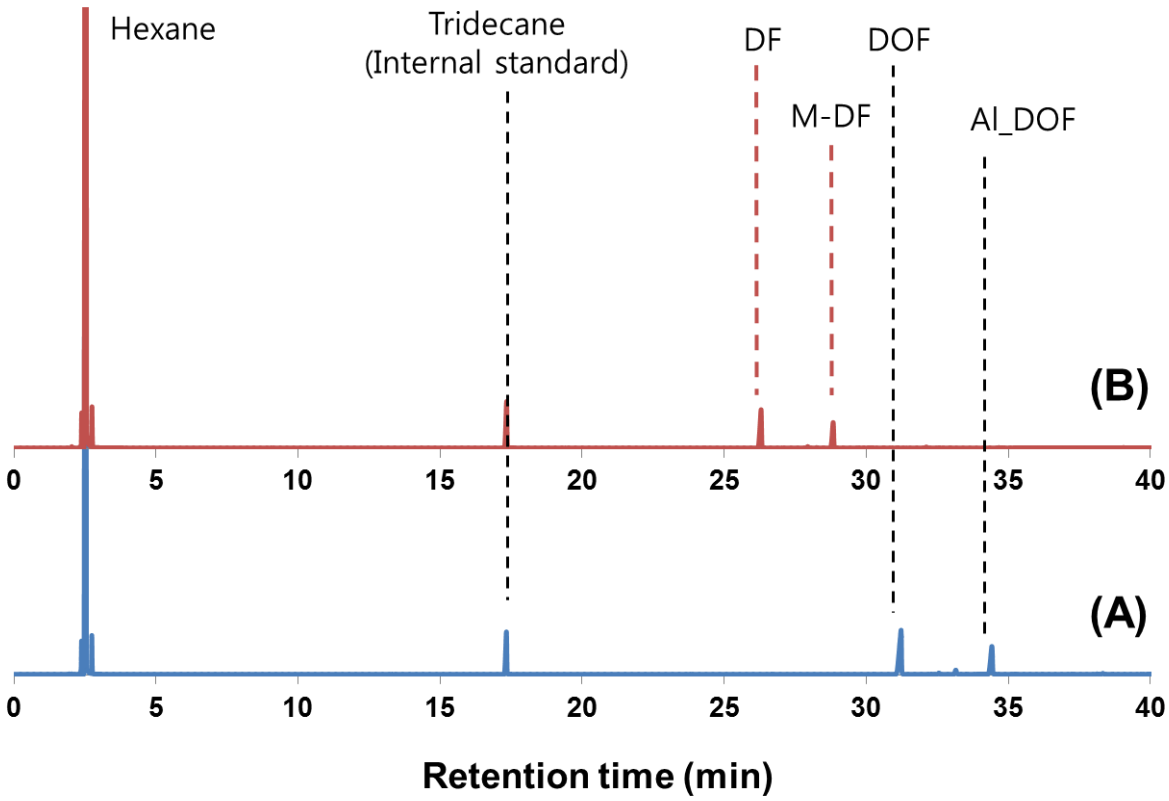

Fig. S41. Typical GC profiles of **A.** reactant mixture and **B.** products in hydrogenation of of DOF and Al_DOF mixture (DOF: 2-dodecanoylfuran, Al_DOF: aldol product, DF: 2-dodecylfuran, M-DF: Mono-ethyl branched dodecylfuran).

6.0 NMR spectra

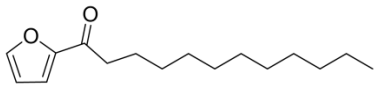

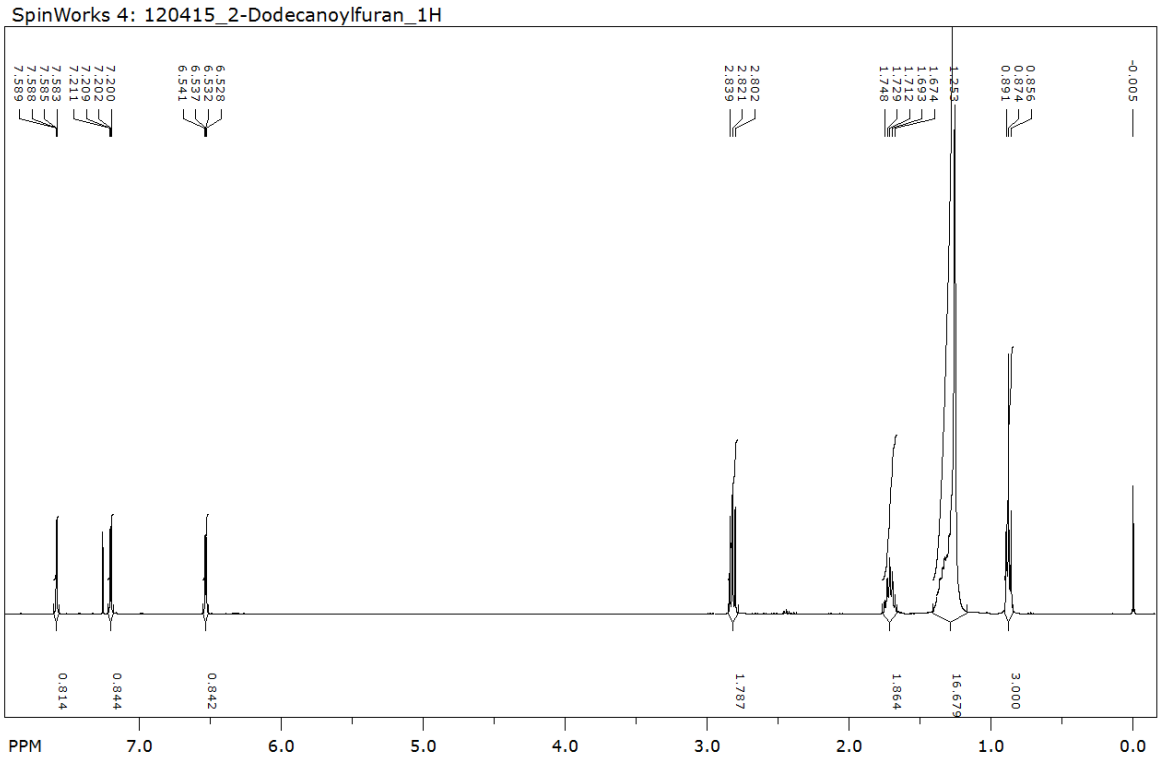

Fig. S42. ^{1}H NMR of 2-dodecanoylfuran (furyl-2-dodecyl-ketone) in $CDCl_3$.

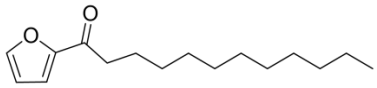

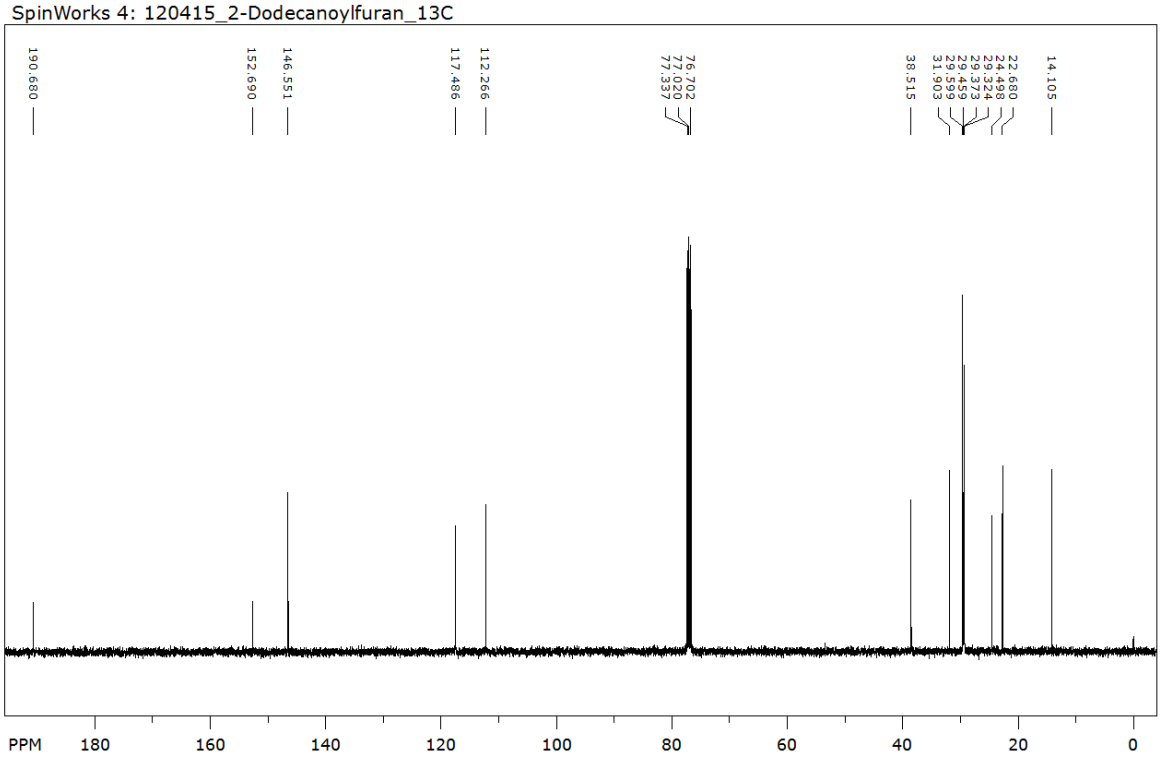

Fig. S43. ^{13}C NMR of 2-dodecanoylfuran (furyl-2-dodecyl-ketone) in $CDCl_3$.

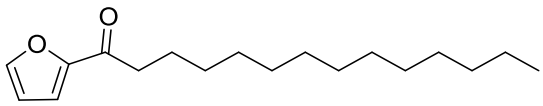

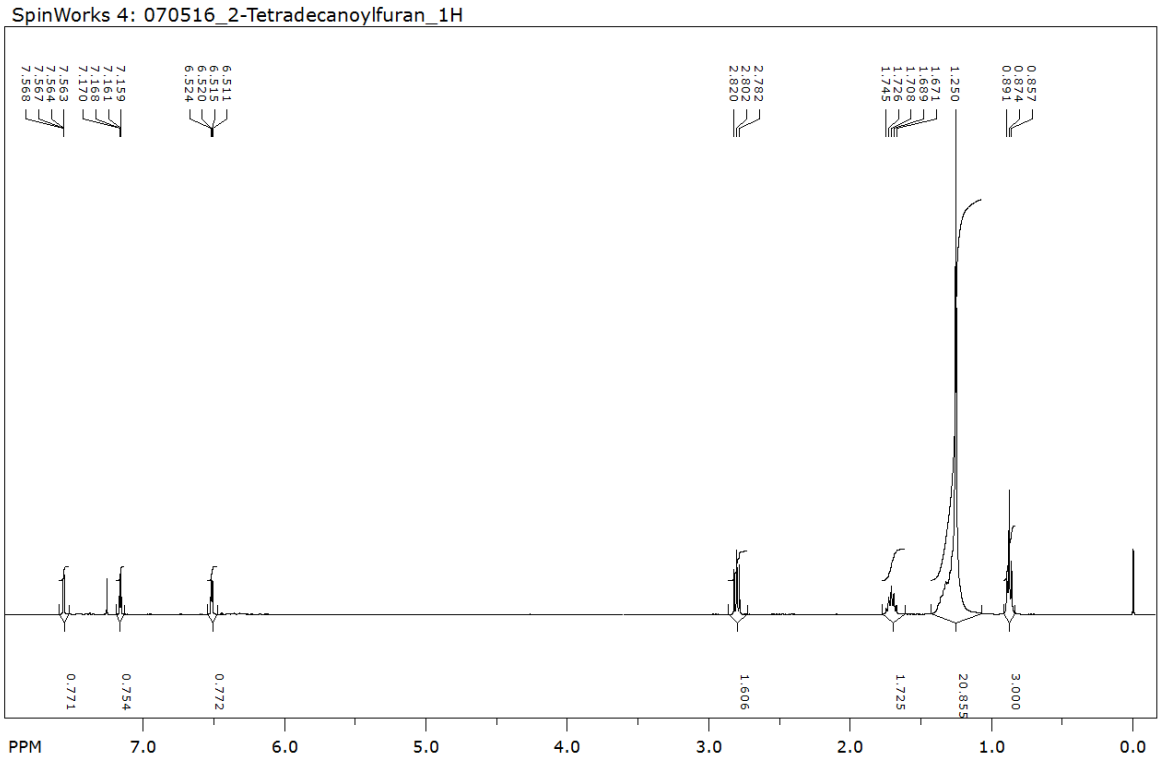

Fig. S44. ^{1}H NMR of 2-tetradecanoylfuran (furyl-2-tetradecyl-ketone) in $CDCl_3$

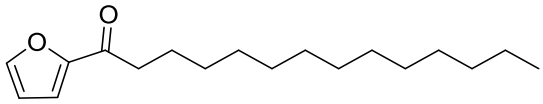

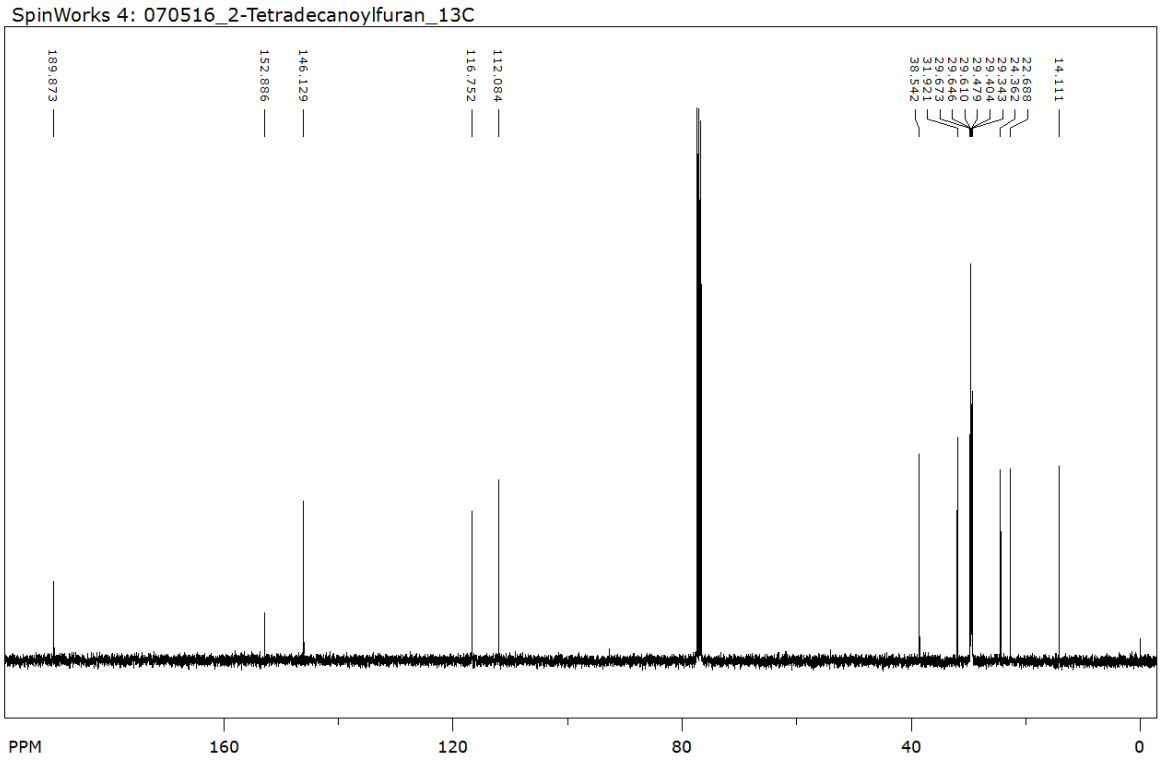

Fig. S45. ^{13}C NMR of 2-tetradecanoylfuran (furyl-2-tetradecyl-ketone) in $CDCl_3$.

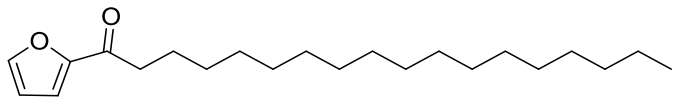

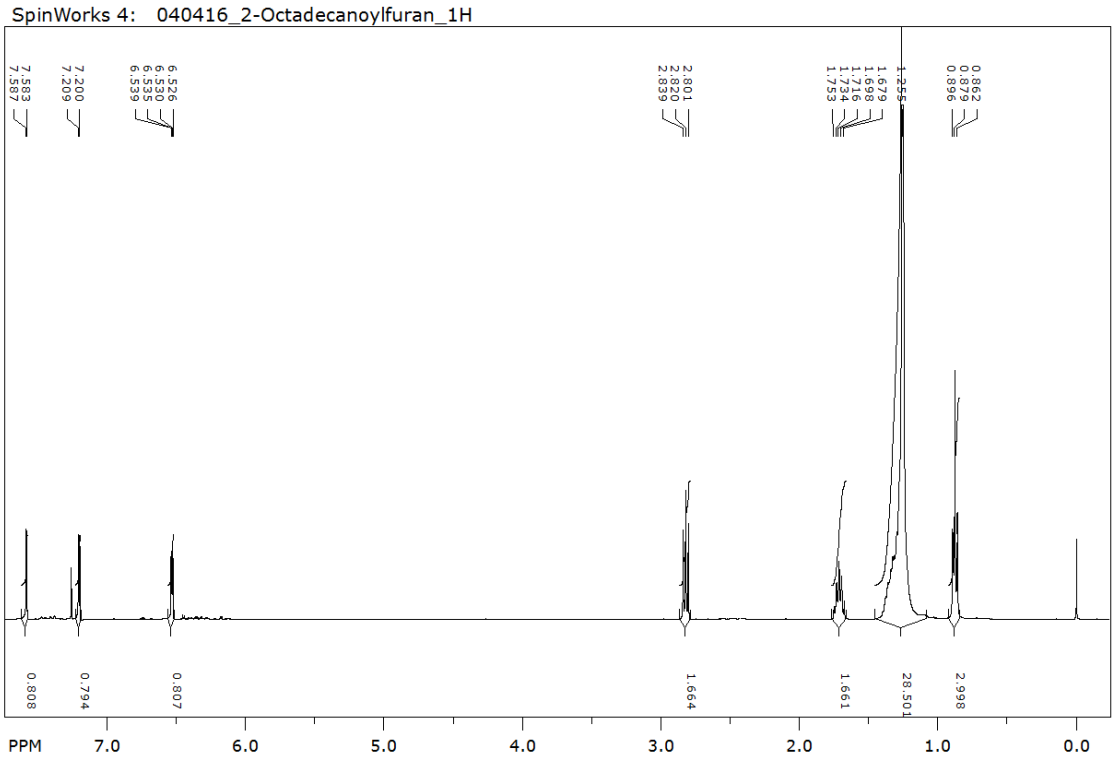

Fig. S46. ^{1}H NMR of 2-octadecanoylfuran (furyl-2-octadecyl-ketone) in $CDCl_3$.

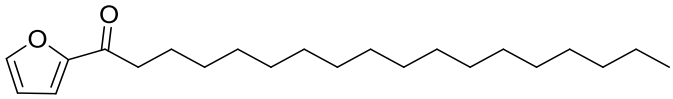

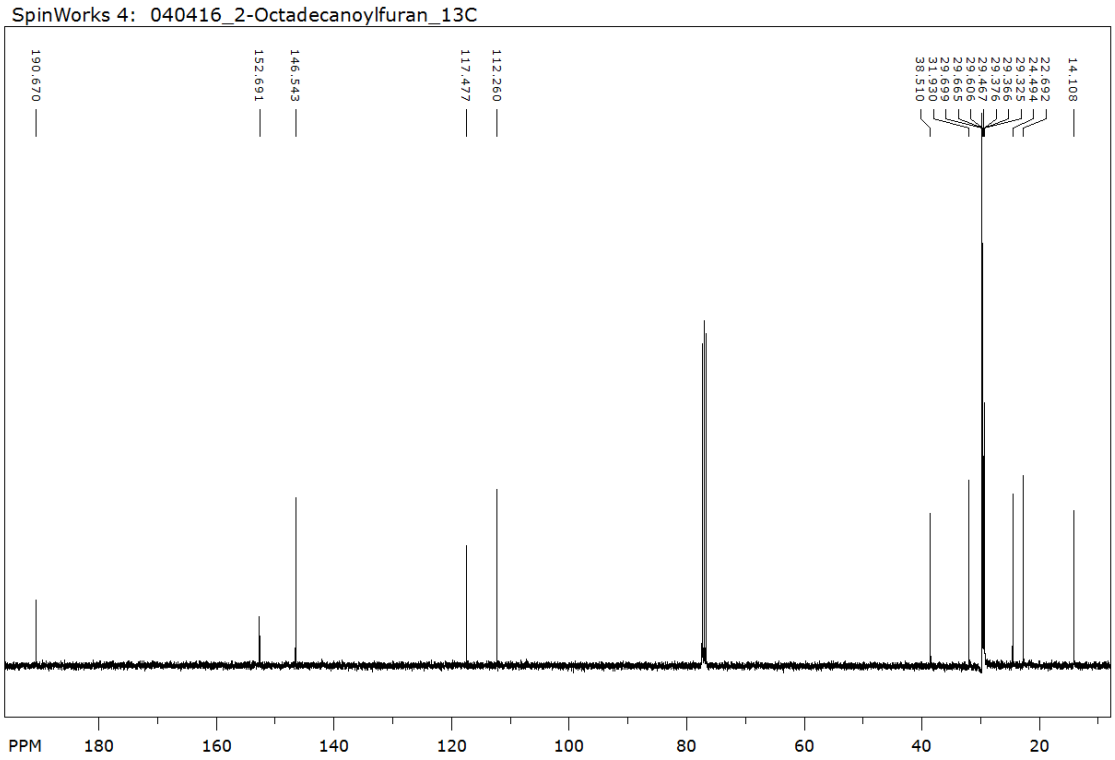

Fig. S47. ^{13}C NMR of 2-octadecanoylfuran (furyl-2-octadecyl-ketone) in $CDCl_3$.

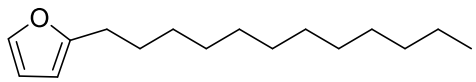

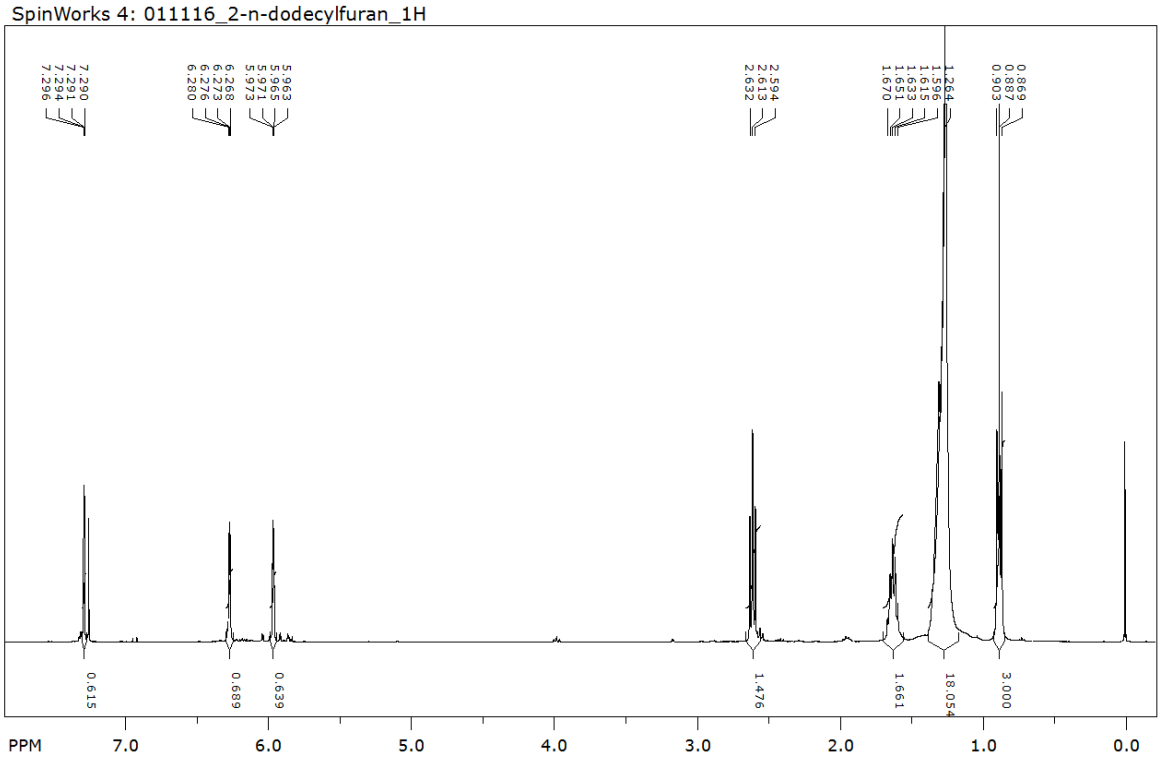

Fig. S48. ^{1}H NMR of 2-n-dodecylfuran in $CDCl_3$.

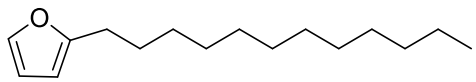

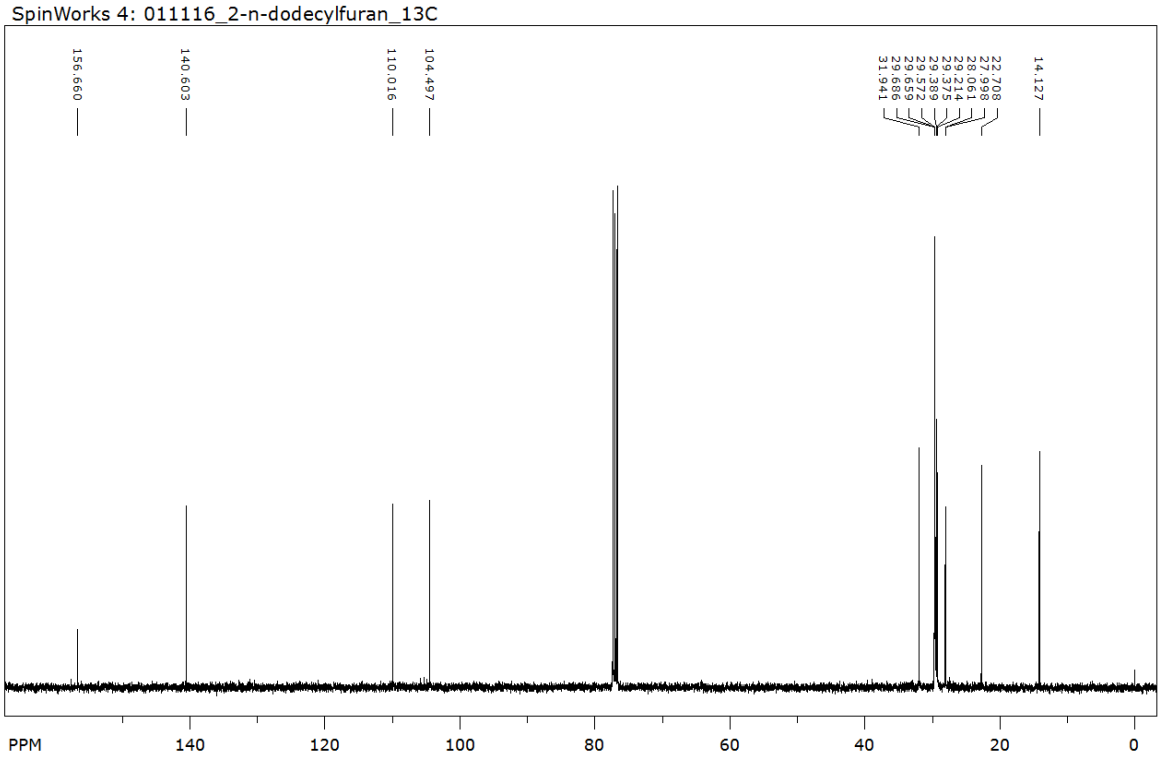

Fig. S49. ^{13}C NMR of 2-n-dodecylfuran in $CDCl_3$.

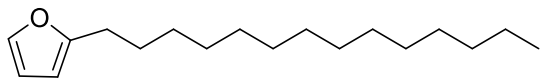

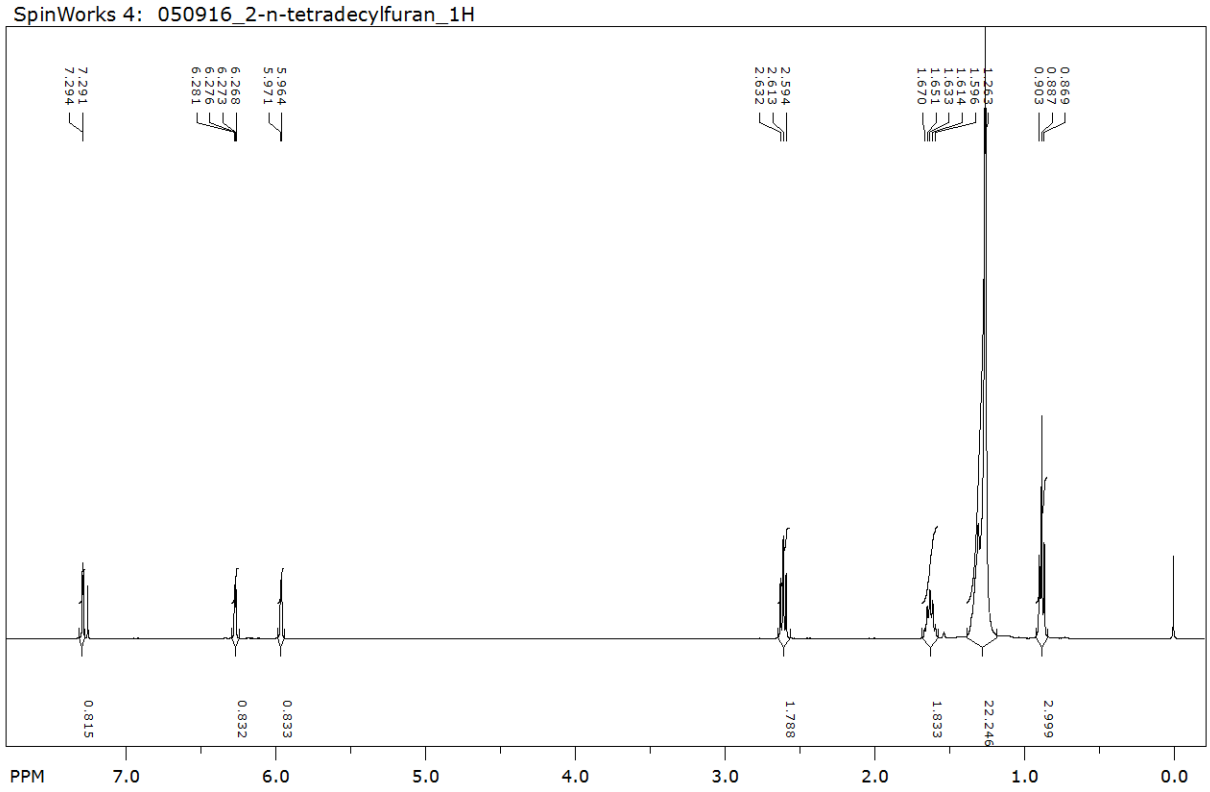

Fig. S50. ^{1}H NMR of 2-n-tetradecylfuran in $CDCl_3$.

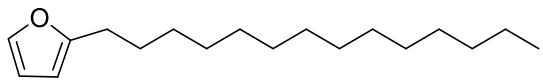

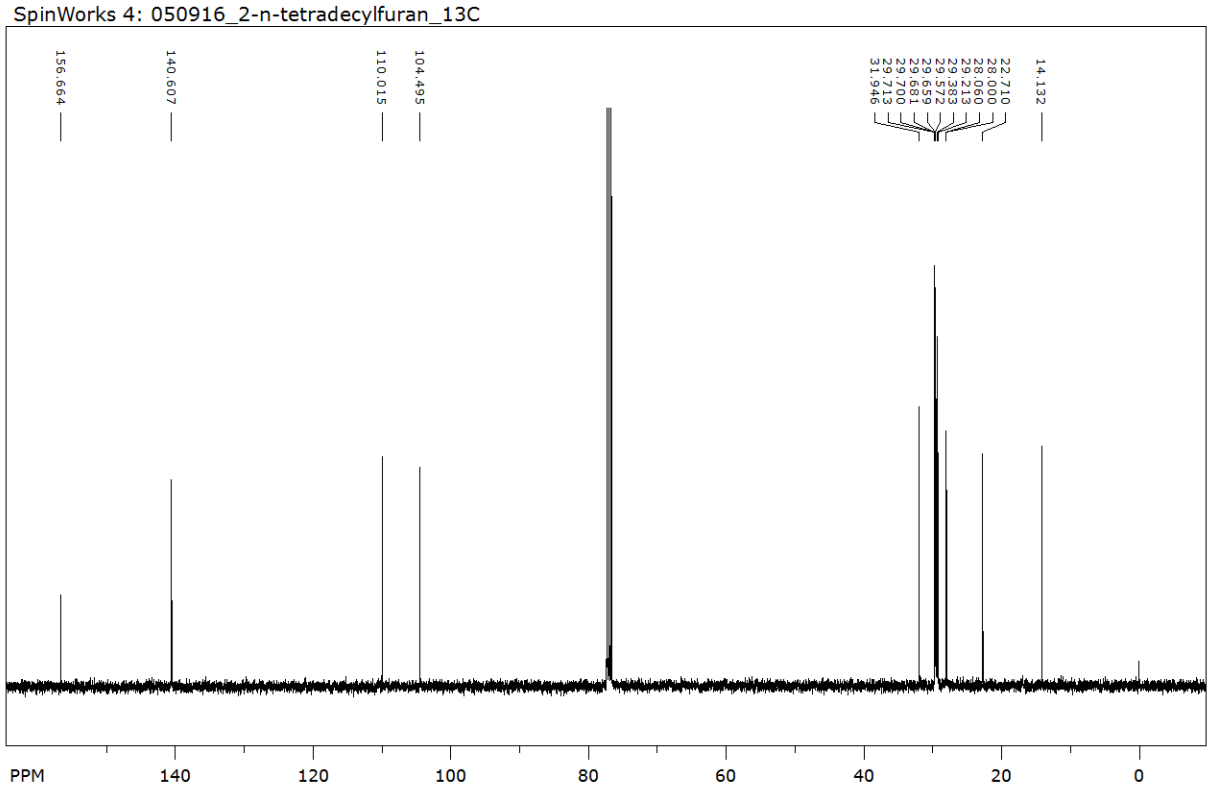

Fig. S51. ^{13}C NMR of 2-n-tetradecylfuran in $CDCl_3$.

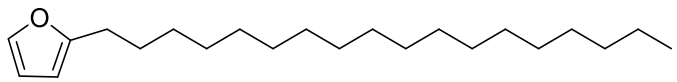

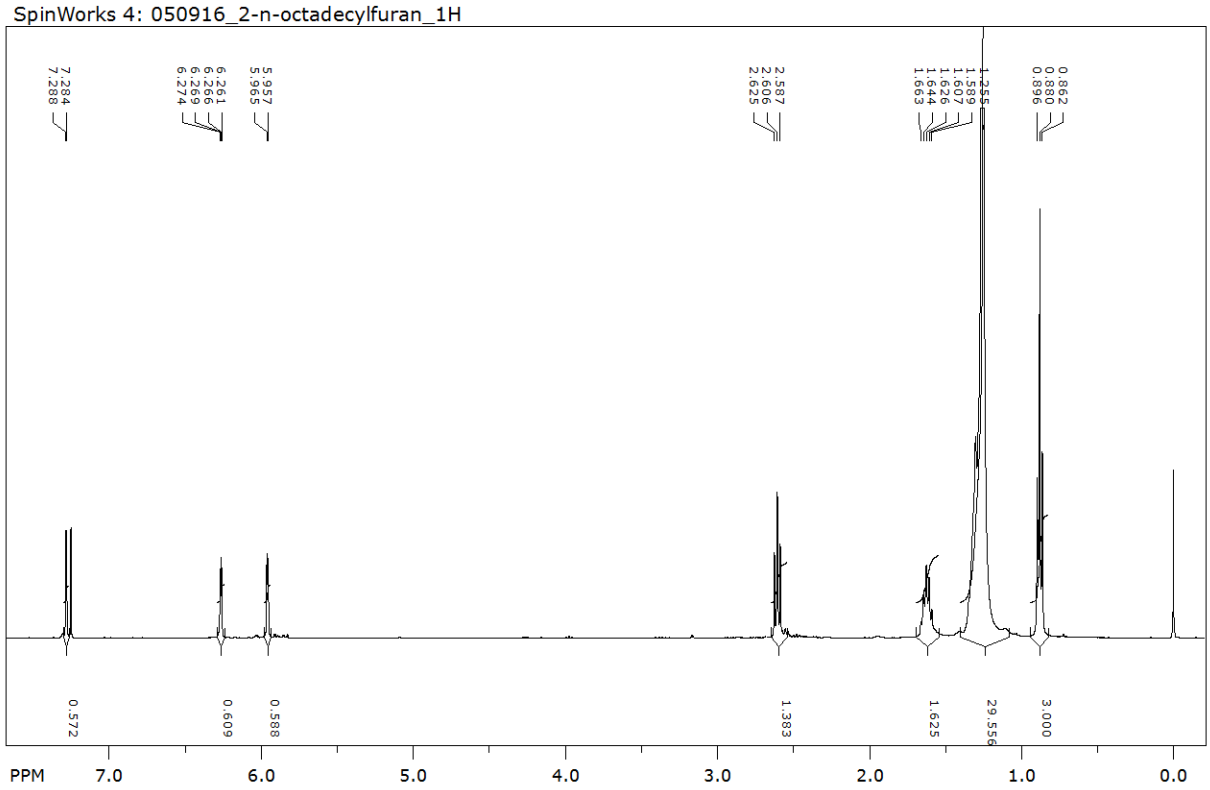

Fig. S52. ^{1}H NMR of 2-n-octadecylfuran in $CDCl_3$.

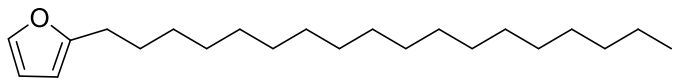

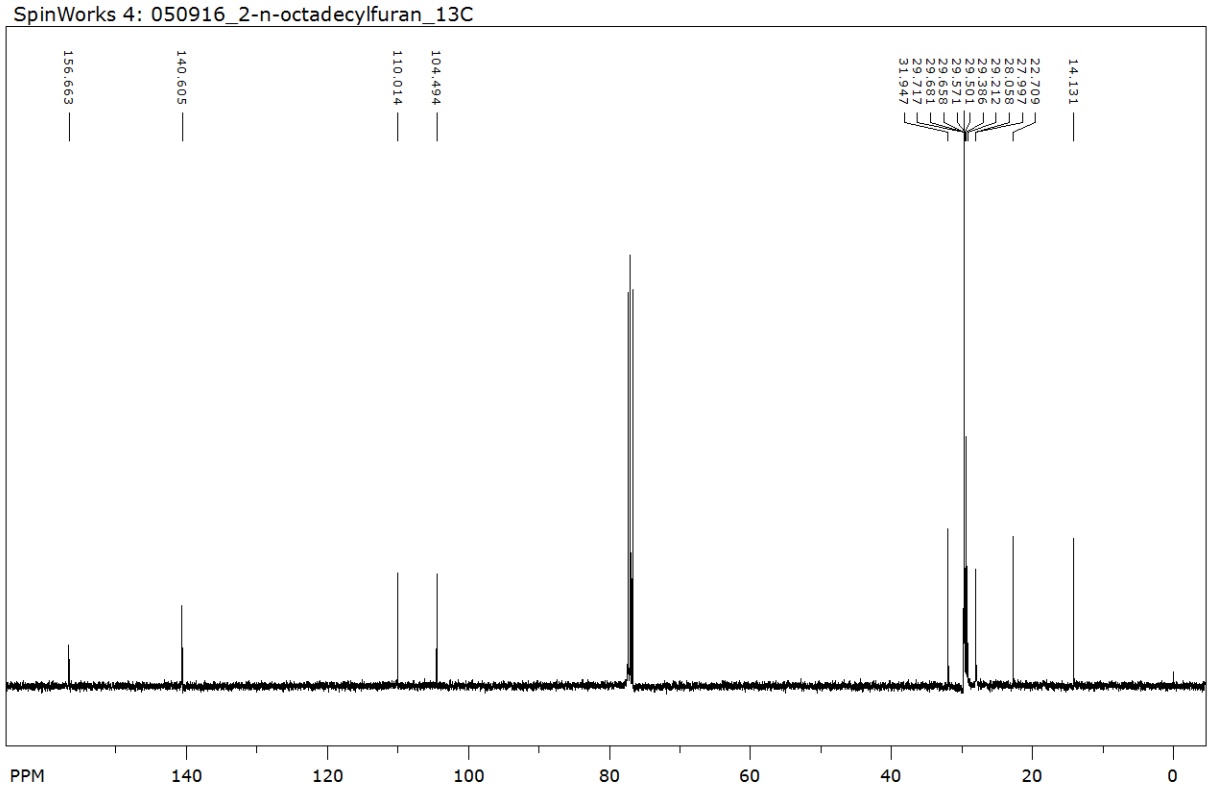

Fig. S53. ^{13}C NMR of 2-n-octadecylfuran in $CDCl_3$.

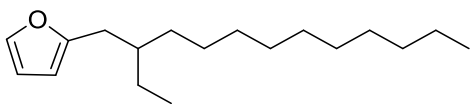

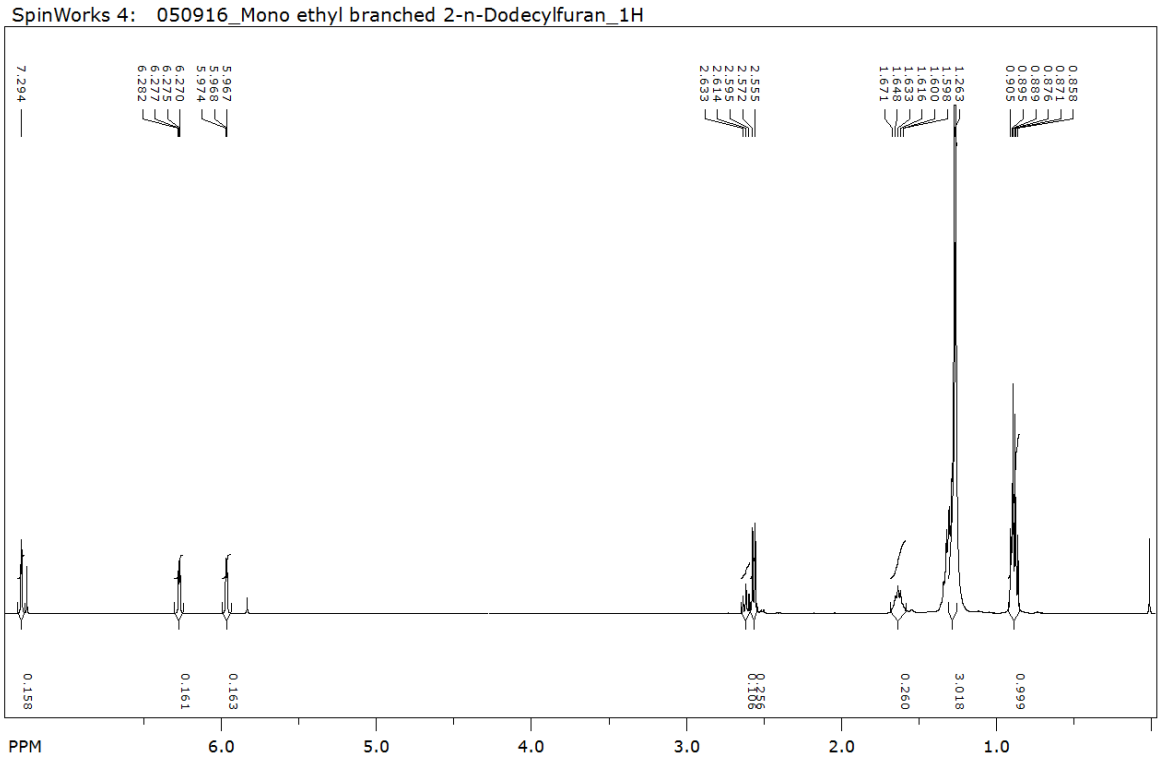

Fig. S54. ^{1}H NMR of mono ethyl branched 2-n-dodecylfuran, M-DF (Mixture with 60 % of 2-n-dodecylfuran) in $CDCl_3$.

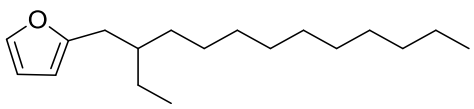

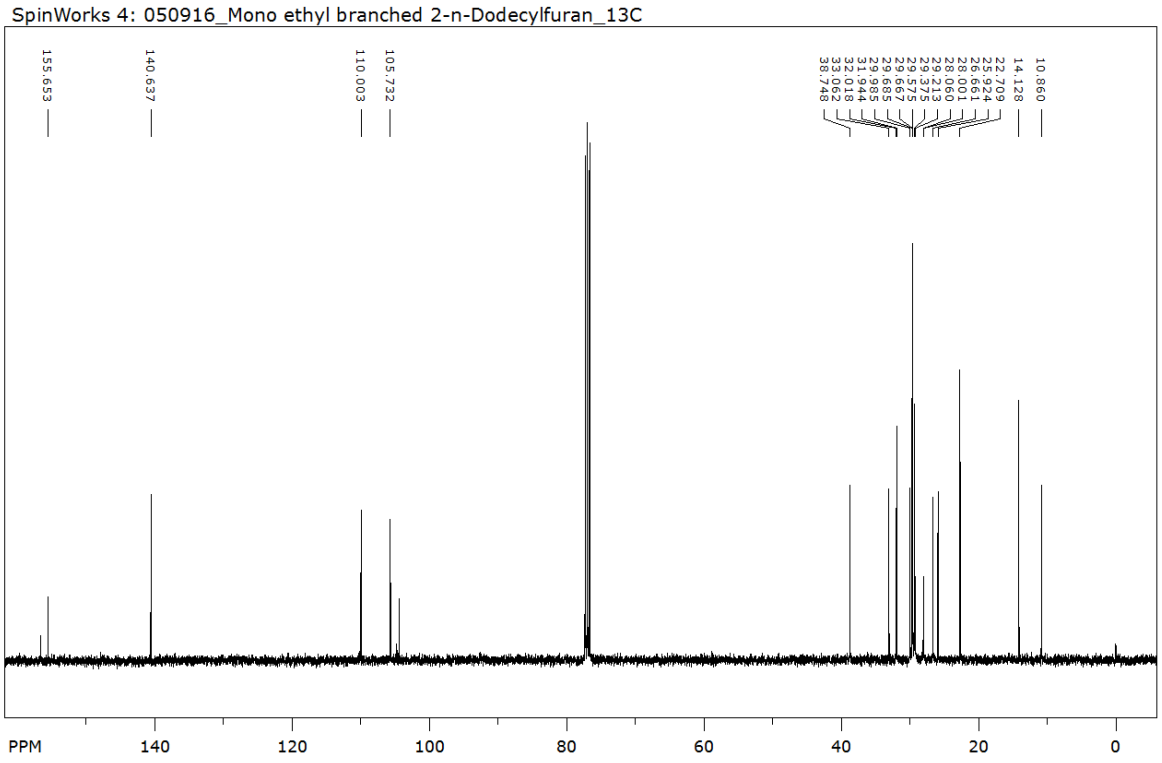

Fig. S55. ^{13}C NMR of mono ethyl branched 2-n-dodecylfuran, M-DF (Mixture with 60 % of 2-n-dodecylfuran) in $CDCl_3$.

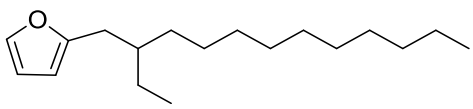

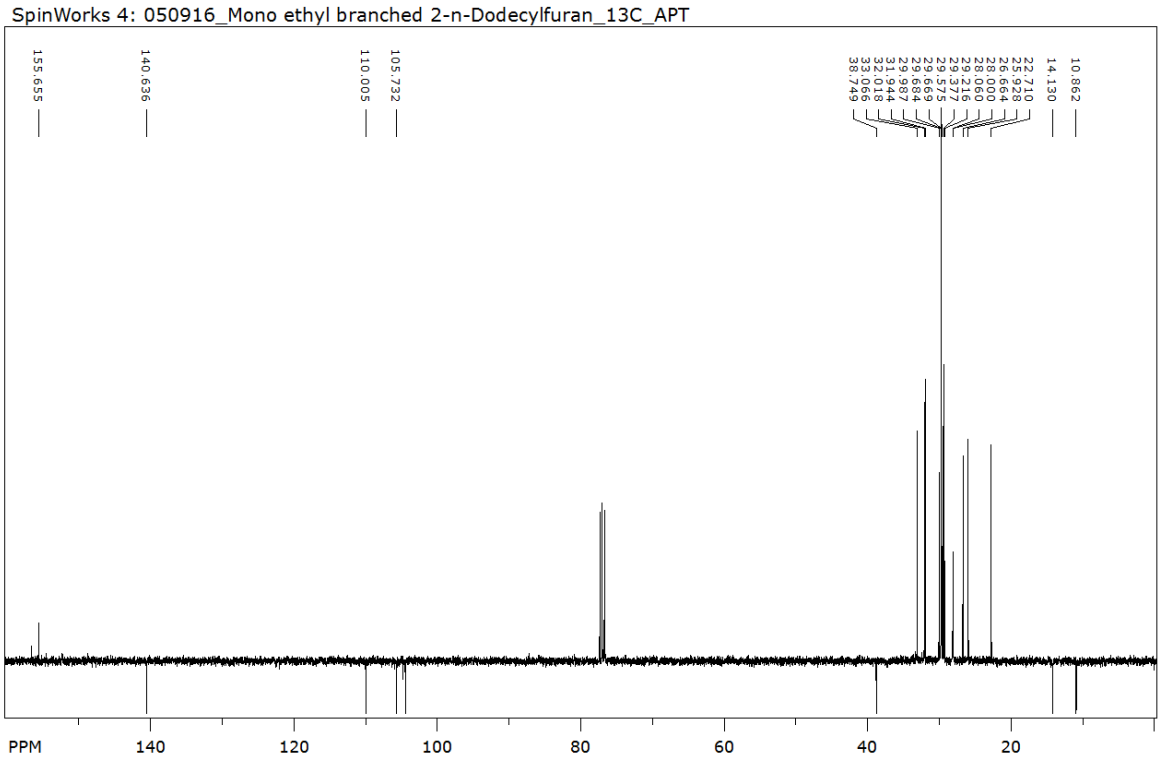

Fig. S56. ^{13}C-APT NMR of mono ethyl branched 2-n-dodecylfuran, M-DF (Mixture with 60 % of 2-n-dodecylfuran) in $CDCl_3$.

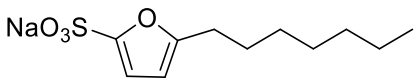

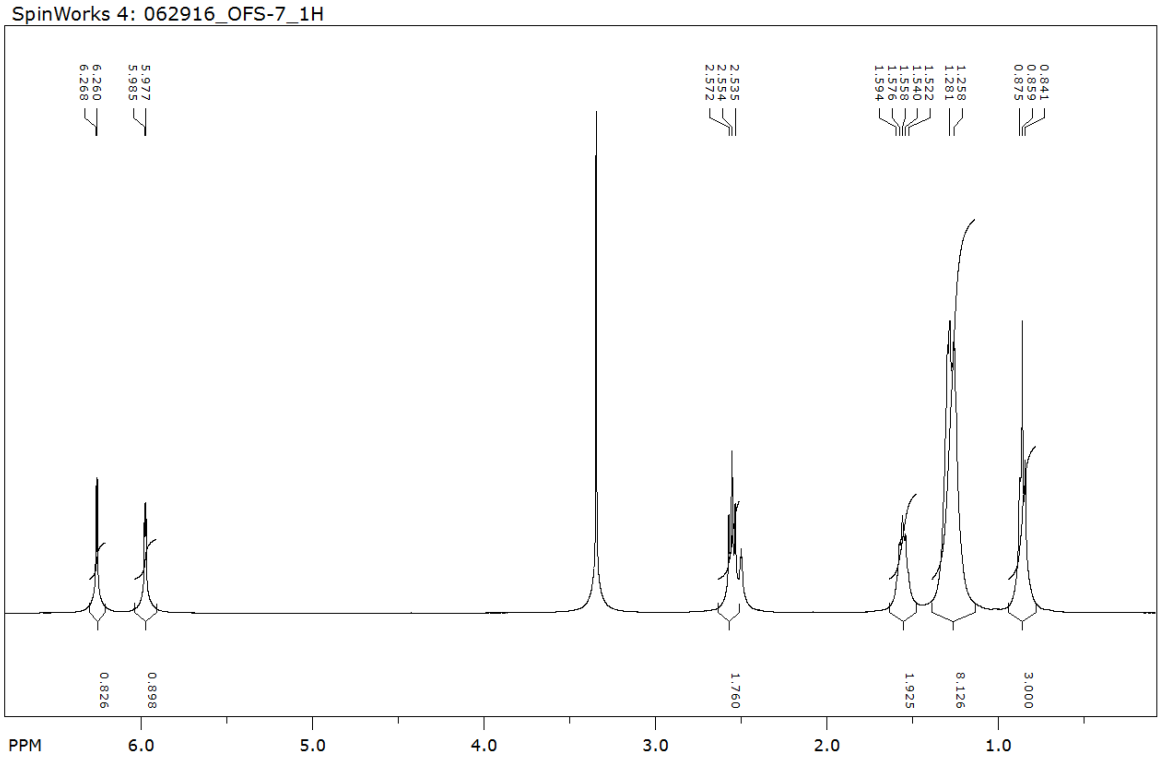

Fig. S57. ^{1}H NMR of OFS-7 in DMSO-d$_6$.

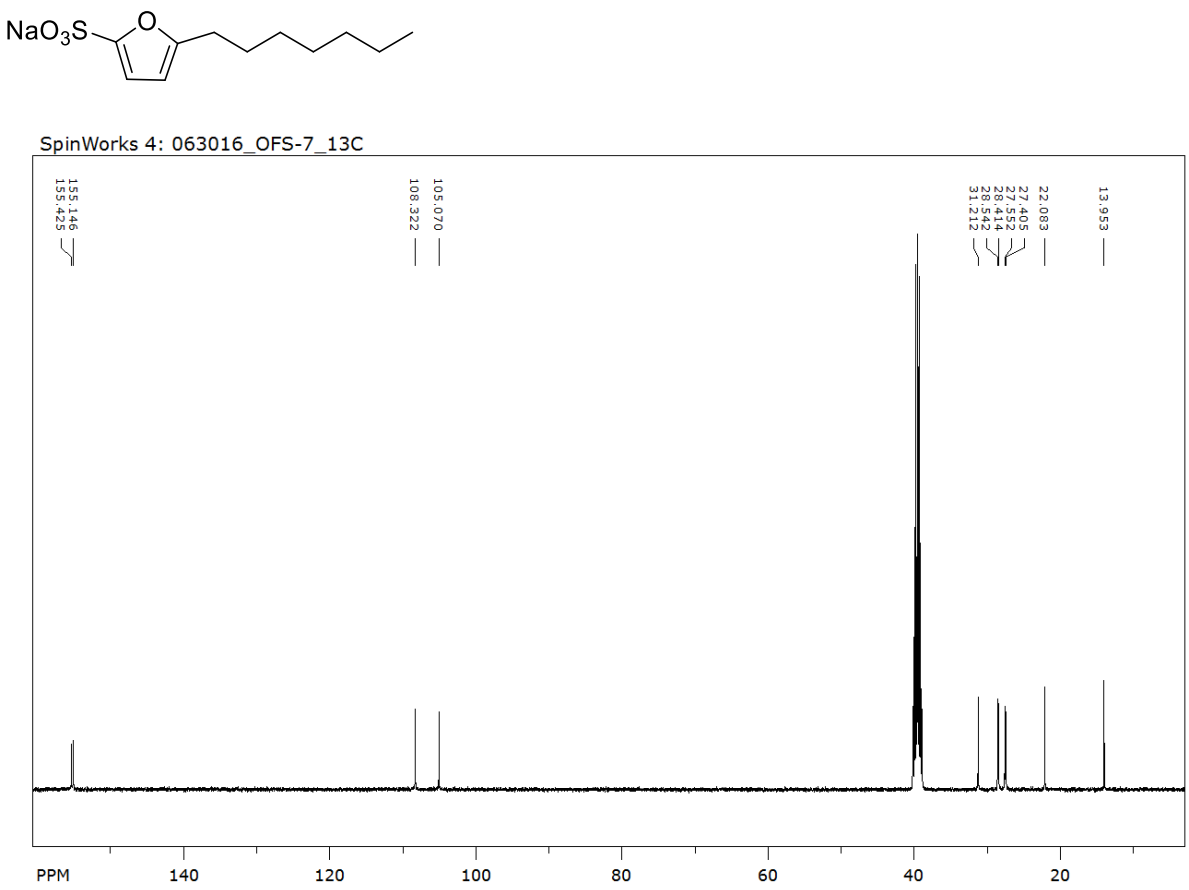

Fig. S58. ^{13}C NMR of OFS-7 in DMSO-d$_6$.

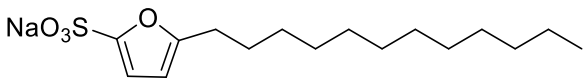

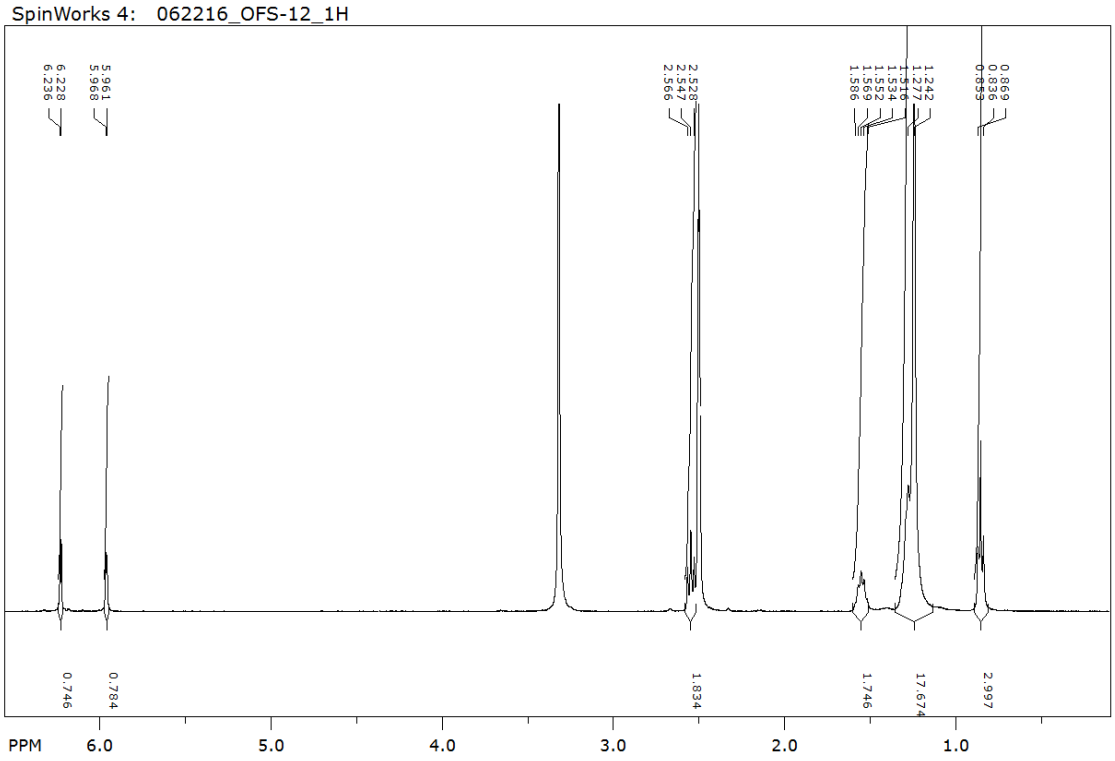

Fig. S59. ^{1}H NMR of OFS-12 in DMSO-d$_6$.

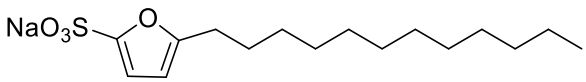

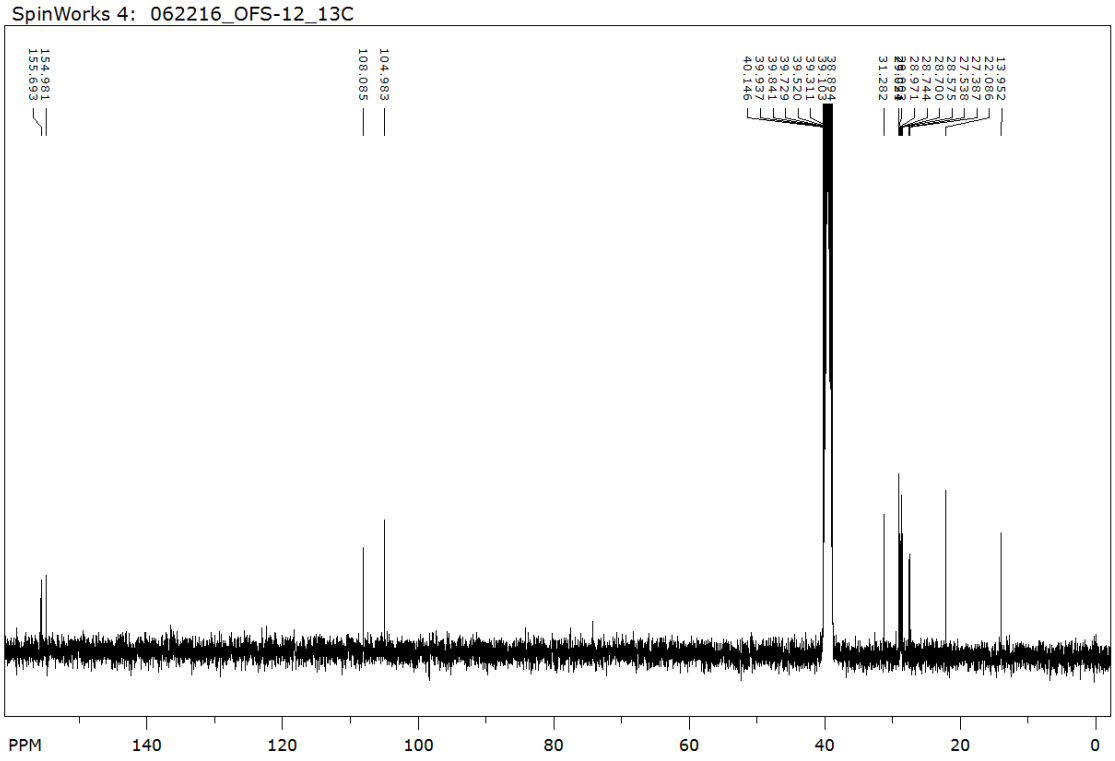

Fig. S60. ^{13}C NMR of OFS-12 in DMSO-d_6.

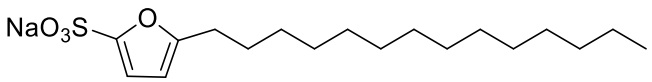

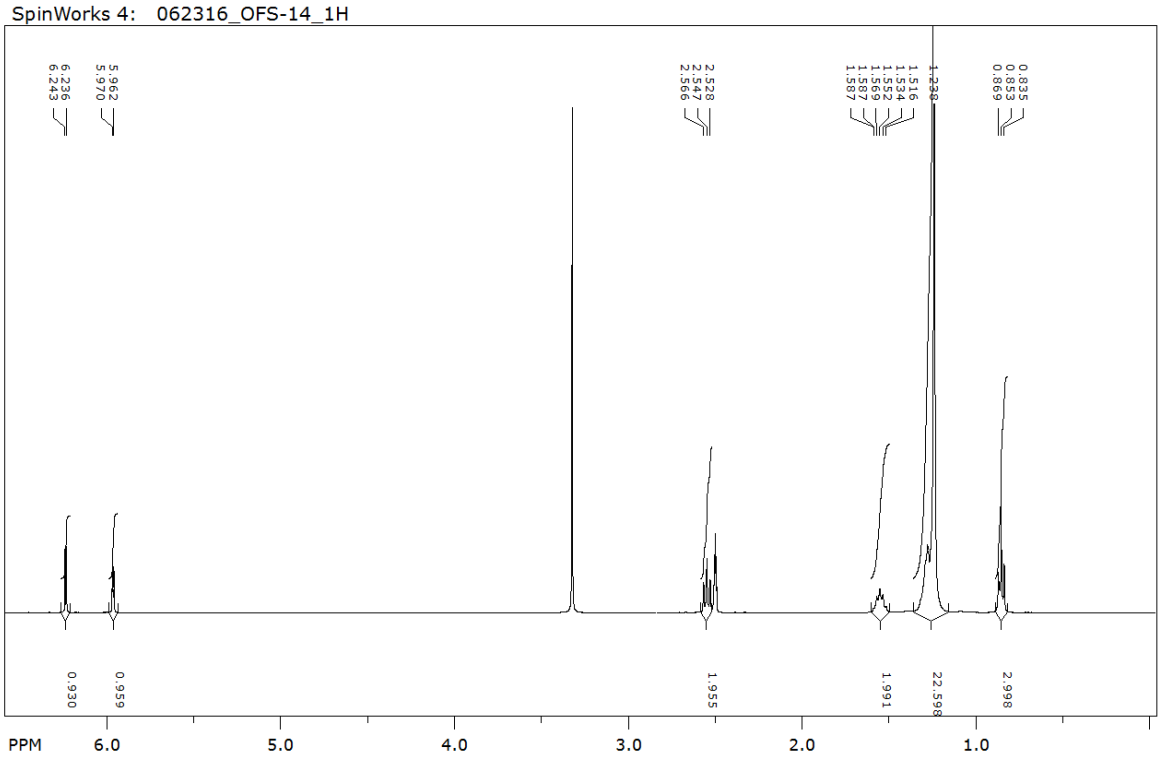

Fig. S61. ^{1}H NMR of OFS-14 in DMSO-d_6.

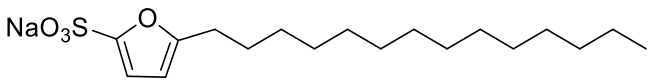

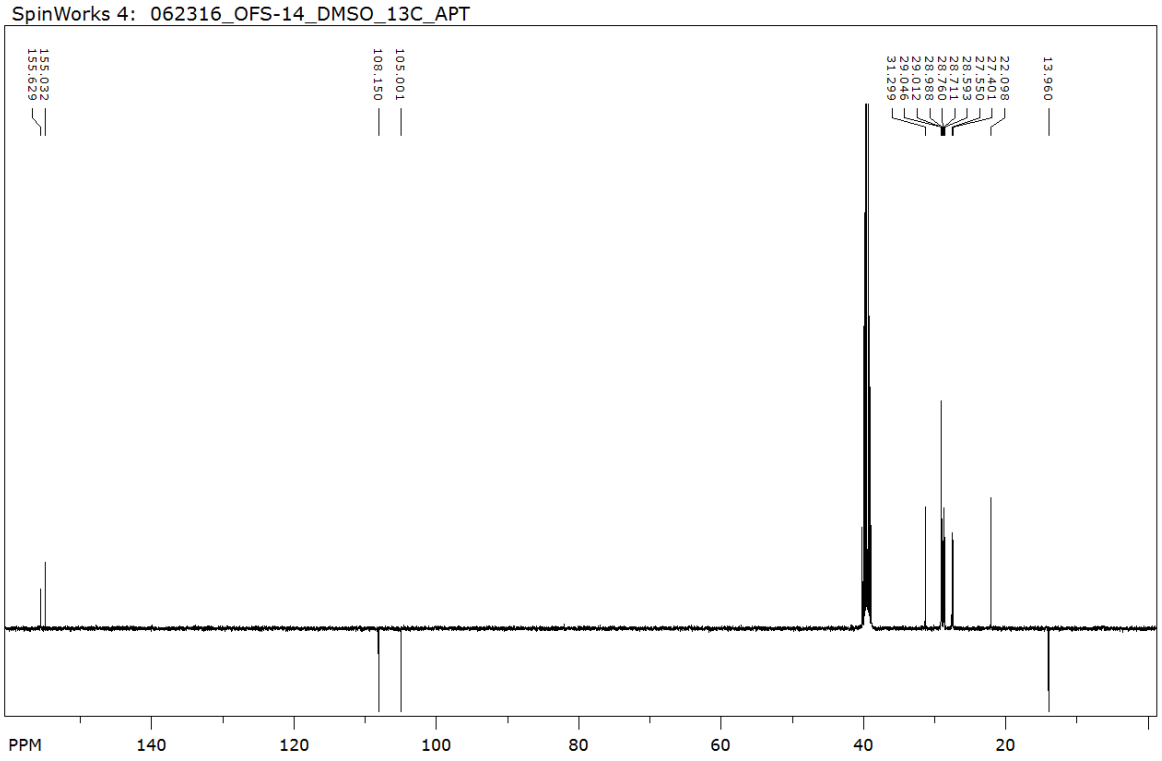

Fig. S62. ^{13}C-APT NMR of OFS-14 in DMSO-d$_6$.

7.0 Small Angle X-Ray Scattering (SAXS)

Small angle X-ray scattering (SAXS) experiments were performed at the beamline 12-ID-B of the Advanced Photon Source, Argonne, IL. The data was obtained at 42 ºC using a quartz capillary flow cell to minimize beam damage to the sample. The flow cell is equipped with a peltier heating/cooling device to control the temperature of the sample in the capillary. The X-ray energy was 14 keV (corresponding to a wavelength of 0.886 Å). To avoid radiation damage, the exposure time for each image frame was set to no more than one second. 20-40 images were collected for each sample/solvent to obtain good signal-to-noise ratio. The 2D isotropic scattering images were azumithally averaged to 1D data sets using the computer program provided at the beamline, followed by averaging of the 1D data sets.

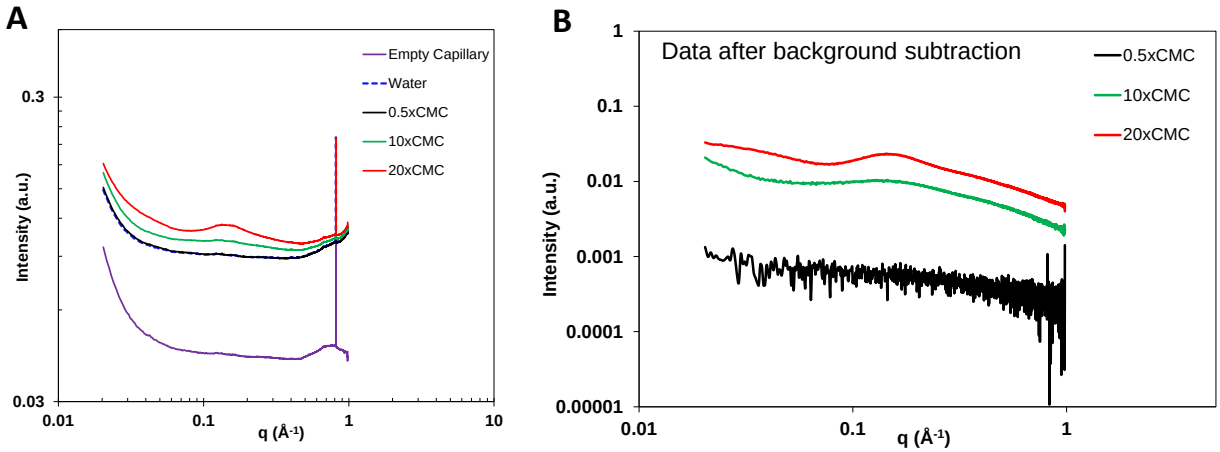

Fig. S63. Small Angle X-Ray Scattering. **A.** Experimental SAXS profiles for varying concentrations of OFS-12 surfactant below and above CMC and for the solvent (water) **B.** Scattering profiles obtained after subtracting the background (capillary with water).

Fig S63A shows the SAXS scattering plots obtained for different concentrations of the OFS-12 surfactant in water while Fig. S63B depicts the background subtracted data. From Fig. S63A, we see that, at a surfactant concentration corresponding to 0.5 times the critical micelle concentration (0.5xCMC, 0.035 wt%), the sample scattering profile resembles that of water and there is no scattering feature in the background subtracted SAXS profile (black curve in Fig. S63B). This conforms to the fact that no micelles are formed in solution below its CMC. As we increase the concentration above CMC (10xCMC and 20xCMC corresponding to 0.7 and 1.4 wt%), the appearance of a form factor oscillation at $q > 0.1$ Å^{-1} is indicative of the formation and presence of micelles within the aqueous system. Similar profiles are also reported in literature, where SAXS experiments have been conducted for a commercial sodium lauryl/dodecyl sulfate (SLS/SDS) sample.[15]

7.1 OFS-12 SAXS – PDDF (Pair Distance Distribution Function)

SAXS data of surfactant micelle have been analyzed using pair distance distribution function (PDDF), which is defined as,

$$P(x) = x^2 \langle \int \eta(\vec{u})\eta(\vec{x}+\vec{u})d\vec{u} \rangle$$

where $\eta(\vec{u}) = \rho(\vec{u}) - \rho_{solvent}$ and $\rho(\vec{u})$ and $\rho_{solvent}$ are the electron density at position $\vec{u}$ and solvent, respectively. Thus $\eta_{\text{solvent}} = 0$. The bracket depicts the orientational average.

In a micelle, $\eta_{shell} > 0$ and $\eta_{core} < 0$. When both ends of the vector $\vec{x}$ ($\vec{u}$ or $\vec{x}+\vec{u}$) is either in the shell or core, $\eta(\vec{u})\eta(\vec{x}+\vec{u})$ is positive. When one of its end is on solvent phase, $\eta(\vec{u})\eta(\vec{x}+\vec{u})$=0. When one end is on the shell and the other is on the core, $\eta(\vec{u})\eta(\vec{x}+\vec{u})$ becomes negative.

Therefore, it is possible to approximately picture the shape of the PDDF function of a core-shell structure. When x is shorter than the shell thickness, $P(x)$ is likely positive. When x is longer than the shell thickness, it may become negative. When x is larger than maximum size of the core, it can be positive again. Finally, when x is larger than d_{max}, $P(x) = 0$. If an object is made of only single phase without a shell, $P(x)$ will be positive at any x smaller than d_{max} and will be $P(x) = 0$ for x larger than d_{max}.

The PDDF was calculated from an experimental data using software program such as GNOM.[16] Our PDDF plot shown in Figure S64B obtained via the fit in Figure S64A of the SAXS data shows a typical PDDF expected from the core-shell structure.[15] The largest dimension obtained from the PDDF is about 7~8 nm determined from Figure S64B. This agrees with the DLS data of Figure S1C (which is the same sample at 20xCMC) with particle sizes of 4-8 nm.

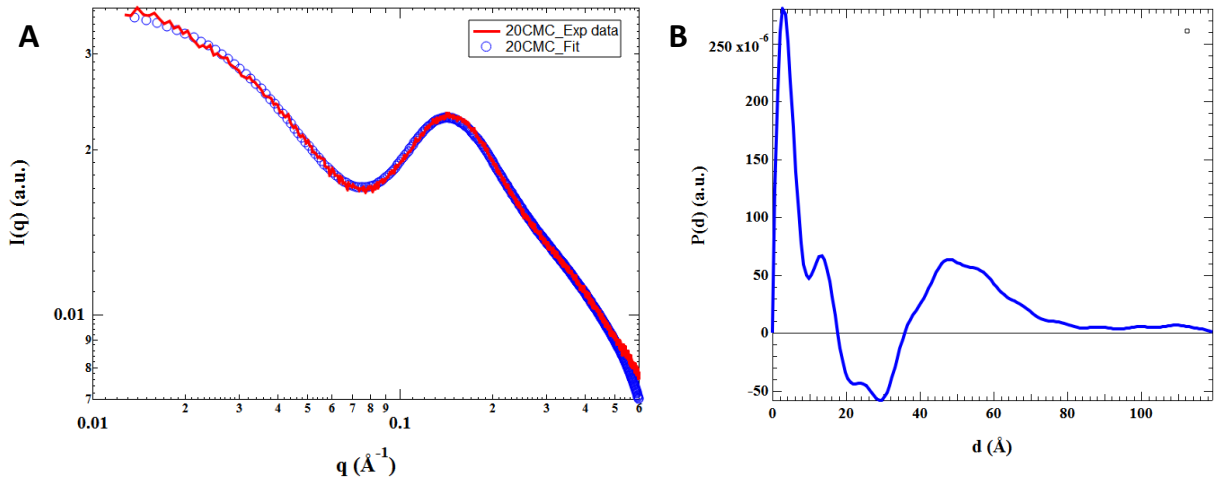

Fig. S64. PDDF of OFS-12 SAXS Data. A. The SAXS data (red) and fit (blue). **B.** Intraparticle Pair Distance Distribution Function.

References

1. Guo, Q.; Fan, F.; Pidko, E. A.; van der Graff, W. N. P.; Feng, Z.; Li, C.; Hensen, E. J. M. Highly active and recyclable Sn-MWW zeolite catalyst for sugar conversion to methyl lactate and lactic acid. *ChemSusChem* **2013**, *6*, 1352-1356.

2. Corma, A.; Fornés, V.; Martinez-Triguero, J.; Pergher, S. B. Delaminated zeolites: Combining the benefits of zeolites and mesoporous materials for catalytic uses. *J. Catal.* **1999**, *186*, 57-63.

3. Faba, L.; Díaz, E.; Ordóñez, S. Performance of bifunctional Pd/MxNyO (M= Mg, Ca; N= Zr, Al) catalysts for aldolization–hydrogenation of furfural–acetone mixtures. *Catal. Today* **2011**, *164*, 451-456.

4. Tago, T.; Konno, H.; Ikeda, S.; Yamazaki, S.; Ninomiya, W.; Nakasaka, Y.; Masuda, T. Selective production of isobutylene from acetone over alkali metal ion-exchanged BEA zeolites. *Catal. Today* **2011**, *164*, 158-162.

5. Fisher, J. W. Manufacture of carboxylic acids. U.S. Patent, 2,411,567, **1946**.

6. Goel, A. B.; Richards, H. J. Preparation of carboxylic acid anhydrides. U.S. Patent 4,477,382, **1984**.

7. Trummlitz, G.; Seeger, E.; Engel, W. 4-5-Dimethyl-thieno[3,2-d]ISO- thiazolo-3(2H)-one-1,1-dioxides, compositions, and methods of use as a sweetener. U.S. Patent, 4,233,333, **1980**.

8. West, R.M.; Wu, R.; Silks, III, L.A. Furan Based Composition. U.S. Patent Application, WO 2015084813 A1, **2015**.

9. Vlachy, N.; Drechsler, M.; Verbavatz, J.-M.; Touraud, D.; Kunz, W. Role of surfactant headgroup on the counterion specificity in the micelle-to-vesicle transition through salt addition. *J. Colloid Interface Sci.* **2008**, *319*, 542-548.

10. Rosen, M. J. *Surfactants and interfacial phenomena*, 3rd ed.; Wiley-Interscience: New Jersey, 2004.

11. ASTM D2281-10. Standard test method for evaluation of wetting agents by the skein test; ASTM International, West Conshohocken, PA, 2010, DOI: 10.1520/D2281-10, www.astm.org.

12. Rodriguez, C. H.; Lowery, L. H.; Scamehorn, J. F.; Harwell, J. H. Kinetics of precipitation of surfactants. I. Anionic surfactants with calcium and with cationic surfactants. *J. Surfactants Deterg.* **2001**, *4*, 1-14.

13. Rodriguez, C. H.; Chintanasathien, C.; Scamehorn, J. F.; Saiwan, C.; Chavadej, S. Precipitation in solutions containing mixtures of synthetic anionic surfactant and soap. I. Effect of sodium octanoate on hardness tolerance of sodium dodecyl sulfate. *J. Surfactants Deterg.* **1998**, *1*, 321-328.

14. Scamehorn, J. F. Precipitation of mixtures of anionic surfactants. In *Mixed surfactant systems*; ACS Symposium Series, vol. 501, American Chemical Society: Washington DC, 1992; pp. 392-401.

15. Itri, R.; Amaral, L. Q. Distance distribution function of sodium dodecyl sulfate micelles by x-ray scattering. *J. Phys. Chem.* **1991**, *95*, 423-427.

16. Semenyuk, A. V.; Svergun, D. I. GNOM - A Program Package for Small-Angle Scattering Data Processing. *J. Appl. Crystallogr.* **1991**, *24*, 537-540